

**Investigating the Thermal Performance of a Solar Water Heating
System Integrated with Phase Change Material as a Thermal
Energy Storage: A Case of Adama Hospital Medical College**

M.Sc. Thesis

By

Hasen Yune Shemsi



**Thermal and Aerospace Engineering Program
School of Mechanical, Chemical and Materials Engineering
Adama Science and Technology University**

Adama, Ethiopia

2011/2019

Investigating the Thermal Performance of a Solar Water Heating System Integrated with Phase Change Material as a Thermal Energy Storage: A Case of Adama Hospital Medical College

M.Sc. Thesis

By

Hasen Yune Shemsi



A Thesis Submitted to Thermal and Aerospace Engineering Program, School of Mechanical, Chemical and Materials Engineering, Adama Science and Technology University in partial fulfillment of the requirement of the degree of Masters of Science in Thermal Engineering

Advisor:

Dr. Gezahegn Habtamu

Adama, Ethiopia

2011/2019

DECLARATION

I declare that this thesis work entitled "Investigating the Thermal Performance of a Solar Water Heating System Integrated with Phase Change Material as a Thermal Energy Storage" fulfilling the nature and standard required for the partial fulfillment of the degree of Master of Science in Thermal and Aerospace Engineering is legal thesis work carried out under my supervision and guidance of Dr. Gezahegn Habtamu, Assistant Professor of Thermal Engineering program, Adama Science and Technology University.

The matter presented in this report has not been submitted by any one of us for the award of any other degree of this or any other University. Any literature, data or works done by others and cited within this thesis has been given due acknowledgement and listed in the reference fragment. All relevant resource information used in this paper has been properly admitted.

_____	_____	_____
Student	Signature	Date

This is to certify that the above statement made by the candidate is correct to the best of our knowledge and credence. This has been submitted for examination with my approval.

_____	_____	_____
Advisor	Signature	Date

Adama Science and Technology University
School of Mechanical, Chemical and Materials Engineering
Thermal and Aerospace Engineering Program



APPROVAL BOARD OF EXAMINERS

We, the undersigned, members of the Board of Examiners of the final open defense by Hasen Yune Shemsi have read and evaluated his thesis entitled "*Investigating the Thermal Performance of a Solar Water Heating System Integrated with Phase Change Material as a Thermal Energy Storage*" and examined the candidate. Therefore to certify, the thesis has been accepted in partial fulfillment of the requirement of the Degree of Master of science in Thermal Engineering.

_____	_____	_____
Chair Person	Signature	Date
_____	_____	_____
Internal Examiner	Signature	Date
<i>Dr. Abdulkadir Arman</i>		<i>24/10/19</i>
External Examiner	Signature	Date

ACKNOWLEDGEMENT

First and foremost my deepest and utmost gratitude to Almighty God, for his overwhelming love, strength and protection throughout and by his power I become successful after enormous challenges and also gives me patient, courage and wisdom to finish my study. Then, I am greatly indebted to my thesis advisor **Dr. Gezahegn Habtamu**, for providing me with a definite direction, professional guidance, boundless support, and constant encouragement from the beginning of the work-study and moral support in many ways during the study period.

I would like to express my sincere thanks to **Dr. Addisu Bekele and Mr. Leulseged Tarekegn** of Thermal and Aerospace Engineering staffs, for their outstanding suggestions and continuous inspiration during my study period. I would also like to thank all my best friends for their encouragement, suggestion, and assistance, and gave a worthy comment on my work and through the process of researching.

I must express my very profound gratitude to my parents (especially my Dad and Mam) for providing me with unfailing support and continuous encouragement throughout my years of study from elementary to higher education level in every direction and through the process of studying and writing this thesis. Without them I would have never been able to achieve my dream and thanks for their support, in always having my back.

Finally, I would like to thank Adama Science and Technology University for allowing me to join a master's program with a full scholarship.

ABSTRACT

The technology of solar energy has led to the development of several solar appliances used for water heating, lighting, cooking and solar thermal systems. The most encouraged among them is the solar thermal system that achieves the energy necessary for different applications at domestic as well as at the industry level both for day and night time use. In solar systems, an available energy supply does not usually coincide in time with the demand and is intermittent in nature. So, the utilization of solar energy can be more attractive and trustworthy if accompanied with a thermal energy storage system (TES).

This thesis studied in detail the design of flat plate solar collector and performance analysis of TES incorporating with and without Phase Change Materials (PCM) with flat plate solar collector for use in domestic water heating purposes. The TES system holds shell and tube configuration using paraffin wax (n-Heptacosane) as PCM in shell side and the water used as HTF in tube side to transferring heat to storage tank from solar collector.

A transient 1D method with the Finite Difference Scheme is used to investigate of flat plate collector and developed numerically to obtain the temperature profiles of both the phase change material (paraffin wax) and heat transfer fluid (HTF) during the melting process. The comparison of conventional sensible storage and latent heat thermal storage with incorporating Paraffin wax was studied and the simulation results are also analysed. As well, the pipe network and water distribution system numerical developed and simulated. Last, cost analyses for TES integrating with the SWH system were performed. Entirely, the results from a numerical simulation performed with meteorological data from Adama and estimated as 54 m³ of the total hot water demand per day, 5.6 m³ of PCM volume and two storage tank with each 30 m³ needs and with 265 units of flat plate collectors can satisfy the energy needed for the designed PCM based solar water heating system for supply domestic hot water to Adama hospital medical college (AHMC).

Key words: *solar energy, Flat plate collector, solar water heating system, Thermal energy storage. Heat transfer fluid, Phase change materials, Paraffin wax.*

TABLE OF CONTENTS

CONTENTS	PAGE
ACKNOWLEDGEMENT.....	III
ABSTRACT.....	IV
TABLE OF CONTENTS	V
LIST OF FIGURE	X
LIST OF TABLE	XIII
LIST OF SYMBOLS AND NOMENCLATURE.....	XIV
ABBREVIATION	XV
GREEK LETTERS.....	XV
SUBSCRIPTS.....	XV
CHAPTER 1.....	1
1. Introduction	1
1.1 Background of the study	1
1.2 Physical description and principles of SWH system integrating with PCMs	3
1.3 Statement of the problem	4
1.4 Objectives.....	5
1.5 Significance of the study.....	5
1.6 Scope and Limitations of the study.....	5
1.6.1 Scope of the study.....	5
1.6.2 Limitation of the study	6
1.7 Research Question.....	6
1.8 Research Methodology.....	6
CHAPTER 2.....	8
2. Literature Review	8
2.1 Solar Water Heating (SWH) System.....	8
2.1.1 Classification of Solar Water Heating System (SWHS)	8
2.2 Solar Thermal Energy Collectors.....	9
2.2.1 Flat-plate collectors (FPC).....	10
2.3 Thermal Energy Storage (TES) System.....	11
2.3.1 Sensible Heat Thermal Energy Storage (SHTES).....	11

2.3.2 Latent Heat Thermal Energy Storage (LHTES).....	12
2.4 Phase change materials (PCM)	13
2.4.1 Classification Phase Change Materials (PCM)	13
2.4.2 Selection of Phase Change Materials	15
2.5 Application of a PCM integrated into a SDHW storage Unit.....	16
2.6 Related work of Latent Heat Thermal Energy Storage for SWH system	16
2.6.1 International Relate work	16
2.6.2 Local Related work.....	20
CHAPTER 3	22
3. Hot Water and Steam Demand of AHMC	22
3.1 Data collected from Adama Hospital Medical College	22
3.2 Hot water consumption of the Hospital.....	22
3.3 Hot Water Consumption Pattern	24
3.4 Hot Water Storage Tank Capacity	25
3.5 Boiler-Conventional Steam Generation	25
CHAPTER 4	28
4. Performance Analysis of Solar Flat Plate Collector for SWH	28
4.1 Estimation of Available Solar Radiation.....	28
4.1.1 Estimation of global solar radiation using sunshine duration.....	28
4.1.2 Preliminary Terminology and sign conventions for estimation solar radiation	29
4.1.3 Estimation of Hourly Solar Radiation on a Horizontal Surfaces (HS).....	30
4.1.3.1 Extraterrestrial (ETR) daily Solar Radiation on a Horizontal Surface	30
4.1.3.2 Prediction of Monthly Average Daily Global Radiation on a HS (H)	31
4.1.3.3 Prediction of Monthly Average Daily Diffuse Radiation on HS (Hd)	32
4.1.3.4 Prediction of Monthly Average Hourly Global Radiation on a HS (I)	33
4.1.3.5 Prediction of Monthly Average Hourly Diffuse Radiation on a HS.....	34
4.1.4 Estimation of Hourly Solar Flux on Inclined Surfaces.....	34
4.1.5 Adama Climate Condition and Estimation Hourly Variation of Ambient Temperature.....	36
4.1.5.1 Climatic condition.....	36
4.1.5.2 Estimation of Diurnal Variation of Ambient Temperature.....	36

4.2 Transient thermal performance analysis of Flat Plate Collector	37
4.2.2 Technical Specification and Assumption of Flat Plat Collector Model	38
4.2.3 Basic Energy Balance Equation for Flat Plate Collector.....	40
4.2.4 Incident solar radiation and solar energy input	40
4.2.5 Overall Heat Loss Coefficient of Solar Flat Plate Collector	42
4.2.5.1 Overall Top-Loss Coefficient - U_t	43
4.2.5.2 Bottom Loss Coefficient.....	45
4.2.5.3 Side Loss Coefficient.....	45
4.2.6 Collector efficiency factor F' and temperature distribution between tubes	46
4.2.7 Transient Analysis and Energy Balance Equation of Flat Plate Solar Collector Components.....	50
4.2.8 Transient Analysis of Flat Plate Solar Collector Using Finite Difference Method.....	52
4.2.9 Estimating total heating load and solar energy.....	54
4.2.10 Determining sizing of collector system	54
4.2.11 Flat Plate Solar Collector Arrays Configuration	55
4.2.12 Clearance between collector arrays	56
4.2.13 Length of Pipe between solar collector and storage.....	57
4.2.14 Pressure drop in solar collector system	58
4.2.15 Total Pressure Drop through the solar thermal system.....	60
4.2.16 Selection of Pump.....	63
CHAPTER 5.....	64
5. Design and Performance Analysis of Solar Thermal Storage system for SHW	64
5.1 Numerical Investigation of Conventional Solar Thermal Storage System	64
5.1.1 Material Selection of Thermal Storage Tank	65
5.1.2 Modeling of the Sensible Thermal Storage for Solar System	65
5.1.3 Optimization of Storage Tank and Insulation Thickness	66
5.1.3.1 Insulation Thickness	66
5.1.3.2 Sensible Thermal Storage Tank Thickness.....	68
5.1.4 Transient Analysis of Thermal Storage for Solar Hot Water System	70
5.2 Performance Analysis of Solar Thermal Storage Tank Integrated with Phase Change Materials (PCM).....	72

5.2.1 Thermal Storage Tank Integrated with incorporating PCM.....	72
5.2.2 Benefits of integrating PCM with Solar DHW Storage System.....	72
5.2.3 Modes of Thermal Energy Storage System.....	73
5.2.4 Design Consideration	73
5.2.5 Design Assumption.....	74
5.2.7 Sizing of Latent Heat TES System for Solar Heating application	74
5.2.8 General Procedure for sizing LHTES unit for Solar Water Heating System	75
5.2.9 Modeling and Simulation of Shell and Tube LHTES with integrating paraffin wax...	77
5.2.10 Heat stored and available during charging and discharging process.....	80
CHAPTER 6.....	82
6. Pipe Network and Water Distribution system.....	82
6.1 Water Demand Pattern and Distribution System Design.....	84
6.2 Water Distribution system and Hospital Building Geometry	85
6.3 Estimation of discharging rate and head loss for each Room	85
6.4 Pressure drop through water distribution system	88
6.5 Investigation of hot water flow from storage tank through pipeline.....	88
6.6 Selection of pump for water distribution system	90
6.6.1 The performance or characteristic curve of the pump.....	90
CHAPTER 7.....	92
7. Result and Discussion.....	92
7.1 Solar Intensity Radiation.....	92
7.2 Variation of Hot water Stream (HTF) Temperature.....	92
7.3 Solar Fraction	94
7.4 Instantaneous thermal efficiency.....	95
7.5 Estimated solar sizing system	96
7.6 Variation of Storage tank Temperature throughout the day.....	97
7.7 Useful Energy gained by Solar Collector.....	98
7.7.1 Hourly average useful solar energy throughout the day.....	98
7.7.2 Monthly average of useful solar energy throughout a year	99
7.7.3 Solar thermal energy losses throughout the day.....	100

7.8 Fluctuation Temperature of Thermal Storage Tank integrating Phase Change Materials (Paraffin wax).....	100
7.8.1 Variation temperature of Paraffin storage tank during charging process.....	100
7.8.2 Validation.....	101
7.9 Summary and Comparison of LHTES and Conventional SHS solar water heating system.....	102
7.9.1 Validation.....	104
7.10 Water distribution system and pipe network.....	104
CHAPTER 8.....	106
8. Estimation of Economic Analysis of DHW for AHMC.....	106
8.1 Economic Analysis of Solar Thermal System.....	106
8.2 Financial and Unit prices of components of SHW system with integrating PCM as Thermal energy storage.....	107
8.3 Maintenance, Operating and Replacement Cost.....	108
8.4 Analysis of investment cost.....	108
8.5 Summary of Cost Estimation for the project installation.....	110
CHAPTER 9.....	111
9. Conclusions and Recommendations for Future work.....	111
9.1 Conclusions.....	111
9.2 Recommendations.....	112
9.3 Future work.....	112
References.....	113
APPENDIX.....	116
ANNEX A: Incident solar radiation on inclined surface collector.....	116
ANNEX B: Graph of Outlet heat transfer fluid temperature.....	116
ANNEX C: Temperature of plate absorber, air gap and glass cover.....	117
ANNEX D: Useful solar energy gain for every months.....	118
ANNEX E: Variation of daily temperature of hot water with and without phase change materials for June 17.....	119
ANNEX F: Moody chart.....	120

LIST OF FIGURE

Figure 1.1 Adama Hospital medical college (AHMC).....	2
Figure 1.2 Schematic diagram of SWH system for AHMC; A) SWH system with conventional storage tank and B) SWH system integrating with PCM as energy storage.....	3
Figure 2.1 Classification of solar water heating system	8
Figure 2.2 a) Side cross–section view of single glazed flat-plate collector. b) Components of glazed flat-plate collector (Kalogirou, 2014).	10
Figure 2.3. Classification of Thermal Energy Storage and processes	11
Figure 2.4 Classification of phase change materials (PCMs) from Sharma et al., (2009).....	13
Figure 3.1 Daily Hot Water consumption pattern and distribution over the time of the day of Adama Hospital.	24
Figure 3.2. Installed diesel fuel steam generation of AHMC new building	25
Figure 4.1 Monthly averagely sunshine duration for each months of Adama.....	29
Figure 4.2 The solar radiation incident on a horizontal plane outside of the atmosphere (Extraterrestrial (ETR) daily Solar Radiation).....	31
Figure 4.3 Graph of Monthly Average Daily Global Radiation on a Horizontal Surface	32
Figure 4.4 Graph of Monthly Average Daily Diffuse Radiation on a Horizontal Surface.....	32
Figure 4.5 Graph of Monthly average daily global, diffuse and beam of solar radiation.....	33
Figure 4.6 Monthly average hourly global radiation on a horizontal surface (Wh/m^2) at Adama	33
Figure 4.7 Monthly average hourly diffuse solar radiation on horizontal surface (W/m^2).....	34
Figure 4.8 Global hourly solar radiation on 22.5° tilted surface (W/m^2).....	35
Figure 4.9: Maximum Hourly Global, Diffuse and Beam SR on inclined surfaces (22.5°) on Febr 16 th	35
Figure 4.10: Result of average variations of ambient temperature of Adama	37
Figure 4.11 Cross section of a typical liquid flat-plate collector (Duffie & Beckman, 2013).....	38
Figure 4.12 Monthly average hourly incidence solar radiation on a tilted surface (22.5°) for all seasons in a year (A, B, C & D).....	42
Figure 4.13 Thermal resistance network collector losses (Kalogirou, 2014).	42
Figure 4.14. Various heat losses from absorber to ambient (Tiwari, 2016).	43
Figure 4.15 Bonding material placed between the plate and the tube.	46

Figure 4.16 Energy flow on fin element (a) Fin with Insulated Tip and (b) Energy balance Over Finite Volume.	46
Figure 4.17 Variation of desired outlet temperature for heat transfer fluid versus mass flow rate.....	49
Figure 4.18 Energy balance and heat transfer techniques on single glass cover	50
Figure 4.19 Energy balance and heat transfer techniques of air gap between glass and abs. plate.....	51
Figure 4.20 Energy balance and heat transfer techniques on absorber plate	51
Figure 4.21 Energy balance and heat transfer techniques of insulation	51
Figure 4.22 Energy balance and heat transfer techniques by working fluids	52
Figure 4.23 Diagram of FPC Parallel array configuration.....	56
Figure 4.24 Clearance of collector arrays angle of inclinations	56
Figure 4.25 Schematic diagram of total length of pipe and network between solar collector and thermal storage system.....	58
Figure 5.1 Schematic diagram of Sensible thermal storage tank for solar water heating system.	64
Figure 5.2 Optimization of insulation thickness from Sahu et al., (2015).....	66
Figure 5.3 Optimum insulation thickness and cost.....	68
Figure 5.4 Sensible thermal storage tank thickness	69
Figure 5.5 Schematic configuration of shell and tube latent heat thermal energy storage system (LHTES) unit with complete system, and concentric cylinders.	74
Figure 5.6 Schematic diagram of transient heat transfer flow through the shell and tube latent heat thermal storage system.....	80
Figure 6.1 Layout of hot water discharging from storage tank to all floor building	83
Figure 6.2 The selection chart to determine the appropriate Centrifugal pump model and size for water pumping application.....	91
Figure 7.1 The hourly average SR for February, January, June and August in Adama.	92
Figure 7.2. Fluctuation of Hot water stream temperature throughout the day in 24 hours for Winter Season (High solar radiation incidence).	93
Figure 7.3. Fluctuation of Hot water stream temperature throughout the day in 24 hours for Summer Season (Low solar radiation Incidence).	93

Figure 7.4 Temperature Fluctuation of absorber Plate, Glass Cover, Air Gap throughout the Day for February 16.	94
Figure 7.5 Monthly solar fraction (sf).....	94
Figure 7.6 Variation of instantaneous efficiency of a flat plate collector for February 16.....	95
Figure 7.7 Variation of instantaneous efficiency of a flat plate collector for July 17.	95
Figure 7.8 Simulated hourly variation temperature of hot water during summer season.....	97
Figure 7.9. Hourly variation temperature in storage hot water tank during winter season.....	98
Figure 7.10 Hourly average useful energy collected throughout the day from a single FPC for Summer Season (Minimum value of Useful energy gain).....	98
Figure 7.11 Monthly average daily average useful energy collected by a single FPC.....	99
Figure 7.12 Simulation of Useful Energy losses throughout the day for February 16 th and July 17.....	100
Figure 7.13: Temperature variation of Paraffin wax during melting process during February 16.....	101
Figure 7.14: Variation Temperature of phase change materials for different heat transfer inlet Temperature during charging process Reddigari et al., (2012).	102
Figure 7.15 The time wise variation of the hot water temperature in the solar water heating system with and without PCM during charging processes on July 11 th	102
Figure 7.16: The time wise variation of the hot water or HTF average temperature of the storage tank for the SWH system with and without PCM on February 16 th during charging processes	103
Figure 7.17. Depth of hot water in thermal storage tank	105
Figure 7.18. Quality of hot water withdrawal rate capacity versus operating time used.....	105
Figure A.0.1 Incident solar radiation on inclined surface collector.....	116
Figure B.0.2 Outlet temperature of HTF during all months in a year	117
Figure C.0.3 Temperature of Glass cover, absorber plate, and air gap during summer season..	117
Figure D.0.4 Hourly average useful energy solar gain by a single flat plate collector.....	118
Figure E.0.5 Variation of daily temperature of hot water with and without phase change materials, and ambient temperature.....	119
Figure F.0.6 Moody chart	120

LIST OF TABLE

Table 2.1: Solar thermal collector type (Sarbu & Sebarchievi, 2015).....	10
Table 3.1. Collected data of Adama Hospital Medical College.	22
Table 3.2. Standard Hot Water Demand for Hospital (Brochure, 2015)	22
Table 3.3. Hot Water Demand for each Appliance of the Hospital.....	23
Table 3.4. Hot water demand of the Adama Hospital medical college per Services.....	24
Table 4.1 Sunshine hourly duration for five years (source; East Shoa Meteorology).....	28
Table 4.2. Estimation of five years average sunshine hour duration.	29
Table 4.3 Monthly average annual climatic condition of Adama (Ethiopia National Meteorology Agency).....	36
Table 4.4 The main specification reference for Solar Flat Plate Collector used in analyses.....	39
Table 4.5 Total pressure drop in Solar Flat Plate Collector system.....	59
Table 4.6 Absolute Roughness Coefficient (enggcyclopedia.com, 2011).....	61
Table 4.7 Total pressure drop through the solar thermal system for SWH system	62
Table 5.1 Thermophysical properties of selected Paraffin wax (n-Heptacosane) in design of SWH system.	75
Table 6.1 Design parameters ranges	84
Table 6.2 Summary of discharging rate or demand for a hospitals	87
Table 6.3 Total pressure drop throughout the pipe flow in a hospital.	88
Table 7.1 Average effective area and total number of flat plat collector needed for each months.....	96

LIST OF SYMBOLS AND NOMENCLATURE

SYMBOL	NAME	UNITS
A_c	Area of the collector	m^2
C_p	Specific heat capacity	$kJ/kg.k$
C_t	Total daily Hot water consumption	Liter or m^3
D	Diameter of storage tank	mm
E	Equation of time	min
F_R	The collector's heat removal factor.	
G_T	The incident radiation.	W/m^2
h_c	Convective Heat transfer coefficient	W/m^3K
h_r	Radiative Heat transfer coefficient	W/m^3K
H_{sr}	Sunrise hour	hr
H_{ss}	Sunset hour	hr
K	Thermal conductivity	$W/m.k$
L_p	Length of the pipe	m
L_{st}	Length f storage tank	m
P	Power	W
Q	Amount of heat storage	W
Q_d	Amount of energy demand	W
Q_s	Amount of heat storage by solar	W
Q_L	Amount of heat storage losses	W
Q_{HWD}	Heat energy of hot water demand	W
T_a	Ambient Temperature	$^{\circ}C$
$T_c \& T_h$	Cold Temperature	$^{\circ}C$
T_p and T_g	Temperature of absorber plate and cover	$^{\circ}C$
T_{pcm}	Temperature of phase change materials	$^{\circ}C$
U_L	Overall heat transfer coefficient	$^{\circ}C$
V_{st}	Total volume of storage tank	m^3
W	Distance b/n the centres of the two tubes	mm
$\Delta T \& \Delta P$	Temperature difference and pressure drop	$^{\circ}C$ and Pa

ABBREVIATION

AHMC	Adama Hospital medical college	HTF	Heat transfer fluid
FPC	Flat plate collector	NTU	Number of transfer unit
ETC	Evacuated tube collector	FDM	Finite difference method
HWD	Hot water demand	ST	Shell and tube
SHS	Sensible heat storage	LCC	Life cycle cost
LHS	Latent heat storage	LCS	Life cycle saving
LHTES	Latent heat thermal energy storage system	CI	Investment cost
PCM	Phase change material	CF	Cash flow
HS	Horizontal surface	NPV	Net present value

GREEK LETTERS

η	Efficiency	ε	Emissivity
τ	Transmittance	σ	Stefan Boltzmann
ρ	Density kg/m ³	φ	Latitude angle (°)
β'	Thermal expansion coefficient [1/K]	δ	Declination angle (°)
Δ	Delta change	ω	Solar hour angle (°)
\dot{m}	Mass flow rate [kg/s]	θ_i	Incidence of angle (°)
\dot{V}	Volume flow rate [m ³ /s]	θ_z	Zenith angle (°)
μ	Dynamic viscosity	β	Surface slope angle (°)
ν	Kinematic viscosity	α	Thermal absorptivity

SUBSCRIPTS

avg	Average	s	Steam
ins	Insulation	out	Outer
a	Ambient or atmosphere	in	Inner
surr	Surrounding	t	Tube
c	Convection	f	Fluid
r	Radiation	ref	Reference
L	Loss	w	Wall
st	Storage tank	m	Melting point

CHAPTER 1

1. Introduction

1.1 Background of the study

Energy is an essential aspect of the well-being of any application for human life to prosper and develop in the economic front. Hence, the energy requirement is increasing day to day and may affect all aspects of modern economic development. In Ethiopia, electricity power has been serving as the main source of energy for domestic water heating systems. The inevitable rise of the price of electricity caused by increased investment cost of power generation that searches for an alternative source of energy application. The fossil fuels are considered as an alternative source, but its cost rate is extremely increasing and make pollution that affects an environment.

As we know, most of the hospitals in our country uses an electric power and fuel boiler for water heating system and for another appliance. Among them, Adama Hospital Medical College (AHMC) is one of the 1st Medical Hospital in Adama town located in Oromia region, 100 km to southeast of Addis Ababa, Ethiopia. AHMC was previously known by the names of Hayile Mariam Mamo Memorial Hospital and Adama Referral Public Hospital at different times. The hospital developed its facilities, technology, service standards and personnel to become a renowned institution under government since 1970 E.C.

The hospital was upgraded to Medical College in 2003 E.C because of its position, patient load and staff capacity. The College is led by the board and has three major wings (academic and research, health service and the development and administration). The Hospital is serving a catchment population of more than six million from five regions: Oromia, Amhara, Afar, Somali, and Dire-Dawa. It has 232 beds capacity and serving on average 1000 patients per day. AHMC is providing services using all available material, financial and human resources. Because of improved services, the number of patients coming to the Hospital increasing from day to day.

The Hospital College has tried to expand its existing facilities for the fundamental transformation, and the construction of the new Hospital College complex was designed and started to be constructed with the cost of nearly one billion ETB. The construction of hospital was completed in 2010 E.C. and started functioning since October, 2011 E.C.



Figure 1.1 Adama Hospital medical college (AHMC).

The hospital uses energy for various activities. Due to the hospital building upgrade and expansion (new), the number of society's increases, and the increasing number of patients day to day; the diesel fuel and electric energy consumption of the hospital is high. Consequently, the hospital's consumption and demand of hot water required were approximately 50,000 liters per day and functions for 24 hours. The Adama hospital uses a diesel fuel at least 2400 liters per every month. This shows that, energy costs from fuel sources are increasing at a considerable rate by increasing operating costs and reducing profitability due to the continuous escalating of diesel fuel price.

The remaining option as an energy source is to exploit the inexhaustible and freely available solar radiation. When the solar energy has to be used for such a purpose, it has to bring economic benefit to the potential user and decrease the use of fossil fuels. Solar energy is one of the green technologies and stands as a feasible candidate for obtaining heat for both industrial and domestic processes. To reduce the cost of energy consumption, increase profitability and make free pollution environments; the solar thermal system for supplying hot water to AHMC is proposed as a sustainable alternative energy source.

Although solar energy is available, the discontinuity of the sun irradiation could cause a heat supply disruption and being an intermittent energy source. Hence, the utilization of solar energy

can be more attractive and trustworthy if associated with a thermal storage system (TES). TES is used to equalize instantaneous differences between demand and supply of thermal energy using off-peak excess energy which may be lost otherwise, increasing the reliability of solar thermal systems. The heat that is not required by the process during peak sun hours can be stored to be later used when there is no solar irradiation. Besides, the hospital gives a function for 24 hour operation, then thermal energy storage system is required. Therefore, proposed schematic diagrammatic solar water heating system for Adama hospital is shown in Figure 1.2.

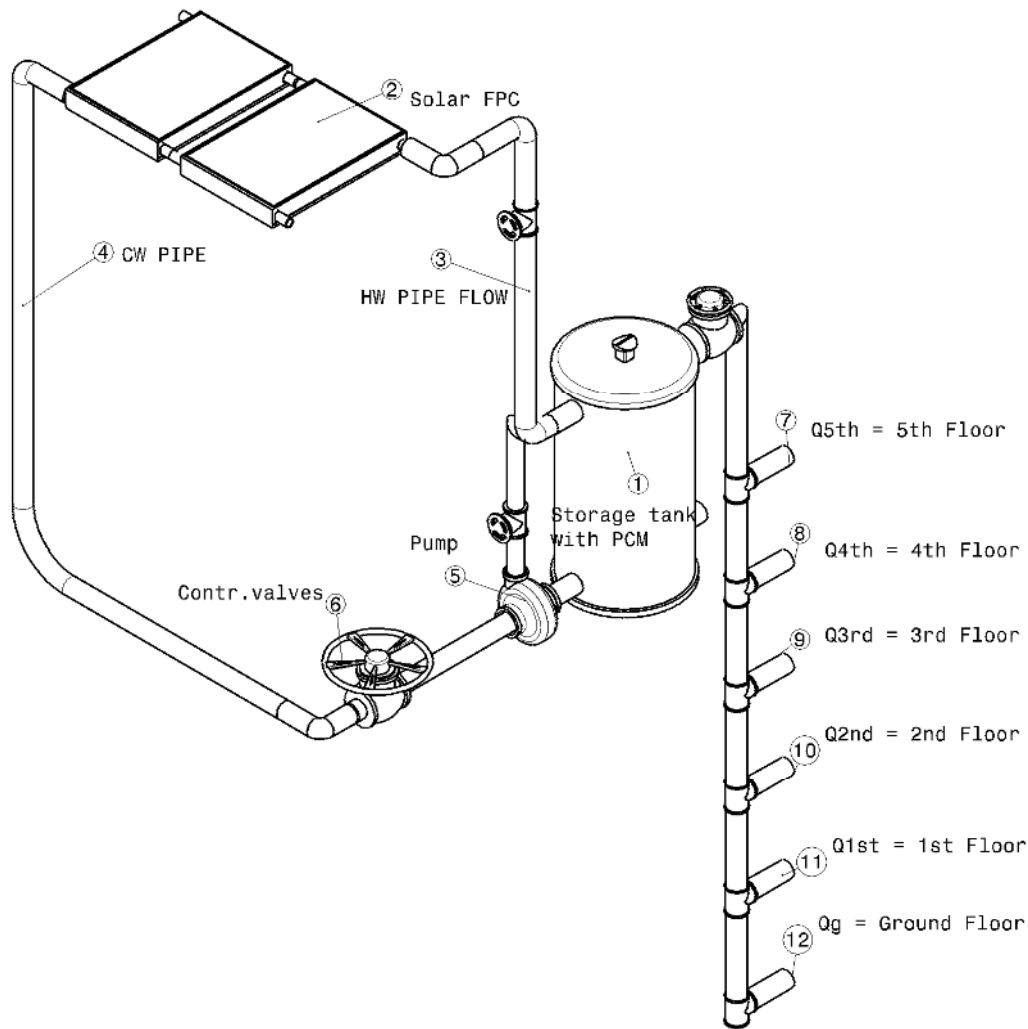


Figure 1.2 Schematic diagram of SWH system for AHMC; A) SWH system with conventional storage tank and B) SWH system integrating with PCM as energy storage.

1.2 Physical description and principles of SWH system integrating with PCMs

Solar heating systems are composed of solar flat plate collectors, heat transfer fluid, insulated thermal storage system, connecting pipes and instruments, accessories and supporting stand. The

heat from the sun fall on the solar FPC. The solar thermal devices captures and transfers the heat energy available in solar radiation. Then, a cold water forced upward by pump is heated by the solar thermal energy absorbed by the collectors. A bank of collectors can be arranged in a parallel combination to get higher quantity of hot water. After the cold water is absorbed heat, the hot water is flows through insulated pipe in to storage tank. Then, some of the hot water is used for standby and distributed through water distribution system to its point of usage which can be used for meeting the requirements of heat in different temperature ranges, while some hot water is stored by phase change materials TES system for later usage. Finally, Hot water from the system is transferred to various utility points through insulated pipelines. For designing this overall system the components such as solar thermal analysis, storage analysis, water distribution system and pipeline should separable designed.

Some minor components should be raised here are accessories and regulating system such as temperature pressure valve (TPV), air vent, pressure relief valve (PRV), drain valve and check valve and temperature gauges and their functions are as the following:

Allows air that has entered the system to escape, and in turn prevents air locks that would restrict flow of the HTF. TPRV is Protects system components from excessive pressures and temperatures. TG is Provide an indication of system fluid temperatures. A temperature gauge at the top of the storage tank indicates the temperature of the hottest water available for use. Drain valves are used to drain the collector loop, the storage tank and, in some systems, the heat exchanger or drain-back reservoir. Check valve is allow fluid to flow in only one direction.

Generally, this thesis focus on analysis of solar water heating system such as transient flat plate collector performance, estimation of HWD for AHMC, thermal energy storage system, phase change material, pipe network and water distribution system and minor economic analysis.

1.3 Statement of the problem

In our country, almost all public health centers are dependent on the electrical power supplied and fossil fuel for an energy source. Thus, energy charges are growing day to day and also using fossil fuel that influences an environment. The heating water system for Hospital is supplied from boiler steam and the fuel used is diesel to meet daily hot water demand. Continuously, electric power does not provide energy properly. So, partial replace it when electric power off, the hospital uses four diesel generators and each used diesel fuel of 800 liters per month. The total paid cost of this

fuel is about 60,800.00 ETB per month. And also the hospital gives a function of 24 hours. These show that the energy costs are considerable. Besides, the energy and the temperature level required to be supplied to carry out everyday tasks will high. To fulfill the gabs, a solar thermal energy source is proposed and is the foremost way to solve the problems mentioned. Since the hospital operates for 24 hour, the solar water heating accompanying with a thermal storage system for a hospital is a sustainable alternative to partially or wholly supply hot water demand of the hospital.

1.4 Objectives

The general objective is the design, and performance analyses of a solar thermal water heating system integrated with phase change material energy storage that supplies hot water to AHMC.

The specific objectives of this thesis are

- ✦ Estimate HWD and sizing overall dimension of the solar system (area of the collector, number of collector and thermal storage) that fulfill the demand of hot water to AHMC.
- ✦ Thermal Modelling, simulation and investigating the transient performance of solar system components, flat plate collector and thermal storage units using finite difference scheme.
- ✦ Numerical compare the conventional sensible thermal storage with a latent thermal storage unit integrating phase change material.
- ✦ Analyze pipe network system of water distribution and pump selection

1.5 Significance of the study

AHMC was used diesel boiler for water heating system. This thesis tends to the hospitals to use solar technology rather than boiler. If the hospitals uses the product obtained of this study, it will be benefited more by reducing cost for electricity and a cost for diesel, and also environmental free pollution. The solar thermal energy storage system proposed for this hospital is functions during both day and night. Solar energy is an affordable energy which are good physical well-being, reduce dependence to electricity and fossil fuel energy consumption of the hospital for hot water supply system. I hope that, the results of this research will open an opportunity for further application of solar thermal storage system for a hot water supply system in the country.

1.6 Scope and Limitations of the study

1.6.1 Scope of the study

This thesis begins with a comprehensive literature review tracing the history of solar heating system and energy storage for thermal application. The analysis of this research covers the thermal

performance and simulation of FPC and TES units that would partially replace of steam boiler in AHMC. In this work, the water distribution system after storage unit and pipe network is investigated up to the end user.

1.6.2 Limitation of the study

This study is developed on Adama weather condition to design, and simulate a solar thermal system integrating PCM as energy storage for providing hot water demand to AHMC. Consequently the result of this study is applicable for a tropical area like Adama and health centers that demands are less than the demands of this hospital. Since the multi-dimensional heat transfer phenomenon is complicates the analysis of the solar collector and TES system, this study specify the one-dimensional heat transfer analysis and modeled to investigating the systems.

1.7 Research Question

There are numerous questions arise regarding the solar-assisted water heating system with an improvement of solar thermal systems. However, for this thesis specific research questions are: -

- i. How many amounts of energy delivery to cover the energy demand of hospitals?
- ii. How many numbers of flat plat collectors used to cover the daily energy requirement?
- iii. What are the factors that influence the hot water storage tank performance?
- iv. How to achieve the desired output temperature of water from solar water heating system?
- v. How and by what methods the thermal performance of a storage tank could enhance?

1.8 Research Methodology

This study is concerned with the design and thermal performance of analyzing the solar thermal system with solar FPC and thermal storage investigating to supply hot water for AHMC new building. Primarily, the latest literature review of relevant materials on solar water heating systems, flat plate collectors, conventional storage tanks, latent heat thermal storage unit, and pipe network systems are conducted. Secondary, the data are referred from related research and previous done, existing statistical information, etc. In general, the following activities were accomplished to achieve the thesis objectives.

- Data collecting from Hospital and weather data taken from Adama meteorology agency.
- Estimating the hot water consumption to cover the daily demand for hospital and estimating solar radiation on inclined solar collectors using collected data and standard.
- Modeling and transient thermal performance analysis of flat plate collector

- Compare the sensible storage tank and latent heat thermal storage tank with incorporating phase change material.
- Simulate the offered system and components functionally using MATLAB and Excel Microsoft package
- Analyzing the pipe network and hot water distribution system to each room of the hospitals
- Writing the study results with the help of graph, table, figure, number, and give the discussion of the result and final validating with published paper.
- Lastly, prepare and arrange the full paper and make a presentation.

CHAPTER 2

2. Literature Review

Under this portion, a detailed review of the previous work that related to the current research is presented. A literature review concerning to solar-assisted water heating system, types of SWH, the configuration of a storage tank, solar collector, phase change materials and its classification, performance and effects of thermal-physical properties, overall dimension and geometry are discussed below.

2.1 Solar Water Heating (SWH) System

Solar water heating is an acceptable technology with the help of solar radiation and is increasingly being used as one of the cost-effective means of heating water in residential and public buildings such as hotels, restaurants, hospitals, health centers and industries such as textile, paper, and food processing of dairy & edible oil. With the abundance of solar energy, the domestic solar water heating system is very promising. It converts solar energy into thermal energy and can replace any type of conventional heating system or fuel and there is a re-emerging market today with the need for renewable sources of energy by Christopher et al., (2010). Domestic hot water supply at temperatures in the range of 50 to 60°C is considered to be acceptable.

2.1.1 Classification of Solar Water Heating System (SWHS)

SWH systems are categorized depending on how the domestic water is heated or how the heat transfer fluid flows through the collector (Panapakidis, 2016).

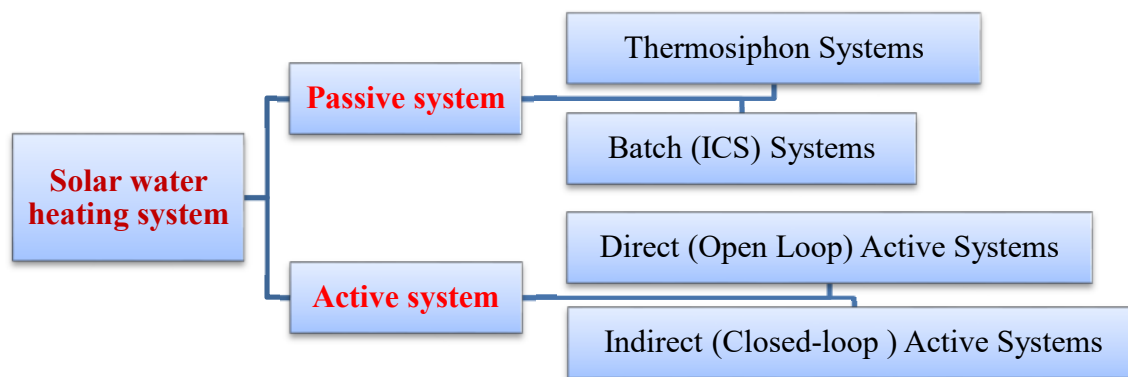


Figure 2.1 Classification of solar water heating system

1. Passive Systems

Passive systems move water or a heat-transfer fluid through the system without forced circulation and a storage tank located above the collectors. The systems have no electric components to

circulate a fluid. It is less costly and have extremely low or no maintenance, but the efficiency of a passive system is significantly lower than that of an active system. Two types of passive system:

- I. Thermosiphon Systems- Natural convection
- II. Batch Systems (Integral Collector Storage Systems)

2. Active Systems

Active systems use pumps, valves and controllers to circulate water or other heat-transfer fluids through the collectors. They are usually more expensive than passive systems but it more efficient. In Active systems, storage tanks can be situated lower than the collectors and can be hidden from view, reducing heat loss, superior efficiency, and uses increased control over the system. There are two common active systems are:

- I. Direct or Open Loop Active Systems
- II. Indirect or Closed-loop Active System

Direct System is the most common systems in use in tropical and sub-tropical climates. They use an electric pump to circulate water from the storage tank to the collector and back to the storage tank. Factors that influence the selection of a specific system type are depends on: - the amount of water that needs to be heated, relative cost and efficiency, simplicity of operation, and climate conditions. Depending on the above factors and considerations, direct active system is selected for analyzing of solar assisted water heating system. Active SWH systems are more reliable and affordable than passive that provides a financial benefits along with environmental sustainability.

2.2 Solar Thermal Energy Collectors

A solar collector is the special energy exchanger which converts solar irradiation energy to the thermal energy of the working fluid in solar thermal applications. The major component of any solar system is the solar collector which is a device which absorbs the incoming solar radiation, converts it into heat, and transfers this heat to a fluid (usually water) flowing through the collector. SWH systems typically utilize three different kinds of stationary collectors: -

- ❖ Flat plate collectors (FPCs)
- ❖ Evacuated tube collectors (ETCs) and
- ❖ Concentrating parabolic collectors (CPCs)

Table 2.1: Solar thermal collector type (Sarbu & Sebarchievi, 2015)

Stationary Solar Collector type	Absorber plate	Temperature range (°c)	Concentration Ratio
Flat plate collector (FPC)	Flat	30-80	1
Evacuated tube collector (ETC)	Flat	50-200	1
Concentrating parabolic collector (CPC)	Tubular	60-240	1-5

2.2.1 Flat-plate collectors (FPC)

FPCs are the most common collectors for water heating and also it is simple and effective means of collecting solar energy for applications that require heat temperatures up to 80 °c. The FPC is the heart of any solar energy collection system. The flat-plate collectors are characterized by their high efficiency compared with other types of collectors. For most residential and small commercial hot water applications, the solar FPC tends to be more cost effective due to their simple design, low cost, and relatively easier installation compared to other forms of hot water heating systems. Also, solar FPCs are more capable of delivering the necessary quantity of hot water at the required temperature. A typical FPC consists of an absorber, a header and riser tube arrangement or a single serpentine tube, a transparent cover, a frame, and insulation. They use both direct and diffuse solar radiations, do not require tracking of the Sun, and require little maintenance. (Rai, 2001).

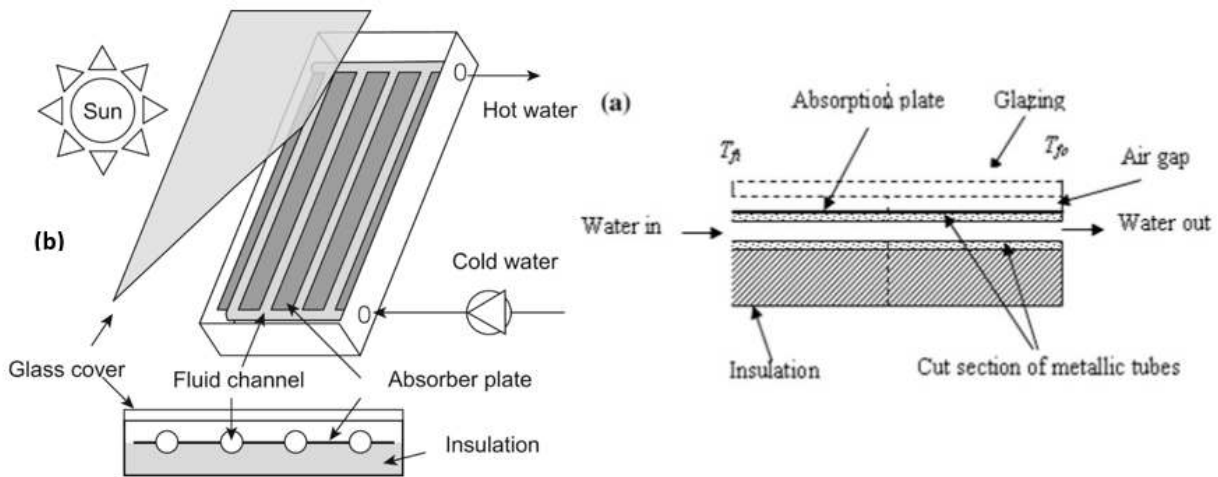


Figure 2.2 a) Side cross-section view of single glazed flat-plate collector. b) Components of glazed flat-plate collector (Kalogirou, 2014).

2.3 Thermal Energy Storage (TES) System

Today, the storage of energy in suitable forms can conventionally be converted into the required form is the popular technologies. TES systems are currently undergoing a revolution, vowing to their influential involvement in modern technology, and their extensive applications such as space heating, water heating, waste heat utilization, cooling and air conditioning. Energy storage is substantial, whenever there is a gap between the supply and consumption of energy. Solar thermal energy storage devices need heavier research attention due to irregular and unpredictable nature of solar energy which is quite efficient, economical and reliable energy resource. The goals of TES units are to obtain heat from renewable energy other than fossil fuels, increase the efficiency of heating appliances, and provide energy security. There are three methods for storing thermal energy, the first two being the most widely used in TES systems (Dincer & Rosen, 2007):

1. Sensible heat storage
2. Latent heat storage
3. Thermochemical storage.

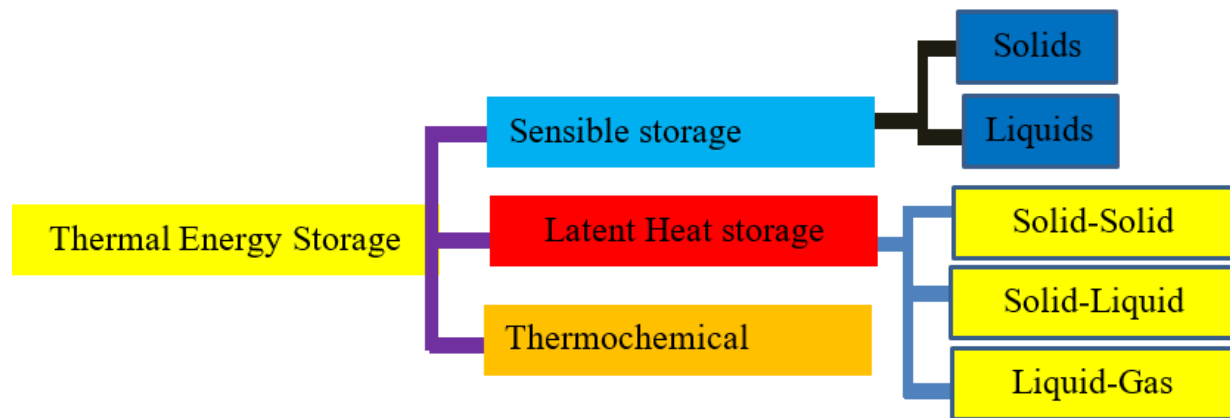


Figure 2.3. Classification of Thermal Energy Storage and processes

2.3.1 Sensible Heat Thermal Energy Storage (SHTES)

In SHS, thermal energy is stored by raising the temperature of a solid or liquid. The sensible heat storage is a system that uses heat capacity of a substance to store heat energy due to the temperature difference. It utilizes the heat capacity and the change in temperature of the storage medium during the process. The amount of heat stored depends on the specific heat of the medium, the temperature change, and the amount of storage material.

$$Q_{sensible} = \int_{T_1}^{T_2} m C_p dT \text{-----} 1.1$$

$$Q_{sensible} = m C_p \Delta T \text{-----} 1.2$$

Where, Q is sensible heat storage [kW], m is the flow rate of the storage substance [kg/s].

C_p is specific heat capacity [kJ/kg °c] and $\Delta T = T_2 - T_1$ is the difference in temperature [°c]

2.3.2 Latent Heat Thermal Energy Storage (LHTES)

The LHS systems offer high storage capacity as compared to sensible heat storage and also involve low heat losses. Phase change materials are latent heat storage materials. The thermal energy transfer occurs when a material changes from solid to liquid or liquid to solid. It is based on the heat absorption or release when a storage material undergoes a phase change from solid to liquid or to gas or vice-versa.

LHTES units are mostly used to store solar energy for high temperature application with simultaneously works. The storage capacity of the latent heat thermal energy storage (LHTES) system with a PCM medium is given by

$$Q = \int_{T_1}^{T_2} m c_{p,s} dT + m\Delta H_{pcm} + \int_{T_1}^{T_2} m c_{p,l} dT \text{-----} 1.3$$

$$Q = m [C_{sp} (T_2 - T_1) + \Delta H_{pcm} + C_{lp} (T_2 - T_1)] \text{-----} 1.4$$

Where, Q is the total amount of LHES [kW]; m is the mass of the material (kg); C_{sp} and C_{lp} are specific heat of the PCM in solid and liquid respectively [kJ/kg °c]; T_1 and T_2 are the initial and final temperature respectively (°c); ΔH_{pcm} is heat of fusion at the PCM temperature, T_m (°c).

Amongst above thermal heat storage techniques, LHTES is particularly attractive due to its ability to provide high-energy storage density and its characteristics to store heat at constant temperature corresponding to the phase transition temperature of phase change material (PCM). Latent heat storage can be accomplished through solid-liquid, liquid-gas, solid-gas, and solid-solid phase transformations (Rai, 2001)

In solid–solid transitions, heat is stored as the material is transformed from one crystalline to another. These transitions generally have small latent heat and small volume changes than solid–liquid transitions.

Solid–gas and liquid–gas transition through have higher latent heat of phase transition but their large volume changes on phase transition are associated with the containment problems and rule out their potential utility in thermal-storage systems. Large changes in volume make the system complex and impractical.

Solid–liquid transformations have comparatively smaller latent heat than liquid–gas. However, these transformations involve only a very small change in volume. This transitions have proved to be economically attractive for use in thermal energy storage systems. In addition, phase changes can take place at constant temperature and for many materials; the melting and freezing process can be repeated for an unlimited number of cycles with no change to the physical or chemical properties of the material by Garg et al., (2003).

2.4 Phase change materials (PCM)

Thermal energy storage systems based on phase change materials are considered to be an efficient alternative to sensible thermal storage systems. Furthermore, these systems have high energy density compared to sensible heat storage systems. The use of latent heat TES system with PCM has been receiving greater attention because of its large energy storage capacity and isothermal behavior during charging and discharging processes. Thermal energy storage increases by almost 2 to 3.5 times as compared to that what was stored without the use of PCM by Sharma et al., (2009). A PCM is a substance with a high heat of fusion which melting and solidifying at a certain temperature and capable of storing and releasing large amounts of energy. The PCM to be used in the design of thermal-storage systems require desirable thermo-physical, kinetics chemical and economical properties.

2.4.1 Classification Phase Change Materials (PCM)

The PCM may be grouped into three categories: organic, inorganic and eutectic which is a mixture of organic and inorganic materials.

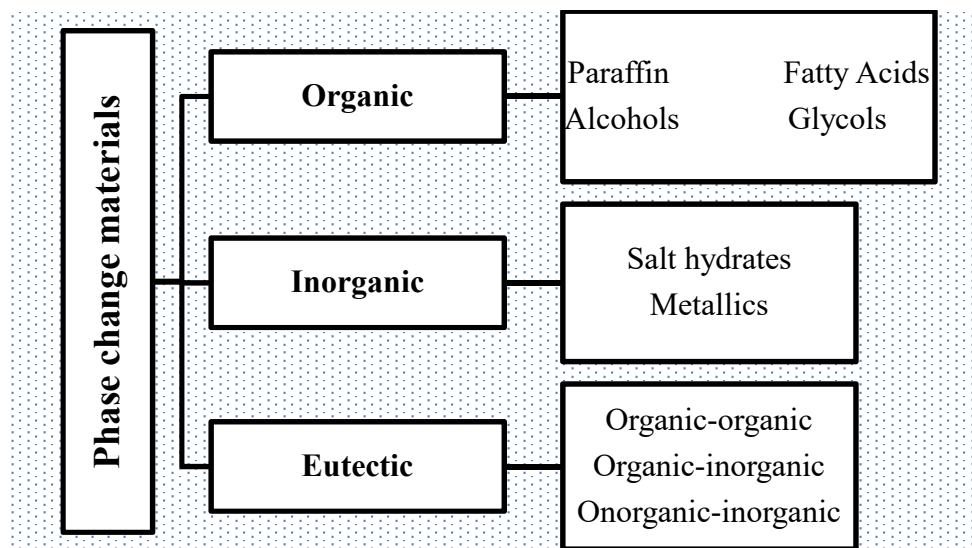


Figure 2.4 Classification of phase change materials (PCMs) from Sharma et al., (2009).

I. Organic PCMs

Organic latent heat storage materials are implemented in many domestic and commercial applications such as solar water heating. Organic materials have inherent characteristic of low thermal conductivity (0.1–0.35 W/m K), hence, a larger surface area is required to enhance the heat transfer rate. In addition, because of the low melting point of organic PCM, they have not yet been explored for high temperature applications. Organic materials are paraffin, non-paraffin, fatty acids, esters, alcohols, and glycols.

Paraffin: -Paraffins of type C_nH_{2n+2} are a group of saturated hydrocarbons with very similar properties, Paraffins between C_5 and C_{15} are liquids and the rest are waxy solids, Paraffin wax is one of the most popular organic heat storage PCM for commercial applications, it consists of a straight chain hydrocarbons having melting temperatures ranging between 23 °C and 67 °C. Paraffin is safe, reliable, predictable, less expensive and non-corrosive. They are chemically inert and stable below 500°C, show little volume changes on melting and have low vapor pressure in the melt form Sharma et al., (2009).

II. Inorganic PCMs

The inorganic LHS materials are grouped into two categories, namely, salt hydrates and metallic.

Salt hydrates: - have a tendency to segregate when they are dissolved with water and form an anhydrous salt. Due to density difference, unmixed salt hydrates settle down at the bottom of the container. They have melting temperature range from 15 °C to 117 °C (Sarbu & Sebarchievi, 2015). Lane and Shamsundar (2012) reported that the behavior of melted salt can be identified as congruent, incongruent and semi congruent. Congruent melting occurs when the anhydrous salt is completely soluble in its water of hydration at the melting point temperature. Else it represents incongruent melting. The most attractive properties of salt hydrates are: High latent heat of fusion, relatively high thermal conductivity as compared to other types of LHS materials and small volume change during phase change process.

Metallics: - can be either metal with low melting point temperature or metal eutectics. These metallics have not yet been seriously considered for PCM technology because of weight penalties. Major advantage of metallic LHS materials is its high thermal conductivity, approximately 20 W/m-K that substantially increases the heat transfer rate. However, only limited studies have been carried out on metallics due to low latent heat of fusion per unit weight.

2.4.2 Selection of Phase Change Materials

A suitable PCM with its melting point in the desired temperature range is one of the most important parameters in the design of a SDHW system using latent heat energy storage. A large range of PCMs is currently available that have melting temperatures ranging from -5 to 190 °C. Phase change materials intended for use in the design of thermal storage systems should possess suitable thermodynamic, kinetic and chemical properties as listed below by Sharma et al. (2009).

Desirable properties of PCMs: -

Thermodynamic properties	
<ul style="list-style-type: none"> ❖ A melting temperature is in the desired operating temperature range ❖ Large enthalpy of transition with respect to the volume of the storage unit ❖ High specific heat to provide for additional significant sensible heat storage ❖ Fixed and clearly determined phase change temperature (freeze/melt point) ❖ High density, so that a smaller container volume holds the material ❖ High latent heat of fusion per unit volume to store more energy in a given volume. ❖ High thermal conductivity to assist charging and discharging of energy. ❖ Small changes in volume during phase change and low vapor pressure to avoid containment problems. 	
Kinetics properties	
<ul style="list-style-type: none"> ✚ High nucleation rates to avoid super cooling of the liquid phase ✚ High rate of crystal growth, so the system can achieve rapid heat recovery from the storage system (Sufficient crystallization rates). 	
Chemical properties	
<ul style="list-style-type: none"> ➤ compatibility with the container ➤ Non-corrosiveness to construction material ➤ Long term sustained chemical stability ➤ Non-poisonous, Non-toxic, Non-flammable and no pollution ➤ Non explosive materials for safety 	
Economic properties	
Abundant resource	good recyclability
Low cost and availability	Friendly environmentally

PCMs, which can be used for such low-temperature solar thermal applications as water heating, baking, and drying, should have a melting temperature in the range of 45°C to 90°C. Depending upon the above desirable property of PCM and the selections of organic PCM (paraffin) are based on the thermodynamic, kinetic, chemical and economic properties. Almost all, paraffins with a melting temperature of around 60 °C have been proven as a good storage material for solar DHW systems, especially due to their melting point temperature, reliability, cost and non-corrosiveness (Hossain, 2011). The use of paraffin wax (n-Heptacosane) as phase changing material as better characteristics and performance improving compared to conventional sensible heat storage system.

2.5 Application of a PCM integrated into a SDHW storage Unit

An integrated PCM in solar DWHS and offer several advantages including high storage capacity, low storage volume, and isothermal operation during the charging and discharging phases. One of the main benefits of TES systems is their ability to store thermal energy in order for it to be applied for later use, either at the harvesting source or elsewhere. Some other benefits of TES are listed below (Dincer & Rosen, 2007):

- ✚ Energy storage reduces the mismatch between supply and demand
- ✚ Improves the performance and reliability of energy systems
- ✚ Affordable maintenance costs
- ✚ Enhanced efficiency in equipment usage
- ✚ Least emissions and free environmental pollution
- ✚ Reduced size of system components or space.
- ✚ Energy consumption and energy costs are reduced
- ✚ Leads to saving of premium fuels and makes the system more cost effective by reducing the wastage of energy and capital cost

2.6 Related work of Latent Heat Thermal Energy Storage for SWH system

2.6.1 International Relate work

Trp (2005) done an experimental and numerical investigation of transient heat transfer phenomenon during paraffin melting and solidification in a shell-and-tube LHTES unit, with the HTF circulating inside the tube and the PCM filling the shell side. A fully implicit 2D control volume FORTRAN computer code developed for simulation. For melting of PCM, the paraffin was initially in the solid phase at the ambient temperature. Inlet temperatures of the HTF varied from 318 to 328 K. Dimensionless geometric parameters of the system, as dimensionless length

L/D and dimensionless outer radius r_o/D have been 20–100 and 1.2–1.8, respectively. The results of numerical analysis reveals that the HTF velocity field reaches the fully developed condition quickly, and also provide guidelines for thermal performance and design optimization.

Mehling et al., (2009) developed an effective hot water system by adding a PCM module to the water tank. The hot water system is a cylindrical vertical tank that has a diameter of 20 cm and a height of 120 cm. The PCM module consists of a brass cylinder with a diameter of 10 cm and a height of 30 cm filled with PCM (6% of the total volume of the tank was PCM). Water at the top of the store was held warm above 55 °C for 50–200% longer and the average energy density was increased by 20–45% compared to the whole tank.

Fortunato et al., (2012) characterize the thermodynamics of a TES system based on the latent heat of a paraffinic PCM and the heat exchange between the heat transfer fluid and the PCM are investigated. The thermal storage system consists of a shell and tube heat exchanger with the HTF flows inside a tubes which are arranged in a regular pattern. Considering assumption and governing equation is derived in terms of enthalpy method for HTF, tube wall and PCM and are numerically solved by finite difference method (FDM) that implemented in MATLAB language. The simulations are conducted in order to derive the temperature profiles inside the PCM and to estimate the time needed to complete the melting of the PCM. It conclude that, the numerical modeled used as guidelines for thermal storage system analysis and processes.

Kibria et al., (2014): A numerical method based on the iteration of temperature and thermal resistance was investigated for the analysis of heat transfer between PCM and HTF in a shell and tube arrangement of thermal storage unit during charging cycles and also an experimental setup was built for validation. A PCM is paraffin wax and filled in the shell and HTF is water that passed inside the tube. For simulation, a numerical method has been discretized and MATLAB code used. The dimension of shell and tube thermal storage unit with length of the copper tube was 1 m long and the inner and outer diameters of the tube were 10.8 mm and 12.0 mm, respectively. The inner diameter of the shell was 36.0 mm. The thermophysical properties of water are 25 °C for solidification and 88 °C for melting used, and with a maximum flow rate capacity of 10 kg/h. a detailed parametric study are carried out with various mass flow rate, inlet HTF temperature and radii of the tube. The result of the study shows that the contribution of inlet T^o has much influence than flow rates in terms of storage operating time.

Murali et al., (2015) experimentally investigate the performance of a solar water heater incorporated with a TES tank with cylindrical PCM tank was conducted using a FPC as heat source, and the hourly based charging efficiency and thermal efficiency of the storage tank were calculated. Discharging without PCM took 1,110 minutes, while discharging with PCM took 1530 minutes. It clearly indicates that the PCM improves the performance of a solar hot water system as the discharging is prolonged by additional 420 minutes. So the incorporation of PCM cylinder improves the performance of the system. An experiment result reveals that the latent heat stored in 2.5 kg PCM improved the thermal efficiency of storage tank by 10 –16%. The results shows that the thermal performance of the PCM incorporation is significantly enhanced in relation to energy capacity, operation time under a temperature ranges.

Abhilash et al., (2016) the thermal energy storage systems incorporating PCMs for use in a solar water heater are investigated. Since the demand of hot water available is inversely proportional to the available of solar energy. Then, the system suggested incorporates PCM inside the water tank of solar water heater to store more heat that can be utilized further. Experimentally done with conventional solar water tank of capacity of 60 L of an evacuated type solar water heater was modified and a cylindrical PCM tank was fabricated holding a volume of 14 liters of PCM made up of steel. Compares the results obtained from both conventional and modified PCM filled storage tank in January 2016 at 8:30 AM and 26°C of ambient temperature. PCM box was filled with Paraffin C-32 as the PCM material which has a melting point of approximately 66 - 69°C. During charging the solar water heater for the case of without PCM, the water ran up to a temperature of more than 90°C in 105 minutes with that of PCM in 120 minutes; that is 15 minutes of time lag was found. He conclude that, incorporating the Paraffin used prolonged time to which hot water was available and the PCM holds the heat till night so as to make available hot water by solar water heater during night time also. In solar water heater an increase in time of 220 minutes was obtained with that of PCM to without PCM.

Kumar et al., (2016): Studied an investigation and analysis of thermal energy storage incorporating with and without PCM for use in solar water heaters. It used the storage unit utilizes cylindrical tubes made of copper and curved cylindrical tubes made of steel filled with paraffin wax as the heat storage medium and an experiment done focuses to maintain 60 liters of water at a temperature of around 70 °C during the day time with a flow rate of 5 ml/sec through a FPC. The melting point of Paraffin is 56 °C. The PCM with in the Copper tube is more effective than the steel tube. The

work is done with 770 gram of PCM. If the amount of PCM increases, the performance also increased. It was found that by the application of PCM the hot water availability can be extended up to 4 hours than the normal condition.

(Agbanigo, 2017) Experimental studied an impact of PCM on performance of solar water heating systems. The experimental set up consists of two insulated flat plate solar collectors 2.13 m, 1.09 m and 0.1m, length, breadth and depth respectively, inclined at 17.5° to the horizontal and latitude 7.5° north and two 0.225 m^3 capacity hot water storage tanks. The water storage tanks were insulated with fiber glass wool and covered with aluminum foil. Experiment show higher daily maximum water temperatures for system with PCM compared with the other without PCM. Average minimum water temperatures in the early hours of the day between 6 – 8 AM were 57.8°C and 46.5°C for system with and without PCM respectively. It concluded that the systems with PCM had higher hot water discharge capacity, with higher demand which would enable use of low cost electricity and thermal energy storage capacity was increased, and could result in reduction in size of hot water tank.

(Liang, et al., 2017): Experimental study on TES performance of water tank with PCMs in Solar Heating System. The WS-PCM-TES is composed of 72 phase change heat storage units, stainless steel fixed support and square heat preservation water tank. The dimensions of the phase change heat storage unit is diameter 50 mm and length is 450 mm. Each unit consumes 0.367 kg of stainless steel and the volume is 0.883 L. The PCMs is encapsulated in a molten state, and a certain volume is reserved to accommodate the volume change before and after the phase transition. Thus, 0.685 kg of PCMs can be encapsulated in single unit, the total mass is 49.32 kg. It was concluded that increasing the heat storage density of the energy storage water tank can increase the heat storage capacity and the heat storage efficiency of the same volume WS-PCM-TES.

Mehrdad et al., (2018) studied a comprehensive evaluation of an SDHW system was carried out in terms of three types of effective parameters, including the system characteristics, the hot water demand profile, and the integration of PCMs. According to the results, in the non-uniform high daily water consumption the thermal stratification is more beneficial which can lead to 9% increase in the annual solar fraction (ASF) and it is found out that a solar water heater system performance is very demand dependent so that it induces up to 8% ASF variation in different demand conditions. So, integration of the PCM in SDHW systems can increase the ASF by 4%.

2.6.2 Local Related work

Bekele (2007): has numerically investigated the solar water heating system for hospital by using FORTRAN package in simulation the transient performance of the system. Among the selected sites for study, the results model of the Jimma hospital was a total daily hot water consumption of 119.24 m^3 , a total of 795 collectors with four storage tanks of each capacity 24.8 m^3 are needed with initial capital cost of 3,216.77 Birr per collector, which will cost a total of 4,205.00 Birr per collector throughout its lifetime and the life cycle cost saving will be 6,197.00 Birr per collector. Since the unit cost of solar energy is less than the unit cost of fossil fuel, the large-scale water heating by solar energy is a viable alternative to heating by fossil fuel.

Kebede (2016) worked on design and analyses solar thermal system for hot water supply to health centres. Designing of the selected solar collector and the heat storage based on the amount of hot water supplied to the hospital throughout the day and the energy needed to heat the demanded hot water. Used Implicit FDM scheme to solve derived equation of a system and performance transient analysis in FPC. It found that the total daily HWD of 30.475 m^3 , a total of 108 collectors with two storage tanks of each capacity 18.3 m^3 are needed. The result shows that, the unit cost of solar energy is less than cost of fossil fuel, and the water heating by solar energy is a viable alternative.

Solomon (2018): studied solar thermal energy as alternatives to energy sources for public Hospitals. Used a MATLAB package for performance evaluation of the system and to compute the numerical heat transfer model and derived an equation of the system by FDM. Uses a U-type ETC system as a heat source with a storage tank. It was found that the daily hot water demand for hospitals was estimated to be 30.022 m^3 per day. The study reveals that ETC would meet the hot water demand is around 52 number of a collector on holding space 82.46 m^2 with two storage capacity each have 15.011 m^3 . Economic analysis shows that investment cost 1,066,388.44 Birr with LCC 2,003,254.14 Birr and a payback period of 5 years and 6 months.

Endale (2019) examines the potential and significance of SWH system to alleviate the challenges of unmet electricity demand, imported oils dependency and unsustainable supply of firewood in Ethiopia. The economic potential saving of these energy sources in future through solar water heaters (SWHs) is estimated. Water heating energy demand of the three major sectors of household, commercial and industrial are analyzed. It concludes that, further study is needed to

estimate the technical and economic potential of SWHs for industrial applications in Ethiopia. The current utilization of SWHs in Ethiopia is insignificant still now.

The above literature review shows many vigorous areas for future study work. To fulfil the HWD for a hospital, the solar energy source is proposed. The study have made a large effort to investigate integration techniques between SWH system and PCM units. As more reviews a literatures, further research is necessary to incorporate the update technologies of PCM units into SDHW systems. Since the PCM unit in a SDHW system substantially escalations the capacity of energy storage in comparison to the sensible SDHW system. TES is a key issue to be addressed the intermittence of solar energy and balances the demand and supply of energy consumption. Solar TES with PCM have a higher energy storage density and energy storage at constant temperature. So, incorporating a solar assisted water heating system with latent heat TES with PCM has a higher enhancement advantages in modern technology.

CHAPTER 3

3. Hot Water and Steam Demand of AHMC

Averagely health centers require approximately 160 liters per day for every occupant. Without enough hot water, a hospital could become dangerous and it is hard to clean without proper hot water. For a large hospital, this amount of water is very substantial. At peak demand rates, each occupant requires on average 50 liters per hour (Christopher & Homola, 2010). In addition to hot water consumption, at certain times of the year the hospital must either be heated or cooled to maintain proper comfort levels for occupants. So, the hot water is the primary requirement things in health services for different appliance. Beforehand, the Adama hospital uses fuel as sources of energy for water heating to meet daily hot water demand.

3.1 Data collected from Adama Hospital Medical College

In developing countries such as Ethiopia, due to lack of measuring instruments and misinformation about hospital hot water system, reliable data of the hospital is not found. In the absence and scarcity of reliable hot water system of the hospital data, assumption and estimation are made based on the standard hot water delivery system of hospital.

Table 3.1. Collected data of Adama Hospital Medical College.

Appliance	Quantity	No of Rooms	Person per Room	Occupancy	Energy source
Shower	Patient	115	4	95%	Fuels and electric power
	Public	31	15	100%	
	Medical Staff	5	15	85%	
Laundry	3	1	10	100%	
Kitchen	1	1	12	100%	

3.2 Hot water consumption of the Hospital

The hot water demand is significant for the sizing or dimensioning of a domestic hot water solar (DHWS) system.

Table 3.2. Standard Hot Water Demand for Hospital (Brochure, 2015)

	Standard Hot Water Demand for Different appliance			
Demand	Kitchen	Shower	Laundry	Restaurant
Hot water	320 l/kitchen/day	60 l/person/day	530 l/laundry/day	160 l/restaurant/day
Temperature	48 °C	43 °C	48 °C	60 °C

For this study determination of the hospital hot water demand per day is performed by make assumptions. Depending on Ethiopian condition it is good to assume that the daily hot water requirement for shower will be determined by multiplying the developed countries hot water requirement for shower by the ratio 3:4 (Brochure, 2015).

Table 3.3. Hot Water Demand for each Appliance of the Hospital

Demand	Appliance of the Hospital		
	Kitchen	Shower	Laundry
Hot water (lit/ L/person)	320 L/person	45 L/person	530 L/person
Temperature (⁰c)	50	44	60
Energy source	Fuels + electric	Fuels + electric	Fuels + electric

Adama Hospital Medical College is found in East Showa at Adama city, sited at latitude 39.28°N and longitude 8.54 °E. Determination of hot water demand of the hospital for different appliance is done by considering only hot water needs of Adama hospital Medical College.

Load of hot water demand for Hospital is calculated as the following:

The hot water consumption (HWD) for each appliance is given by:

$$C = N_{rooms} * Q_{appl} \text{-----} 3.1$$

Hot water demand for showering service is given by:

$$C_{Sh} = N_{rooms} * \frac{person}{Room} * Q_{app} * O_{rate} \text{-----} 3.2$$

Note; public shower, all patients room and medical staff rooms have a shower. So, daily hot water demand needed for shower are the summation of hot water demand spent for each rooms.

Total daily hot water demand of the hospitals is determined as: -

$$C_T = C_{Sh} + C_L + C_k + C_R \text{-----} 3.3$$

Where, C -Hot water consumption (HWD)

N_{rooms} -Number of rooms

C_L - Hot water demand for Laundry

Q_{app} -hot water appliance

C_R - Hot water demand for Restaurant

O_{rate} - Occupancy rate (%)

C_T - Total daily Hot water consumption for

C_{Sh} - Hot water demand for shower

hospital

C_k - Hot water demand for kitchen

The daily and weekly hot water consumption of the hospital can be increase or decrease from the calculated value, to compensate the inaccuracy created it can be multiplied by factor 1.25. The

factor is one fourth of the total calculated daily and weekly hot water demand of the hospital (Christopher & Homola, 2010).

$$C_{T, supplied} = 1.25 * C_T \text{-----} 3.4$$

Generally, the total hot water requirement for each appliance are tabulated as the following. The above equation (3.1 to 3.4) used to solve daily demand per appliance.

Table 3.4. Hot water demand of the Adama Hospital medical college per Services

Consumption	Services				C_T
	C_k	C_L	C_{Sh}	C_R	
hot water demand (Lt/day)	640	1590	33,626.25	0	35,856.25
HW Demand * 1.25 (Lt/day)	800	1987.5	42032.8	0	44820.3125

3.3 Hot Water Consumption Pattern

Totally, daily hot water requirement for Adama hospital medical college will be 44,820 Liter per day. This daily hot water consumption can be distributed as 35 % in the morning, 25% at the mid-day, 32% in the evening and 8% will be distributed over the day time.

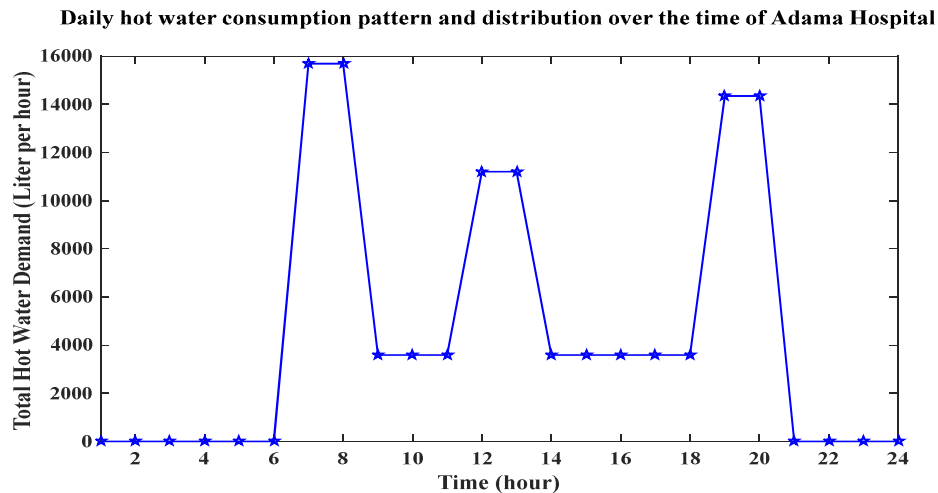


Figure 3.1 Daily Hot Water consumption pattern and distribution over the time of the day of Adama Hospital.

Hot water consumption pattern of the AHMC indicated that hot water requirement of the hospital reaches maximum demand at the morning and afternoon time of the day and the minimum demand is at mid-day time of the day.

3.4 Hot Water Storage Tank Capacity

When the daily hot water demand has been determined, the volume of the storage tank can be specified easily. It should be some 0.8 to 1.2 fold the daily demand for regions with high solar radiation (Brochure, 2015). So that consumption peaks can be met well and cloudy days can be compensated (Homola & Christopher, 2010). So, for total daily hot water demand, the volume of the storage tank required is 54 m³. As the manufacturers do not offer tanks in every possible size as you got the final result by theoretical calculation, the choice has to be made among those generally available on the market. It is recommended that the storage tank capacity is not less than 90% and not more than 120% of the calculated volume (Homola & Christopher, 2010).

3.5 Boiler-Conventional Steam Generation

Conventional steam generation is an equipment, where fuel burns and heat is transferred from fuel gas to energy transfer medium (water), which is heated up or phase change happens (boiling) and used to generate steam. Steam generation is the process of turning water into steam by application of heat and burning a fuel. A boiler used for heat demands which required for several purposes and generate steam for heating water, laundry (washing and drying a clothes), kitchen, auto clave, and other purposes. However, the heat demand characterized according to temperature demand and load demand. In this system, steam is used as heat transfer medium with temperature from ambient to 100°C. Conventional steam generation system or boiler has the following components such as feed water tank, boiler, water treatment and softener, pump and accessories.



Figure 3.2. Installed diesel fuel steam generation of AHMC new building

Feed water tank: Supplies treated water for boiler and regulated by automatic valves with the steam demand. The steam generated would be distribute via steam pipelines to the different

consumes and loads. The types of installed steam generation boiler for hospital is fire tube boiler; feed water converted to steam in the shell side and hot flue gas passes through the tubes.

The Boiler specification used in Adama Hospital Medical College.

Rated evaporation output:	2 ton/h (0.56 kg/s)
Feed water temperature:	20 °C (293 K)
Rated steam temperature	184 °C (457 K)
Rated working pressure	1 Mpa
Heat efficiency	90%

Water treatment: - proper treatment makeup and feed water is necessary before enter to boiler to prevent fouling, corrosion in boiler and provide required steam cleanliness. According to the manufacturer, the boiler has an energy efficiency of 85%. Among the total processes happen in hospitals used almost all of them consume hot water.

Fuel consumption and Steam Demand Cost of Boiler

Enthalpy of heat water and steam at a specification pressure and temperature are

$h_s @ 1\text{MPa} = 2000.6 \text{ kJ/kg}$ and $h_{fw} @ 20^\circ\text{C} = 83.94 \text{ kJ/kg}$ (From steam table).

The heat value of a fuel is the amount of heat released during its combustion and is expressed in energy (J) per specified amount (kg). For diesel fuel heating value range is between 42 to 46 MJ/kg and (GCV = 45 MJ/kg selected). Then, the heat required to the feed water at 20°C raise 2 ton/h of rated evaporation output at 1MPa and 184°C is calculated as the following equation. $h_s @ 1\text{MPa} = 2000.6 \text{ kJ/kg}$ and $h_{fw} @ 20^\circ\text{C} = 83.94 \text{ kJ/kg}$. In a case of steam generator useful heat can be calculated as:-

$$\text{Heat required, } Q_{useful} = m_s(h_s - h_{fw}) = 2000 \frac{\text{kg}}{\text{hr}} * (2000.6 - 83.94) \frac{\text{kJ}}{\text{kg}} = 3833.3 \frac{\text{MJ}}{\text{hr}}$$

From the result, the power required to raise a feed water to steam is 1064.8 kWh

$$\text{Fuel quantity; } m_{fc} = \frac{Q_{useful}}{\eta_b \times \text{GCV}} = \frac{m_s (h_s - h_{fw})}{\eta_b \times \text{GCV}} = \frac{3833.32 \frac{\text{MJ}}{\text{hr}}}{0.85 \times 45,000 \text{ KJ/kg}} = 100.22 \frac{\text{kg}}{\text{hr}}$$

Hence, $100.22 \frac{\text{kg}}{\text{hr}}$ quantity of diesel is required to produce the 2 ton/h of the steam.

Daily oil Tank: -The standby daily oil tank installed to store backup diesel for hospital has the following specification; specific volume is 2000 liter and mass is 645 kg. The boiler uses the daily fuel consumption is around 85 L/day and the cost of this amount of diesel cost is 1,583.55 ETB.

Fuel unit cost

1 liter or 0.85 kg diesel fuel cost is 19.63 birr on a market cost and heating value of diesel fuel is 38.7 MJ (1 liter = 38.7 MJ).

Then, *Unit price of fuel* = $\frac{19.63 \text{ Birr}}{38700 \text{ kJ}} = 4.82 * 10^{-4} \frac{\text{Birr}}{\text{kJ}} = 1.72 \frac{\text{Birr}}{\text{kWh}}$. This indicates that the fuel cost is higher than the cost of electricity. The hospital expenses more costs for fuels also. An average fuel consumption of diesel used to produce a steam is 100.22 kg/hr.

$$\text{Average fuel cost} = \frac{\text{Avg fuel consumption}}{\text{hr}}$$

For the required fuel consumption, the average fuel cost is (*Average fuel cost* = $432.76 \frac{\text{Birr}}{\text{hr}}$).

So, the results indicates that among the total operational cost of the hospital, the amount of cost for fuel paid was 68%. The total cost paid for fuel was about 60,800.00 ETB and from this values approximately 39,397.5 ETB was paid for steam generating fuel. In conclusion, from the results the hospitals pay more money for diesel and electric power. Besides, the hospitals uses four diesel generator as energy source. So, by considering such a problems and other related to this cost, saving time, and performance; the solar thermal system is proposed to the hospitals as alternatives energy sources.

CHAPTER 4

4. Performance Analysis of Solar Flat Plate Collector for SWH

A flat plate solar collector is a core of solar system and required to produce hot water that satisfies the HWD for Adama Hospital Medical College. To estimate a number of solar FPC for the hospital; the solar potential of Adama in a year, transient performance of the single FPC and solar thermal energy storage for supplying hot water for 24 hour function are discussed.

4.1 Estimation of Available Solar Radiation

Solar energy is available in all around the world, especial in tropical zone. Its intensity varies significantly according the place on the earth's surface and for the same place according to the time and the existing meteorological conditions. As a very important renewable energy source, solar radiation parameters and solar-earth angles are most importance factors for the estimation of the energy reaching the earth's surface. Developing country like Ethiopia which has 12 month of sun shined, solar thermal system which is environmental friendly and sustainable source of energy is the best alternative of energy consuming. Ethiopia has an annual mean average solar radiation of about 5.2 kWh/m², and the range of 4 – 6 kWh/m² with average sun light length of more than 10 hours per day throughout the year and has high potential of solar irradiation (UNCC, 2002).

4.1.1 Estimation of global solar radiation using sunshine duration

To estimate solar radiation the data like geographical coordinate of site, sunshine hours and weather condition is the most important and prior requirements. Simply, Sunshine duration is the length of time that the ground surface is irradiated by direct solar radiation and used to characterize the climate of sites. Geographical coordinates of Adama station: -Latitude (ϕ) = 8 33' 23.8'' N = 8.558°; Longitude = 39 17' 2.5'' E = 39.28°; Altitude = 1648 m above sea level. Thus, shows that climate of the city is dominated by hot climate type.

Table 4.1 Sunshine hourly duration for five years (source; East Shoa Meteorology)

Months	Jan	Feb	Mar	Apr	May	Jun	Jul	Aug	Sep	Oct	Nov	Dec
2013	8.9	10.05	8.4	8.12	8.35	7.89	5.3	6.8	7.7	8.3	8.78	10.10
2014	9.46	8.7	8.6	9.0	8.6	8.6	6.4	6.9	6.6	8.7	9.1	8.85
2015	9.7	10.1	9.5	8.7	8.8	7.5	9.3	8.0	8.3	9.0	9.07	8.8
2016	7.7	8.5	9.3	6.7	7.6	7.8	6.4	6.7	7.2	9.8	10.05	9.7
2017	7.9	8.9	9.2	9.5	7.8	8	6.6	5.9	6.8	8.7	9.9	9.4

Table 4.2. Estimation of five years average sunshine hour duration.

Months	Jan	Feb	Mar	Apr	May	Jun	Jul	Aug	Sep	Oct	Nov	Dec
Avg (2012-2017)	8.73	9.25	9.0	8.4	8.23	7.96	6.8	6.86	7.32	8.9	9.38	9.35

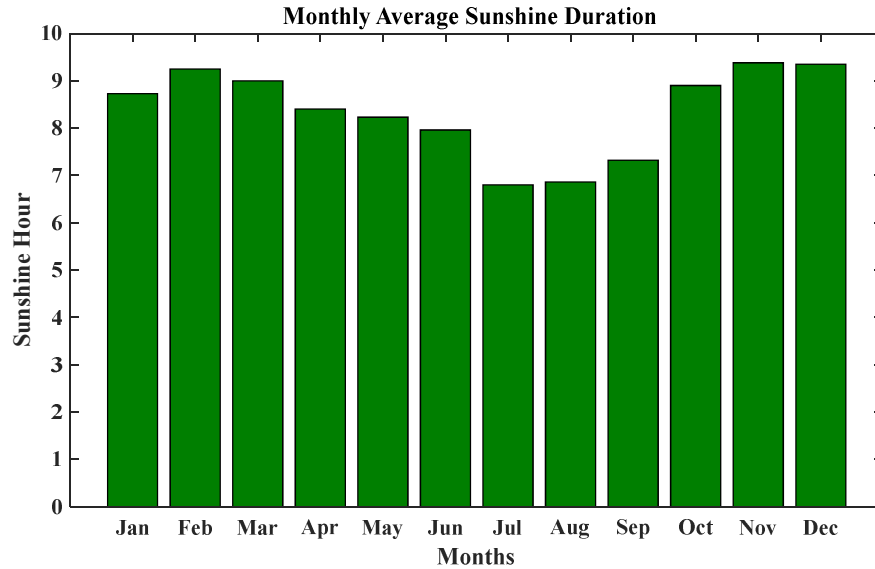


Figure 4.1 Monthly averagely sunshine duration for each months of Adama

4.1.2 Preliminary Terminology and sign conventions for estimation solar radiation

I. Solar Time

Time based on the apparent angular motion of the sun across the sky with solar noon the time the sun crosses the meridian of the observer. Solar time is the time used in all of the sun-angle relationships. So, it is necessary to convert standard time to solar time by applying the equation of time which takes into account the perturbations in the earth’s rate of rotation which affect the time the sun crosses the observer’s meridian.

$$Solar\ time - standard\ time = 4(L_{st} - L_{loc}) + E \text{-----} 4.1$$

Where, L_{st} -is the standard meridian for the local time zone; L_{loc} -is the longitude of the location in question, and longitudes are in (°) West, that is, $0^\circ < L < 360^\circ$.

The parameter E is the equation of time (min) and sited (Kalogirou, 2014).

$$E = 9.87 \sin(2B) - 7.53 \cos(B) - 1.5 \sin(B) [min] \text{-----} 4.2$$

$$B = (N - 81) \frac{360}{365} \text{-----} 4.3$$

Where, N is day of the year, $1 \leq N \leq 365$

II. **Declination angle:** -the angular position of the sun at solar noon with respect to the plane of the equator, north positive ($-23.45^\circ \leq \delta \leq 23.45^\circ$). The declination angle in degrees for

any day of the year (N) can be calculated by the equation (Duffie & Beckman, Solar engineering of thermal processes, 2013):

$$\delta = 23.45 \sin\left[\frac{360}{365} * (284 + N)\right] \text{-----} 4.4$$

III. **Solar Hour angle (ω):** -is the angular displacement of the sun east or west of the local meridian due to rotation of the earth on its axis at 15° per hour (morning negative and afternoon positive) and cited from (Duffie & Beckman, 2013): -

$$\omega = 15 * (\text{solar time} - 12) \text{-----} 4.5$$

IV. Sunrise and sunset times and day length

The sun is said to rise and set when the solar altitude angle (α) is zero. So, the hour angle at sunset, h_{ss} , can be found by (Kalogirou, 2014): -

$$h_{ss} = \cos^{-1}(-\tan\delta * \tan\varphi) \text{-----} 4.6$$

Where, h_{ss} is taken as positive for sunset

Meanwhile, the hour angle at local solar noon is zero, with each 15° of longitude equivalent to 1hr, the sunrise (H_{sr}) and sunset (H_{ss}) time in hours from local solar noon is then given as:

$$H_{ss} = 12 + \frac{1}{15} * \cos^{-1}(-\tan\delta * \tan\varphi) \text{-----} 4.7$$

$$H_{sr} = 12 - \frac{1}{15} * \cos^{-1}(-\tan\delta * \tan\varphi) \text{-----} 4.8$$

The length of sun shine hours (N_s) are computed from: -

$$N_s = \frac{2}{15} h_{ss} \text{-----} 4.9$$

V. **Collector Tilt:** -The tilt of a collector is the angle between the collector and the local horizontal. In most solar water heating applications, a tilt of approximately latitude plus 10° to 15° is near optimum (Duffie & Beckman, Solar Engineering of Thermal Processes, 2013). Slope, $\beta = \varphi + (10^\circ \text{ to } 15^\circ)$

For Adama latitude = 8.54; the slope of the collector is: $-\beta = \varphi + 12.5^\circ = 8.54^\circ + 14^\circ = 22^\circ$

4.1.3 Estimation of Hourly Solar Radiation on a Horizontal Surfaces (HS)

4.1.3.1 Extraterrestrial (ETR) daily Solar Radiation on a Horizontal Surface

At any point in time, the solar radiation incident on a horizontal plane outside of the atmosphere is the normal incident solar radiation as given by Klein relationship Equation: -

$$\bar{H}_0 = \frac{24 * 3600}{\pi} I_{sc} \left(1 + 0.033 \cos\left(\frac{360n}{365}\right)\right) * (\cos\varphi \cos\delta \cos\omega_s + \frac{\pi}{180} \omega_s \sin\delta \sin\varphi) \text{-----} 4.10$$

Where, ω_s = sunrise hour angle

$$\bar{H}_0 \text{ - in Wh/m}^2$$

$$I_{sc} = G_{sc} = 1367 \text{ W / m}^2 \text{ (Solar constant)}$$

n = average days for the month or the day of the year under consideration (1 to 365).

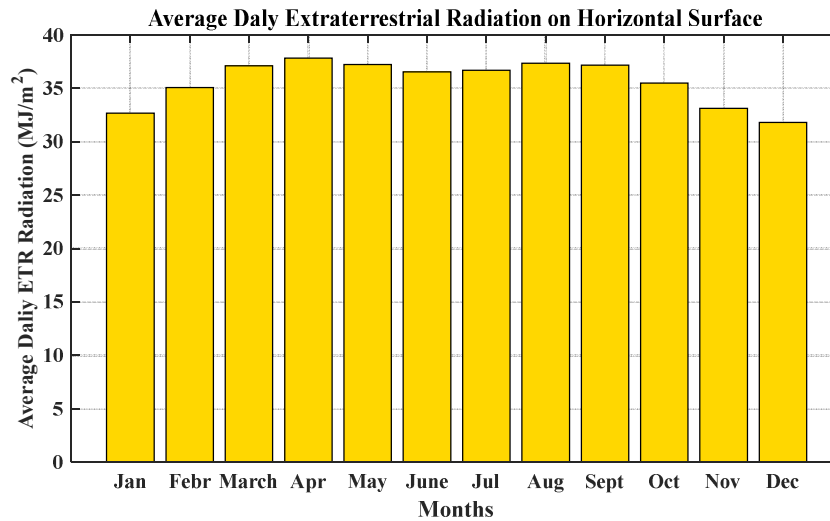


Figure 4.2 The solar radiation incident on a horizontal plane outside of the atmosphere (Extraterrestrial (ETR) daily Solar Radiation)

4.1.3.2 Prediction of Monthly Average Daily Global Radiation on a HS (\bar{H})

The first empirical correlation using the idea of employing sunshine hours for the estimation of global solar radiation was proposed by Angstrom. The Angstrom correlation was modified by Prescott and Page. The simplest model used to estimate monthly average daily solar radiation on horizontal surface is the well-known Angstrom equation.

$$\frac{\bar{H}}{\bar{H}_0} = a + b \left(\frac{\bar{n}_s}{\bar{N}_s} \right) \text{-----} 4.11$$

Where, \bar{H} = monthly average daily radiation on horizontal surface (Global radiation).

\bar{H}_0 = Monthly average radiation outside of the atmosphere (extraterrestrial, ETR on the horizontal surface) for the same location (w/m^2)

a, b – empirical constants.

\bar{n}_s - Monthly average daily hours of bright sunshine (sunshine hour).

\bar{N}_s - Monthly average of the maximum possible daily hours of bright sunshine.

The regression parameters a and b can be determined from; -

$$a = -0.11 + 0.235 \cos \varphi + 0.323 \left(\frac{\bar{n}_s}{\bar{N}_s} \right) \text{-----} 4.11a$$

$$b = 1.449 - 0.533 \cos \varphi - 0.694 \left(\frac{\bar{n}_s}{\bar{N}_s} \right) \text{-----} 4.11b$$

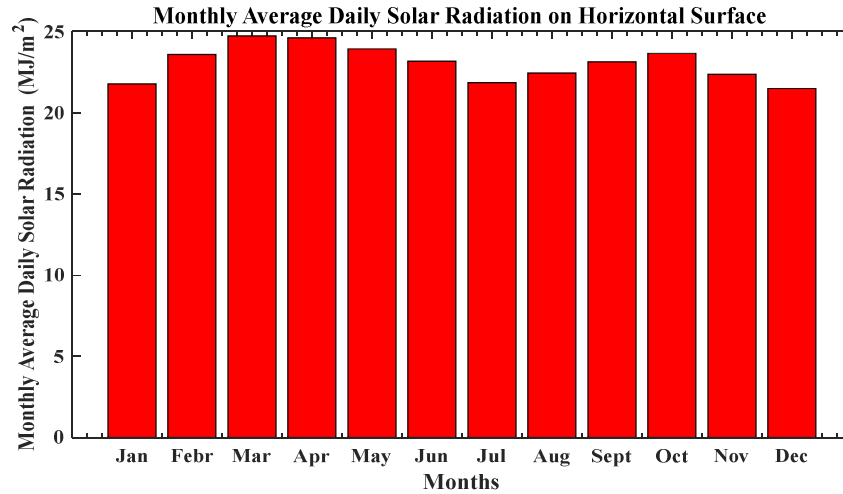


Figure 4.3 Graph of Monthly Average Daily Global Radiation on a Horizontal Surface

4.1.3.3 Prediction of Monthly Average Daily Diffuse Radiation on HS (\bar{H}_d)

The monthly average daily diffuse radiation on a horizontal surface can be determined from the monthly average daily global radiation on a horizontal surface and the number of bright sunshine hours by Dincer et al., (2007).

$$\frac{\bar{H}_d}{\bar{H}} = 0.931 + 0.814 \left(\frac{\bar{n}_s}{\bar{N}_s} \right) \text{-----} 4.12$$

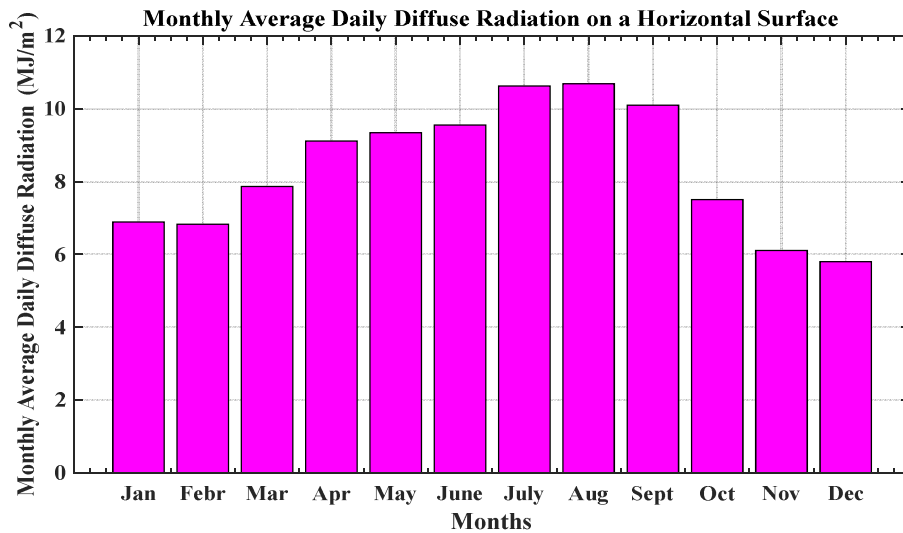


Figure 4.4 Graph of Monthly Average Daily Diffuse Radiation on a Horizontal Surface

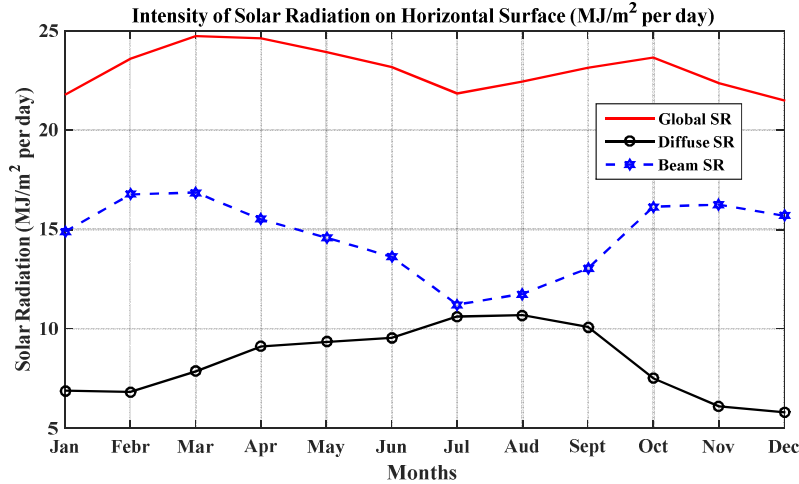


Figure 4.5 Graph of Monthly average daily global, diffuse and beam of solar radiation.

4.1.3.4 Prediction of Monthly Average Hourly Global Radiation on a HS (*I*)

The monthly average hourly global radiation on a horizontal surface can be calculated from the knowledge of the monthly average daily global radiation on a horizontal surface, Dincer et al., (2007). The total hourly solar radiation falling on a horizontal surface, *I* in W.h/m², could be estimated from the daily global radiation, *H* (in kJ/m² per day) in accordance with (Duffie & Beckman, Solar Engineering of Thermal Processes, 2013).

$$\frac{\bar{I}}{H} = \frac{\pi}{24} (a + b \cos \omega) \frac{\cos \omega - \cos \omega_s}{\sin \omega_s - \frac{\pi}{180} \omega_s \cos \omega_s} \tag{4.13}$$

$$a = 0.409 + 0.5016 \sin (\omega_s - 60) \tag{4.13a}$$

$$b = 0.6609 - 0.4767 \sin (\omega_s - 60) \tag{4.13b}$$

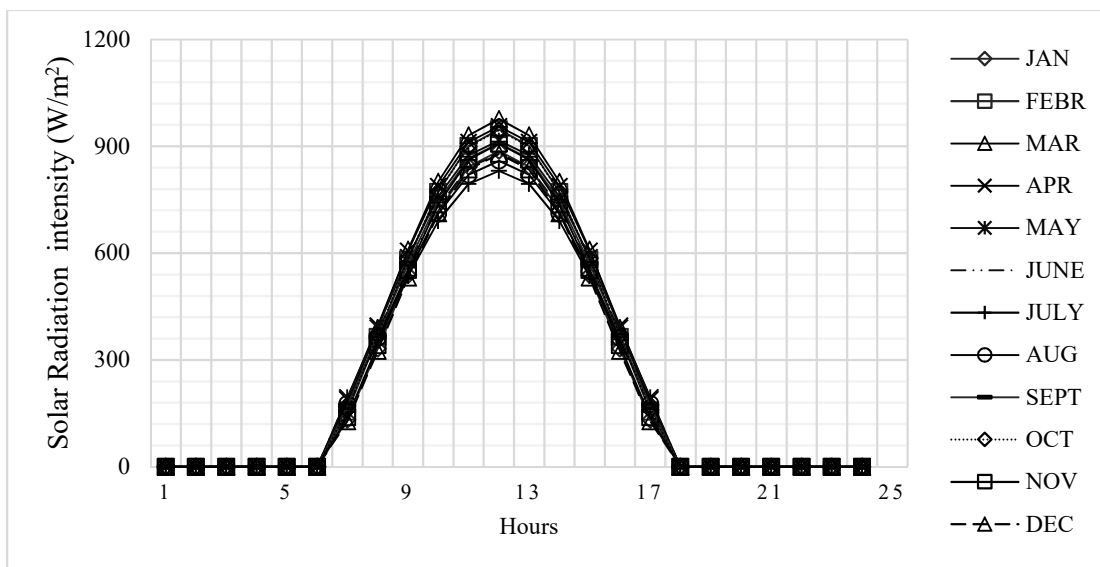


Figure 4.6 Monthly average hourly global radiation on a horizontal surface (Wh/m²) at Adama

4.1.3.5 Prediction of Monthly Average Hourly Diffuse Radiation on a HS

The hourly values of the diffuse solar radiation can be estimated from the equation 4.13.

$$\frac{\bar{I}_d}{\bar{H}_d} = \frac{\pi}{24} \frac{\cos \omega - \cos \omega_s}{\sin \omega_s - \frac{\pi}{180} \omega_s \cos \omega_s} \quad \text{----- 4.14}$$

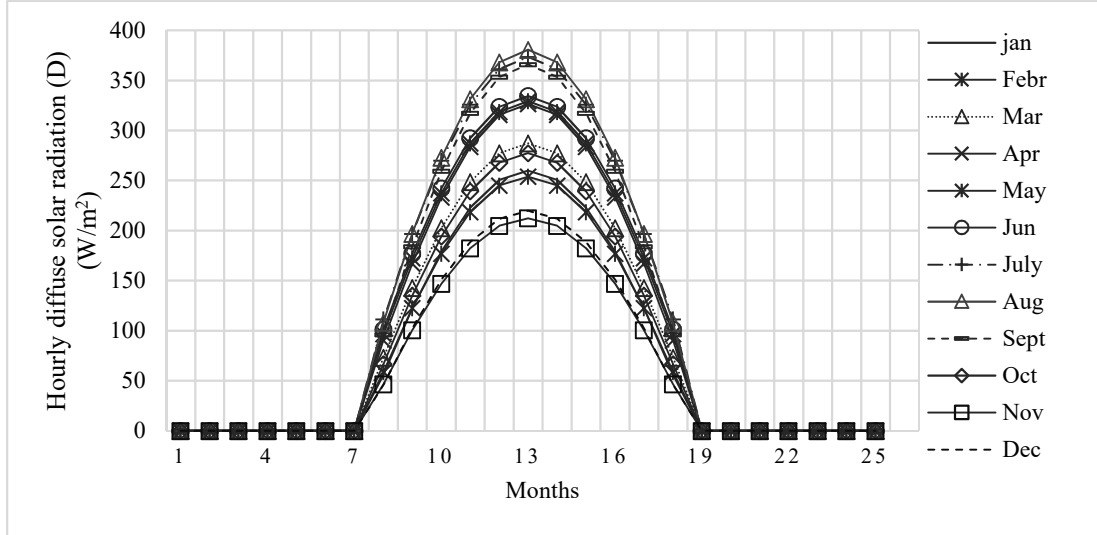


Figure 4.7 Monthly average hourly diffuse solar radiation on horizontal surface (W/m²)

The direct (beam) component of the solar radiation on a horizontal surface is then obtained from:

$$G_b = G - G_d \quad \text{----- 4.15}$$

4.1.4 Estimation of Hourly Solar Flux on Inclined Surfaces

Usually, collectors are not installed horizontally but at an angle to increase the amount of radiation intercepted and reduce reflection and cosine losses. So, system designers need data about solar radiation on such tilted surface. The amount of insolation on terrestrial surface at a given location for a given time depends on the orientation and slope of the surface.

A flat surface absorbs beam (G_{Bt}), diffuse (G_{Dt}) and ground reflected (G_{Gt}) solar radiation and global radiation on tilt surface (G_t) given as: -

$$G_t = G_{Bt} + G_{Dt} + G_{Gt} \quad \text{----- 4.16}$$

General form of total hourly solar radiation energy incident on an inclined surface G_t given by:

$$G_t = G_b R_b + G_d \left(\frac{1 + \cos \beta}{2} \right) + (G_b + G_d) \rho \left(\frac{1 - \cos \beta}{2} \right) \quad \text{----- 4.17}$$

Where, G_t - total hourly irradiance on a tilted surface (w/m²); G_b - Hourly beam irradiance; G_d - Hourly diffuse irradiance

R_b - The ratio of beam radiation on the tilted surface to that on a horizontal surface

$$R_b = \frac{I_{bT}}{I_{bM}} = \frac{I_b \cos \theta}{I_b \cos \theta_z} \text{ (Beam radiation factor)}$$

β – Surface slope angle and ρ – Reflectivity (0.2 for bare earth and 0.7 for snow)

θ_z - is the solar zenith angle

Angle of incidence is angle b/n the beam radiation on a surface and the line normal to surface: -

$$\cos\theta_i = \cos\varphi\cos\beta + \sin\varphi\sin\beta\cos\delta\cos\omega + \sin\delta(\sin\varphi\cos\beta - \sin\beta\cos\varphi) \text{-----} 4.17a$$

Zenith angle is the angle between the sun's ray and the perpendicular line to a horizontal plane: -

$$\cos\theta_z = \cos\varphi\cos\delta\cos\omega + \sin\varphi\sin\delta \text{-----} 4.17b$$

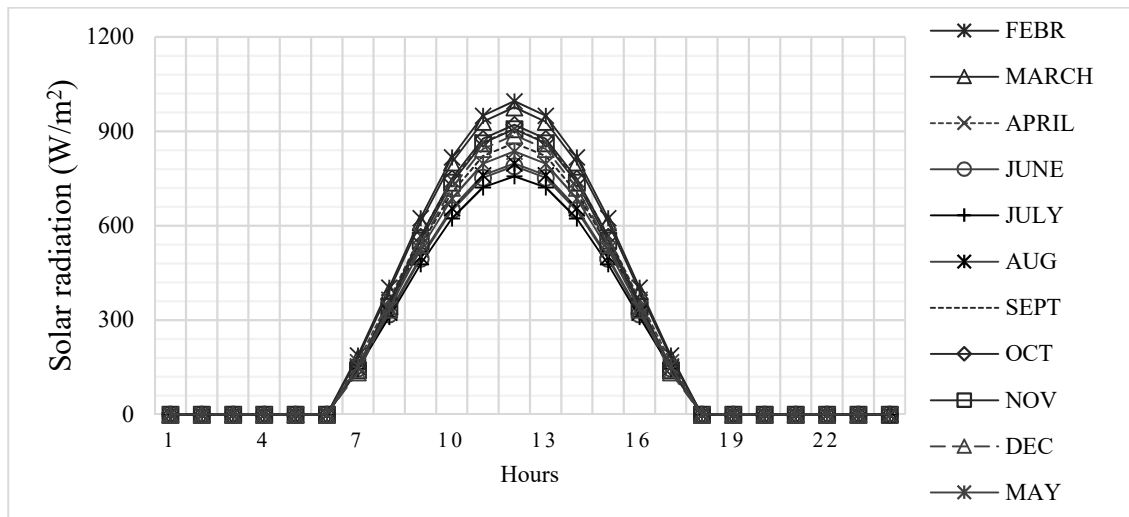


Figure 4.8 Global hourly solar radiation on 22.5° tilted surface (W/m²)

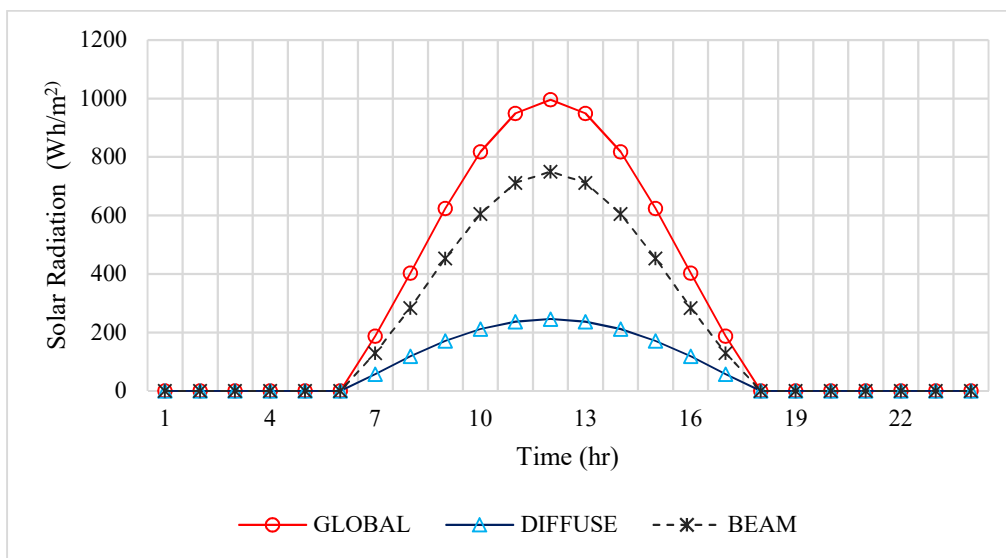


Figure 4.9: Maximum Hourly Global, Diffuse and Beam SR on inclined surfaces (22.5°) on Feb 16th.

4.1.5 Adama Climate Condition and Estimation Hourly Variation of Ambient Temperature

4.1.5.1 Climatic condition

Adama is characterized by a climatic condition of tropical region; It has high intensity of solar radiation. The monthly average temperature of Adama ranges between 18.1°C (December) and 22.6°C (April). Meteorological data are required for evaluating heat transfer between the system and its surroundings. In this paper, for thirty years average climatic conditions of Adama are used to analyze different parameters.

Table 4.3 Monthly average annual climatic condition of Adama (Ethiopia National Meteorology Agency)

		Months in a year												Year
		Jan	Feb	Mar	Apr	May	Jun	Jul	Aug	Sept	Oct	Nov	Dec	
Temperature (°C)	Average max	27	28.1	29.6	30.1	30.5	29.4	24.4	26.1	27.5	27.9	26.7	25.7	27.8
	Daily mean	19.2	20.4	21.9	22.6	22.5	22.4	18.4	20.6	21.1	20.1	18.7	18.1	20.5
	Average min	11.4	12.8	14.3	15.2	14.6	15.3	12.5	15.1	14.7	12.3	10.8	10.6	13.3
Wind speed m/s		3.5	2.7	3.5	3.5	3.5	2.8	2.8	2.7	2.8	3.4	4.3	3.4	

4.1.5.2 Estimation of Diurnal Variation of Ambient Temperature

There are many methods of calculating variation of daylight of ambient temperature. Among them the hourly variation of temperatures can be predicted from the daily maximum and daily minimum temperatures using the sine-exponential model (Brandsma, 2006) was selected. The method was developed by Parton and Logan (1981). This model describes the diurnal cycle by a sine function during daytime connected to a decreasing exponential function during night time.

↗ For daylight hours

$$T(H) = (T_{max} - T_{min}) \sin\left(\frac{\pi * m}{y+2a}\right) + T_{min} \text{-----} 4.18$$

↘ For night time hours

$$T(H) = T_{min} + (T_{sunset} - T_{min}) \exp\left(\frac{-b*n}{z}\right) \text{-----} 4.19$$

Where $T(H)$ is the temperature at any hour of the day or night period determined from m and n , y is day length (h), z is night length (h), T_{sunset} is temperature at sunset (°C), m is number of hours

between time at T_{min} and sunset (h), n is number of hours from sunset to the time of T_{min} (h), a is lag coefficient for $T_{max}=1.80$ (h), b is night time temperature coefficient =2.2 (h).

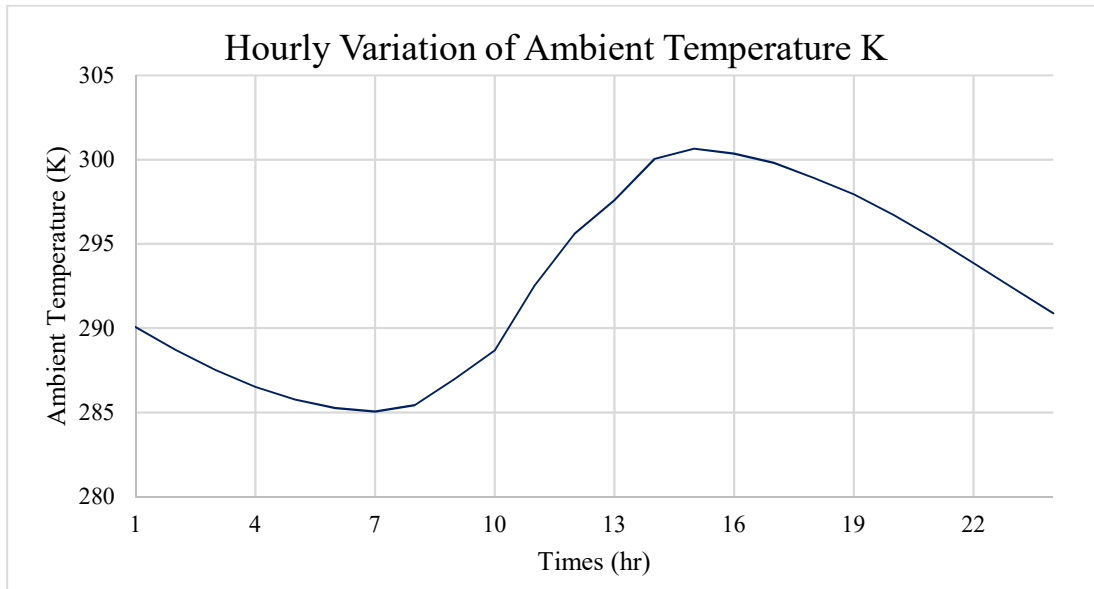


Figure 4.10: Result of average variations of ambient temperature of Adama

4.2 Transient thermal performance analysis of Flat Plate Collector

The mathematical modeling of the flat-plate solar collector (FPC) is concerned under transient conditions. This is done by deriving governing equations for each layer in the solar collector (cover, air gap, absorber, working fluid, and insulation), the derived model will be solved using finite difference method in an iterative scheme utilizing the MATLAB software package. A FPC is a heat exchanger that converts the radiant solar energy from the sun into heat energy. Solar flat plate collector with metal absorber plate and covers are the most successful devices that convert solar energy in to heat at reasonable price without affecting environment. Therefore, solar FPCs are types of solar collectors that are used to absorb and intercept the sun's radiations for water heating. Thermal water obtained using FPC is used in the different low to medium application like hospitals, hotels, homes, industries and etc. (Tiwari, 2016)

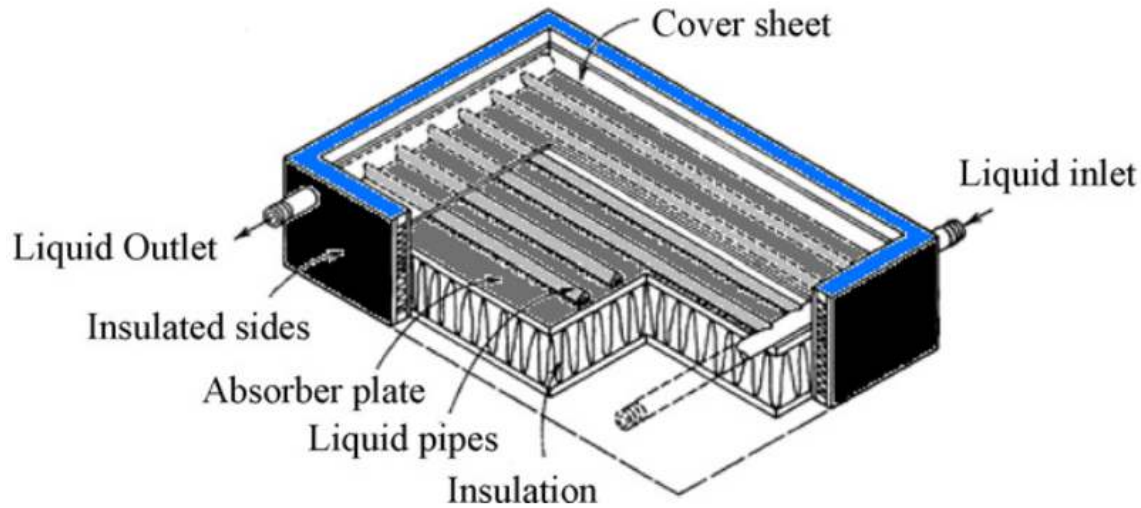


Figure 4.11 Cross section of a typical liquid flat-plate collector (Duffie & Beckman, 2013).

4.2.2 Technical Specification and Assumption of Flat Plate Collector Model

A number of simplifying assumptions can be made to analyse a flat plate collector without complicating the basic physical situation, (Duffie & Beckman, Solar Engineering of Thermal Processes, 2013). These assumptions are mentioned as follows:

- ❖ Performance is steady state.
- ❖ Construction is of sheet and parallel tube type.
- ❖ The headers cover a small area of collector and can be neglected.
- ❖ The headers provide uniform flow to tubes.
- ❖ Heat flow through a cover is one dimensional.
- ❖ There is a negligible temperature drop through a cover.
- ❖ There is one-dimensional heat flow through back insulation.
- ❖ The sky can be considered as a blackbody for long-wavelength radiation at an equivalent sky temperature.
- ❖ Temperature gradients around tubes can be neglected.
- ❖ The temperature gradients in the direction of flow and between the tubes can be treated independently.
- ❖ Loss through front and back are to the same ambient temperature.
- ❖ Dust and dirt on the collector are negligible.
- ❖ Shading of the collector absorber plate is negligible.

Table 4.4 The main specification reference for Solar Flat Plate Collector used in analyses.

Description	Technical specification
Collector type	Flat Plate Collector
Gross Area m ²	2.02
Aperture Area m ²	1.92
Collector Area m ²	2 (2 m *1 m)
Collector thickness	0.078m
Edge insulation thickness	0.021m
Glass cover material & No of glass	Tempered glass, low iron, 3mm thickness & 1
Refractive index or glass relative to air	1.5
Glass cover emissivity/absorptivity	0.85
Length of absorber plate m	1.95
Width of absorber plate m	0.92
Absorber plate Material	Copper
Thermal conductivity of plate material W/mK	386
Density of the plate material kg/m ³	8954
Plate thickness	0.16 mm
Air gap between cove and plate	0.025m
Riser and Header Tube Material	Copper
Diameter of tube	6.33 mm
Diameter of header pipe	12.7m
Riser pipes diameter (outer/inner)	10/8 mm
Tube center to center distance	100 mm
Stagnation temperature °c	197
Transmittance of the glass %	90%
Insulation material	Glass fiber
Thermal conductivity of insulation W/mK	0.04
Thickness and density of insulation material	0.05m and 200kg/m ³ respectively
Emittance of the glass/absorber plate	0.86/0.95
Heat transfer medium	Water

4.2.3 Basic Energy Balance Equation for Flat Plate Collector

Under steady-state conditions, based on the first law of thermodynamics, the energy balance of a conventional FPC that indicates the distribution of incident solar energy into useful energy gain, thermal losses, and optical losses as the follows (Tiwari, 2016):

$$\dot{q}_{ab} = \dot{q}_U + \dot{q}_L \text{-----4.20}$$

$$\dot{q}_{ab} = (\alpha\tau)I(t) \text{-----4.20a}$$

$$\dot{q}_L = U_L(T_{PC} - T_a) \text{-----4.20b}$$

\dot{q}_{ab} is the rate of energy absorbed by the plate per unit area; \dot{q}_U is the rate of useful energy transferred to the fluid and \dot{q}_L is the rate of energy lost per unit area by the absorber plate to the surroundings.

The above equation can be written as:-

$$\dot{q}_U = I(t)(\alpha\tau) - U_L(T_P - T_a) \text{-----4.21}$$

The rate of useful thermal energy for an FPC of area A_c can also be written as

$$\dot{Q}_u = \dot{q}_U A_c = A_c [I(t)(\alpha\tau) - U_L(T_P - T_a)] \text{-----4.22}$$

Furthermore, an instantaneous thermal efficiency can be defined as follows:

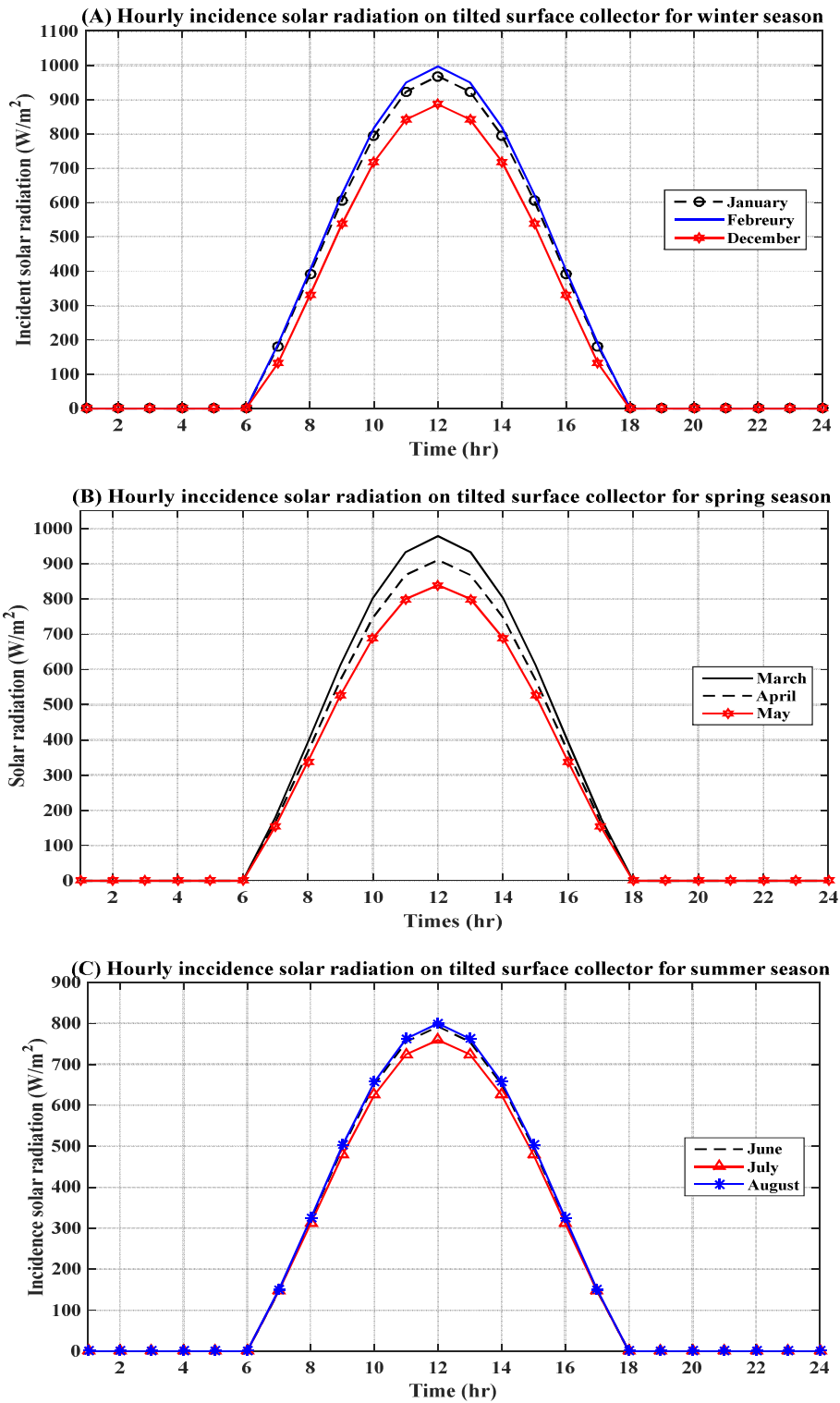
$$\eta_i = \frac{\dot{q}_U}{I(t)} = \frac{\dot{Q}_u}{A_c I(t)} = (\alpha\tau) - U_L \left(\frac{T_{PC} - T_a}{I(t)} \right) \text{-----4.23}$$

Where, α and τ are the absorptivity and transmissivity of the glazing surface of the FPC, respectively, $I(t)$ is the incident total solar radiation in the plane of the absorber (W/m^2), T_{cp} and T_a are an absorber plate and the ambient temperature ($^{\circ}\text{C}$), respectively; and U_L is an overall heat loss coefficient for the FPC ($\text{W}/\text{m}^2 \text{ }^{\circ}\text{C}$). Referring to Equation (4.2a) the rate of useful energy decreases with increasing temperature difference. The higher the rate of thermal losses (q_l), the lower rate of useful energy output (q_u). The rate of heat loss depends on $T_P - T_a$. Hence, for different ranges of temperature difference, different types of collectors are designed to minimize \dot{q}_l and optimize \dot{q}_U (Tiwari, 2016).

4.2.4 Incident solar radiation and solar energy input

Estimation of collector performance and Investigation of solar water heating system needs knowledge of the availability of global solar radiation on the collector absorber plate. Meanwhile the solar radiation reaching the earth's surface depends upon climatic conditions of the place, a study of solar radiation under local climatic conditions is crucial. The solar energy incident on a

tilted collector consists of beam radiation, diffuse radiation, and ground-reflected radiation presented in equation 4.15 and 4.16. Therefore, the results are present graphical as the following.



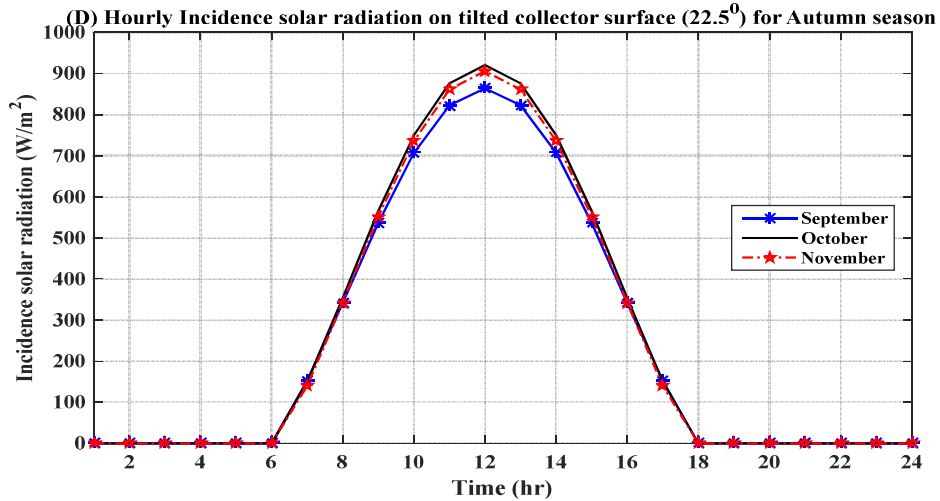


Figure 4.12 Monthly average hourly incidence solar radiation on a tilted surface (22.5°) for all seasons in a year (A, B, C & D).

4.2.5 Overall Heat Loss Coefficient of Solar Flat Plate Collector

Performance of FPC is largely affected by thermal loss to the surroundings through conduction, convection, and radiation. It is useful to develop the concept of an overall loss coefficient for a solar collector to simplify the mathematics (Duffie & Beckman, 2013). Thermal loss from an FPC to the surroundings can occur in the form of:

- a. Top loss: -the absorber plate through the glass cover
- b. Bottom loss: -the absorber plate through the insulation
- c. Side or edge loss: - rate at which heat is lost from the sides

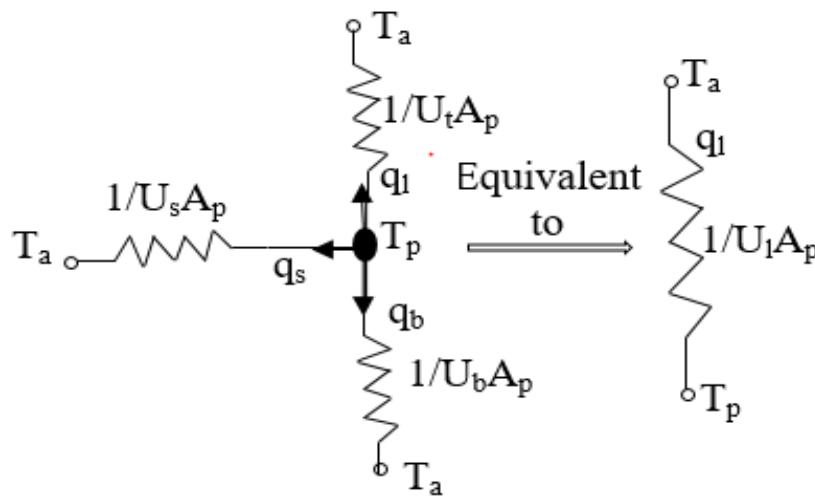


Figure 4.13 Thermal resistance network collector losses (Kalogirou, 2014).

4.2.5.1 Overall Top-Loss Coefficient - U_t

The top loss coefficient U_t is evaluated by considering convection and re-radiation losses from the absorber plate in the upward direction.

a) Convective heat-transfer coefficient:

1. From absorber plate to the glass cover (h_{1c})

The convective heat-transfer coefficient between the absorber plate and the glass cover (inclined at an angle β to the horizontal), can be written as follows:

$$h_{1c} = \frac{NUk_a}{L} \text{-----} 4.24$$

Where, Nu is the Nusselt number; K_a is the thermal conductivity of air between the plate and the glass cover and L is the spacing between the absorber plate and the glass covers.

Hollands et al., (2009) suggested the relationship between the Nusselt number and Rayleigh number for tilt angle β from 0 to 75° as:

$$NU = 1 + 1.44 \left[1 - \frac{1708 \sin(1.8\beta)^{1.6}}{Ra \cos \beta} \right]^+ * \left[1 - \frac{1708}{Ra \cos \beta} \right]^+ + \left[\left(\frac{Ra \cos \beta}{5830} \right)^{\frac{1}{3}} - 1 \right]^+ \text{-----} 4.25$$

$$Ra = \frac{g\beta_v \Delta T L^3}{\alpha\nu} \text{-----} 4.25a$$

$$Pr = \frac{\nu}{\alpha} \text{-----} 4.25b$$

Where, “+” exponent means only the positive value of the term in square bracket is to be considered and Zero is to be used for negative values. g – The gravitational constant; ΔT – Temperature difference between the plate and the glass, and β_v - is the volumetric coefficient of expansion of air.

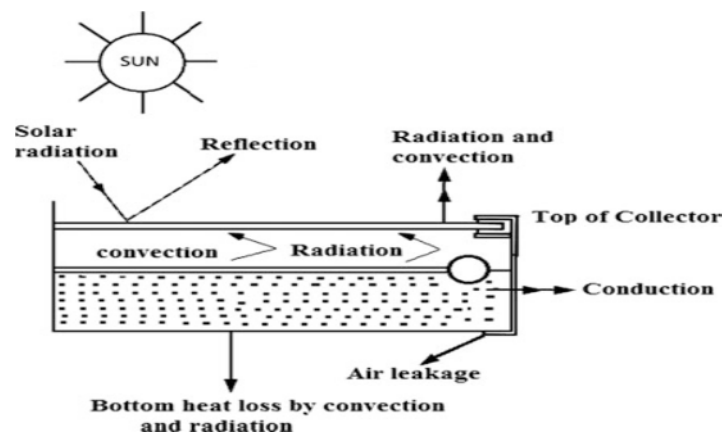


Figure 4.14. Various heat losses from absorber to ambient (Tiwari, 2016).

2. From glass cover to ambient air - h_{2c}

The convective heat transfer coefficient (h_{2c}) from the glass cover to ambient is calculated from the following empirical correlation.

$$h_{2c} = 5.7 + 3.8v \quad \text{-----} \quad 4.26$$

Where, h_{2c} is in $W/m^2 K$, and V is the wind speed over the glass cover of the FPC in m/s.

b) Radiative heat-transfer coefficient:

i. From absorber plate to glass cover - h_{1r}

The h_{1r} is the heat-transfer coefficient by radiation from the absorber plate to the glass cover, and it is expressed as: -

$$h_{1r} = \varepsilon_{eff} \frac{[(T_{pc} + 273)^4 - (T_g + 273)^4]}{T_{pc} - T_g} \quad \text{-----} \quad 4.27$$

The rate of heat transfer from the absorber plate to the glass cover by radiation (W/m^2) can be written as: -

$$(q_{rad} = h_{1r}(T_{pc} - T_g)) \quad \text{-----} \quad 4.28$$

Where, T_{pc} and T_g are the absorber plate and glazing temperatures in $^{\circ}C$, respectively.

$\sigma = 5.67 * 10^{-8} W/m^2 K^4$ is Stefan's constant.

The ε_{eff} is the effective emissivity of plate-glazing system, and it is given by: -

$$\varepsilon_{eff} = \left[\frac{1}{\varepsilon_p} + \frac{1}{\varepsilon_g} + 1 \right] \quad \text{-----} \quad 4.29$$

ii. From glazing cover to ambient - h_{2r}

The heat-transfer coefficient by radiation from a glass cover to the ambient depends on the long-wavelength radiation exchange with the sky at sky temperature T_{sky} , which is given as

$$T_{sky} = T_a - 6 = 0.0552T_a^{1.5} \quad \text{-----} \quad 4.30$$

Thus, the radiative heat-transfer coefficient, h_{2r} can be written as follows:

$$h_{2r} = \sigma \varepsilon_g \frac{[(T_g + 273)^4 - (T_{sky} + 273)^4]}{T_g - T_a} = \sigma \varepsilon_g \frac{T_g^4 - T_a^4}{T_g - T_a} \quad \text{-----} \quad 4.31$$

➤ The total heat transfer coefficient from collector plate to cover is expressed as:

$$h_1 = h_{1c} + h_{1r} \quad \text{-----} \quad 4.31a$$

➤ The total heat transfer coefficient from the cover to ambient is expressed as:

$$h_2 = h_{2c} + h_{2r} \quad \text{-----} \quad 4.31b$$

The thermal resistance due to conduction, heat-transfer coefficient ($h_k = k_g/L_g$) for glass cover is not significant and hence it can be neglected. An overall top-loss heat-transfer coefficient (U_t) from the absorber plate to the ambient is:

$$U_t = \left[\frac{1}{h_1} + \frac{1}{h_2} \right]^{-1} \text{-----} 4.32$$

The rate of heat loss through the top glass cover per unit area, (W/m²), can be written as: -

$$\dot{q}_t = U_L(T_{pc} - T_a) \text{-----} 4.33$$

4.2.5.2 Bottom Loss Coefficient

The bottom loss coefficient U_b is evaluated by considering conduction and convection losses from the absorber plate in the downward direction through the bottom of the collector. Neglecting the convective resistance at the bottom surface of the collector casing and it is expressed as: -

$$U_b = \frac{K_i}{t_i} = \frac{0.044 \text{ W/mK}}{0.06 \text{ m}} = 0.73 \text{ W/m}^2\text{K} \text{-----} 4.34$$

Where, K_i = thermal conductivity of the insulation, t_i = back insulation thickness.

4.2.5.3 Side Loss Coefficient

As in the case of the bottom loss coefficient, it will be assumed that the conduction resistance dominates and that the flow of heat is one-dimensional and steady. The side loss coefficient is always smaller than the top loss coefficient.

$$U_e = \frac{K_i}{t_e} \left(\frac{A_1}{A_c} \right) = U_b \left(\frac{A_1}{A_c} \right) = 0.667 \left(\frac{0.121}{2.02} \right) \text{ W/m}^2\text{k} = 0.1478 \text{ W/m}^2\text{k} \text{-----} 4.35$$

Where, $A_1 = P * h_e = 2(1.95 + 0.92) * 0.078 \text{ m}^2$

P = perimeter of the absorber plate ($L_c * W_c$), h_e = height of the edge (collector thickness) and t_e = edge insulation thickness.

The overall heat loss coefficient U_L is the sum of the top, bottom and side/edge loss coefficient.

$$U_L = U_t + (U_s + U_b) = U_t + (0.73 + 0.1478) \text{-----} 4.36$$

$$U_t = U_L - 0.8778 \frac{W}{m^2K} \text{-----} 4.37$$

The overall rate of heat lost from the absorber to the ambient air through the glass cover and bottom insulation is given by: -

$$\dot{q}_t = U_t(T_{pc} - T_a) \text{-----} 4.37$$

$$\dot{q}_b = U_b(T_{pc} - T_a) \text{-----} 4.38$$

$$\dot{q}_s = U_s(T_{pc} - T_a) \text{-----} 4.39$$

$$\dot{q}_L = \dot{q}_t + \dot{q}_b + \dot{q}_s = U_L(T_{pc} - T_a) \text{-----} 4.40$$

By applying energy balance heat transfer between plate to cover and cover to ambient air and the basic energy equation of top loss coefficient become:

$$Q = h_1(T_p - T_g) = h_2(T_g - T_a) \text{-----4.41}$$

$$U_t = \left[\frac{1}{h_1} + \frac{1}{h_2} \right]^{-1} = U_L - 0.815 \text{ W/m}^2\text{k} \text{-----4.42}$$

By using Iteration method, solving the equation (4.41) and (4.42) simultaneously and after some steps came up with the following results:

$$U_t = 6.87 \text{ W/m}^2\text{k}, U_L = 7.69 \text{ W/m}^2\text{K}, T_p = 367 \text{ K}, T_g = 318.15 \text{ K}, T_a = 296.15\text{K}$$

$$h_{1r} = 6.254 \text{ W/m}^2\text{k}, h_{2r} = 8.43 \text{ W/m}^2\text{k}, h_{2c} = 16.91 \text{ W/m}^2\text{k}, h_{1c} = 4.11 \text{ W/m}^2\text{k}$$

4.2.6 Collector efficiency factor F' and temperature distribution between tubes

Consider the figure 4.17 shows a dimension of one tube below the plate (absorber) configuration.

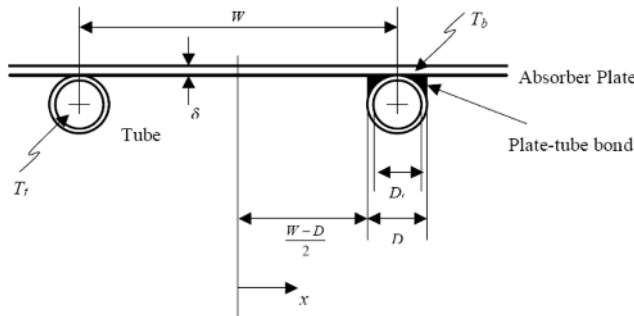


Figure 4.15 Bonding material placed between the plate and the tube.

Where, T_b - local base temperature for sheet above bond; W - Distance b/n the centres of the two tubes; $W/2$ - the distance between the centres of the absorber sheet and the tube; D & d - outer and the inner-tube (riser) diameters are D and d , respectively; δ and $(W - D)/2$ - Thickness of absorber sheet and fin length respectively

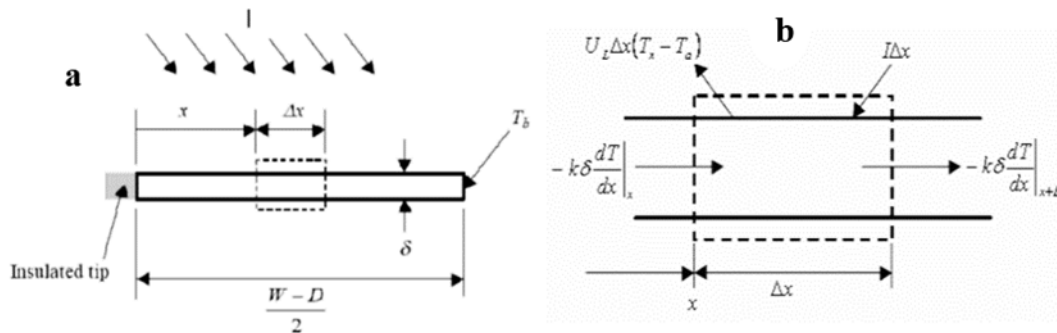


Figure 4.16 Energy flow on fin element (a) Fin with Insulated Tip and (b) Energy balance Over Finite Volume.

Bearing in mind heat transfer occurring in the x-direction and an elemental region of width Δx and unit length in the flow direction as shown above, energy balance on this element can be written as:

$$E_{in} - E_{out} = 0 \text{-----} 4.43$$

$$(\alpha t)I(t)\Delta x + U_L(T_a - T)\Delta x + \left(-k\delta \frac{dT}{dx}\Big|_x\right) - k\delta \frac{dT}{dx}\Big|_{x+\Delta x} = 0$$

$$(\alpha t)I(t)\Delta x + U_L(T_a - T)\Delta x + \left(-k\delta \frac{dT}{dx}\right) - \left(-k\delta \frac{d}{dx}(T + dT)\Delta x\right) = 0$$

$$(\alpha t)I(t)\Delta x + U_L(T_a - T)\Delta x + \left(k\delta \frac{d^2T}{dx^2}\right) \Delta x = 0$$

$$\frac{d^2T}{dx^2} = -\frac{1}{k\delta}[(\alpha t)I(t) + U_L(T_a - T)]$$

Where, $I(t)$ -the absorbed incident solar energy. Dividing all over Δx and using the limit as $\Delta x \rightarrow 0$ yields:

$$\frac{d^2T}{dx^2} = \frac{U_L}{k\delta} \left[T - T_a - \frac{(\alpha t)I(t)}{U_L} \right] \text{-----} 4.44$$

Hence, the second-order differential equation, to solve the two boundary conditions are required.

$$\text{Thus; } \frac{dT}{dx}\Big|_x = 0 \text{ \& } T\Big|_{x=\frac{(W-D)}{2}} = T_b; \text{ Assume } m^2 = \frac{U_L}{k\delta} \text{ and } \Phi = T - T_a - \frac{(\alpha t)I(t)}{U_L}$$

$$\frac{d^2T}{dx^2} = \frac{d^2\Phi}{dx^2} \rightarrow \frac{d\Phi}{dx}\Big|_{x=0} = 0 \text{ \& } \Phi\Big|_{x=\frac{(W-D)}{2}} = T_b - T_a - \frac{(\alpha t)I(t)}{U_L}$$

Finally the equation (4.44) becomes:

$$\frac{d^2\Phi}{dx^2} - m^2\Phi = 0 \text{-----} 4.45$$

The general solution of the second order equation given as: -

$$\Phi = C_1 \sinh mx + C_2 \cosh mx \text{-----} 4.46$$

C_1 and C_2 are constants and obtained by using boundary condition.

$$\frac{d\Phi}{dx}\Big|_{x=0} = mC_1 \cosh(m * 0) + mC_2 \sinh(m * 0) = 0 \rightarrow C_1 = 0$$

$$\Phi\Big|_{x=\frac{(W-D)}{2}} = C_2 \cosh m\left(\frac{W-D}{2}\right) = T_b - T_a - \frac{(\alpha t)I(t)}{U_L} \text{ Then } C_2 = \frac{T_b - T_a - \frac{(\alpha t)I(t)}{U_L}}{\cosh m\left(\frac{W-D}{2}\right)}$$

The general solution becomes:

$$\Phi = \frac{T_b - T_a - \frac{(\alpha t)I(t)}{U_L}}{\cosh m\left(\frac{W-D}{2}\right)} \cosh mx \text{-----} 4.47$$

$$\frac{T - T_a - \frac{(\alpha t)I(t)}{U_L}}{T_b - T_a - \frac{(\alpha t)I(t)}{U_L}} = \frac{\cosh mx}{\cosh m\left(\frac{W-D}{2}\right)} \text{-----} 4.48$$

The temperature distribution found as :

$$T = (T_b - T_a - \frac{(\alpha t)I(t)}{U_L}) \left[\frac{\cosh mx}{\cosh m(\frac{W-D}{2})} \right] + (\frac{(\alpha t)I(t)}{U_L} + T_a) \text{-----} 4.49$$

Or

$$T = (\frac{(\alpha t)I(t)}{U_L} + T_a) - \left[\frac{(\alpha t)I(t)}{U_L} - (T_b - T_a) \right] * (\frac{\cosh mx}{\cosh m(\frac{W-D}{2})})$$

The energy conducted to the district of the tube per unit of length in the flow direction can be found by evaluating Fourier's law at the fin base.

$$\dot{q}_{fin} = -k\delta \frac{dT}{dx} \Big|_{x=(\frac{W-D}{2})} = m \frac{k\delta}{U_L} [(\alpha t)I(t) - U_L(T_b - T_a)] \tanh(\frac{m(W-D)}{2}) \text{-----} 4.50$$

The energy collection for both sides becomes:

$$\dot{q}_{fin} = 2 * m \frac{k\delta}{U_L} [(\alpha t)I(t) - U_L(T_b - T_a)] \tanh(\frac{m(W-D)}{2}) \text{-----} 4.51$$

The equation (4.51) is the rate of heat conducted toward the tube by conduction due to fin per unit length written as; -

$$\dot{q}_{fin} = F(W - D)[(\alpha t)I(t) - U_L(T_b - T_a)] \text{-----} 4.52$$

Where, $F = \frac{\tanh(\frac{m(W-D)}{2})}{m(W-D)}$ is called fin efficiency and $m^2 = \frac{U_L}{k\delta}$

For a fin length L the rate of heat conducted toward the tube can be written as:

$$\dot{Q}_{fin} = F(W - D) * L * [(\alpha t)I(t) - U_L(T_b - T_a)] \text{-----} 4.53$$

Collector Efficiency factor (F') : - is the ratio of the actual energy output of the collector to the energy output in which if the total absorber temperature T_{mp} was at the average fluid temperature T_f with the same fluid quantity of flowing through the tube, ($T_{pm} = T_f$) (Duffie & Beckman, Solar Engineering of Thermal Processes, 2013):

$$F' = \frac{1/U_L}{\frac{1}{U_L[D+(W-D)]F} + \frac{1}{C_b} + \frac{1}{\pi D_i h_{fi}}} \text{-----} 4.54$$

Where; F' is the fin efficiency, h_{fi} is the heat transfer coefficient between the fluid and the tube wall. The bond conductance C_b can be estimated from understanding of the bond thermal conductivity k_b , the average bond thickness γ , and the bond width b and per-unit-length basis:

$$C_b = \frac{k_b b}{\gamma} \text{-----} 4.55$$

It is necessary to have good metal-to-metal contact so that the bond conductance is greater than 30 W/m°C (Duffie & Beckman, 2013).

In this thesis the working fluid circulates through the system, pressurized by external energy source, this lead to forced convection.

The rate of useful energy output from the collector may also be measured by means of the amount of heat carried away in the fluid passed through it and given as: -

$$\dot{Q}_u = \dot{m} c_p (T_{fo} - T_{fi}) \text{-----4.56}$$

Collector Heat Removal Factor, F_R : - is define a quantity that relates the actual useful energy gain of a collector to the useful gain if the whole collector surface were at the fluid inlet temperature and is expressed as (Tiwari, 2016):

$$F_R = \frac{\dot{m}c_p(T_{fo}-T_{fi})}{A_c((\alpha\tau)I(t)-U_L(T_{fo}-T_{fi}))} \text{-----4.57}$$

$$F_R = \frac{\dot{m}c_p}{A_cU_L} [1 - \exp(-\frac{A_cU_LF'}{\dot{m}c_p})] \text{-----4.58}$$

The maximum possible useful energy gain in a solar collector occurs when the whole collector is at the inlet fluid temperature. The actual useful energy gain (Q_u) is found by multiplying the collector heat removal factor (F_R) by the maximum possible useful energy gain.

$$\dot{Q}_u = F_R A_c [I(t)(\alpha\tau) - U_L(T_{fi} - T_a)] \text{-----4.59}$$

The outlet fluid temperature T_{fo} can be calculated by combining equations (4.56 and 4.59):

$$T_{fo} = \frac{F_R A_c}{\dot{m}c_p} [I(t)(\alpha\tau) - U_L(T_{fi} - T_a)] + T_{fi} \text{-----4.60}$$

The instantaneous thermal efficiency of flat plate collector is given by:

$$\eta_{ins} = \frac{\dot{Q}_u}{A_c I(t)} = \frac{F_R A_c [I(\alpha\tau) - U_L(T_i - T_a)]}{A_c I(t)} = F_R \left\{ \tau\alpha - U_L \left(\frac{T_{fi} - T_a}{I(t)} \right) \right\} \text{-----4.61}$$

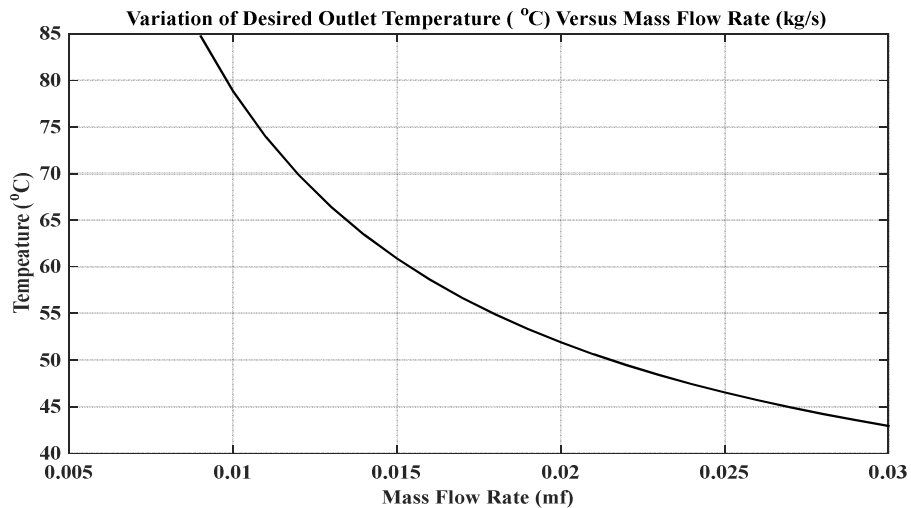


Figure 4.17 Variation of desired outlet temperature for heat transfer fluid versus mass flow rate

From equation (4.60 and 4.61) and shown in figure 4.19; mass flow rate is directly proportional to collector efficiency and inversely proportional to HTF outlet temperature. For the analysis of the collector system, the mass flow rate of heat transfer fluid is preferred for desired outlet water temperature range 60-65°C and the heat transfer fluid mass flow rate is 0.0145 kg/sec.

4.2.7 Transient Analysis and Energy Balance Equation of Flat Plate Solar Collector

Components

With the intention of obtain the appropriate energy supply for a particular fixing of a solar FPC, understanding about the collector operating parameters (temperature of the working fluid) is necessary for the solar collector works under transient conditions. In this topic, the numerical model used to simulate the dynamic behavior of liquid FPC is developed. The collector has divided in to five components (cover, air gap, absorber, fluid, and insulation) which perpendicular to the flow direction. For each node, the equation describing the energy balance is derived. The derived differential equations are solved using the explicit finite-difference method. Assume, all the thermo-physical properties are considered as constant (Salah, 2012).

I. Single Glass cover

The small thickness of the cover makes it reasonable to consider a uniform temperature through it. The governing equation can be derived from an energy balance in a differential volume of thickness δ_g and area of $(L\Delta y)$. The heat transfers into the glass by convection between it and the ambient and by radiation from the sun and the absorber as shown in figure 4.20.

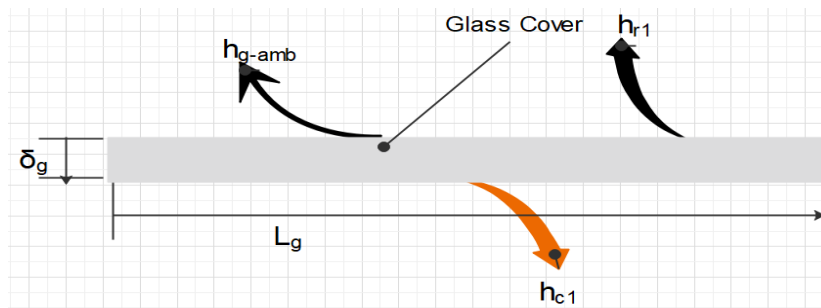


Figure 4.18 Energy balance and heat transfer techniques on single glass cover

For one-dimensional heat transfer through the collector, the general energy balance is given by: -

$$\frac{dU}{dt} = \dot{Q}_{in} - \dot{Q}_{out} + \dot{Q}_{gen} \text{-----4.62}$$

$$C_{pg}\rho_g V_g \frac{dT_g}{dt} = [h_2(T_{amb} - T_g) + h_{1r}((F * T_{mp}) - T_g) + h_{1c}(T_{ag} - T_g) + \alpha I(t)]L\Delta y \text{-----4.63}$$

Where, $h_{g-amb} = h_2 = h_{c2} + h_{r2}$

II. The air gap between the cover and the absorber

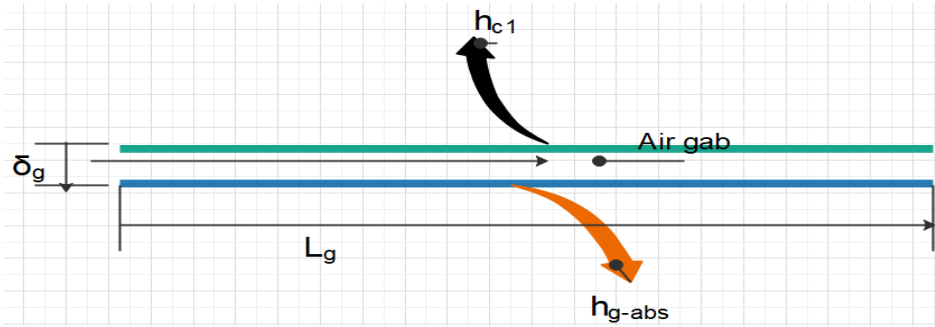


Figure 4.19 Energy balance and heat transfer techniques of air gap between glass and abs. plate

$$C_{pa}\rho_a V_a \frac{dT_a}{dt} = [h_{c1}(T_g - T_{ag}) + h_{g-abs}((F * T_{mp}) - T_g)] L\Delta y \text{-----} 4.64$$

Where, $h_{g-abs} = h_1 = h_{c1} + h_{r1}$

III. Absorber Plate

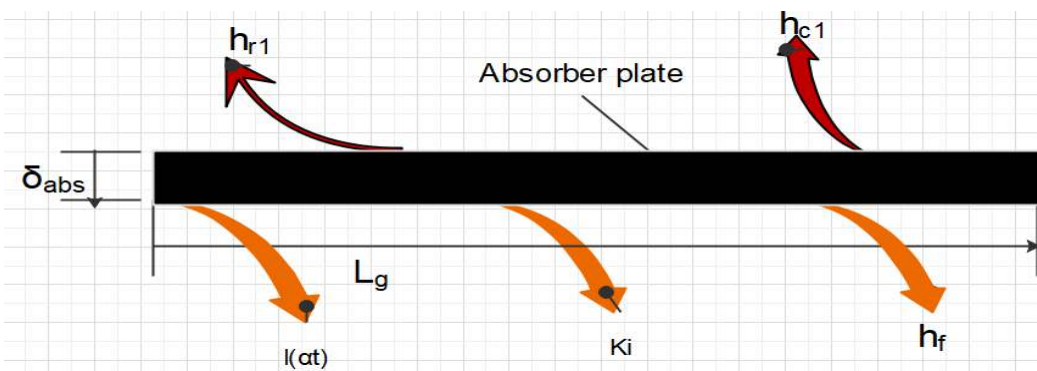


Figure 4.20 Energy balance and heat transfer techniques on absorber plate

$$C_{p abs}\rho_{abs} V_{abs} \frac{dT_{abs}}{dt} = [(\alpha\tau)I + h_{r1}(T_g - (F * T_{abs})) + h_{c1}(T_{ag} - (F * T_{abs})) + \frac{K_{ins}}{\delta_{ins}}(T_{ins} - FT_{abs})] L\Delta y + \pi d_i h_{fi}(T_f - (F * T_{abs})) \text{-----} 4.65$$

IV. Insulation

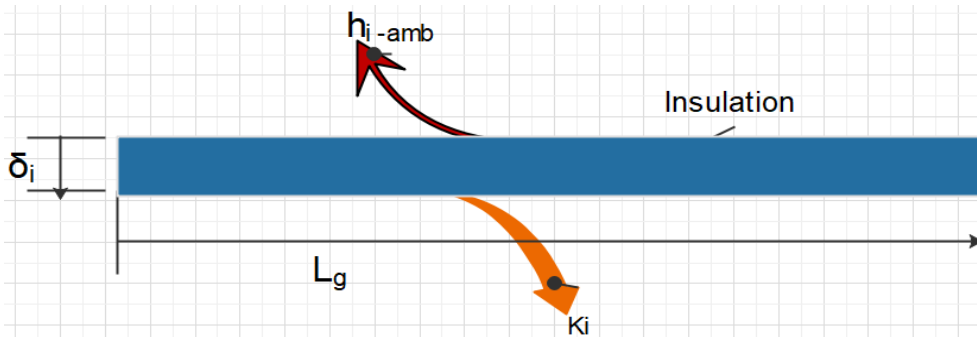


Figure 4.21 Energy balance and heat transfer techniques of insulation

$$C_{p\text{ins}}\rho_{\text{ins}}V_{\text{ins}}\frac{dT_{\text{ins}}}{dt} = \frac{K_{\text{ins}}}{\delta_{\text{ins}}}(FT_{\text{abs}} - T_{\text{ins}}) + h_{\text{ins-amb}}(T_{\text{amb}} - T_{\text{ins}}) \text{-----} 4.66$$

Where, $h_{\text{ins-amb}} = h_{c2}$

V. Working fluid

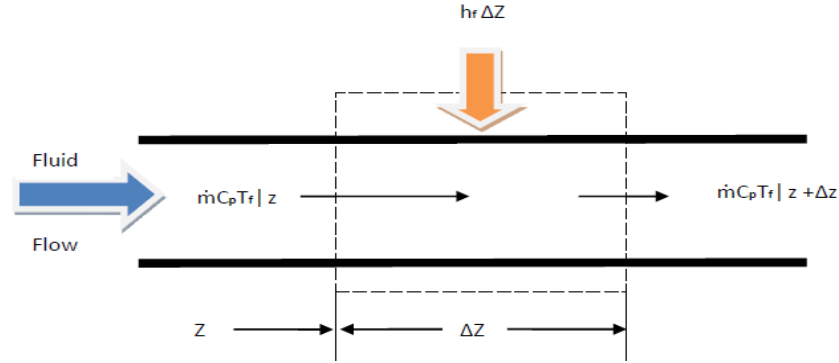


Figure 4.22 Energy balance and heat transfer techniques by working fluids

$$C_{pf}\rho_f A \frac{\partial T_f}{\partial t} = \pi d_i h_f (F * T_{\text{abs}} - T_f) - C_{pf} m_f \frac{\partial T_f}{\partial z} \text{-----} 4.67$$

4.2.8 Transient Analysis of Flat Plate Solar Collector Using Finite Difference Method

The explicit finite-difference method is offered to solve the system of equations. The time derivatives are replaced by a forward difference scheme, whereas the dimensional derivative is replaced by a backward difference scheme.

↻ *For ambient atmosphere*

$$\frac{dT_a}{dt} = \frac{T_{a,m}^{t+\Delta t} - T_{a,m}^t}{\Delta t} \text{-----} 4.68$$

Where, $m = 1, 2, 3, 4 \dots \dots N$ and Δt -is time step increment & t is the time

↻ *For Glass cover*

$$\frac{dT_g}{dt} = \frac{T_{g,m}^{t+\Delta t} - T_{g,m}^t}{\Delta t} \text{-----} 4.69$$

After some steps, the unsteady temperature of differential equation to algebraic equation became;

$$T_{g,m}^{t+\Delta t} = A1 * \Delta t * T_{a,m}^t + A2 * \Delta t * F * T_{p,m}^t + A3 * \Delta t * T_{a,g,m}^t + A4 * \Delta t * T_{g,m}^t + A5 * \Delta t * I_{Tt} \text{-----} 4.70$$

$$A1 = \frac{h_2}{\rho_g C_g \delta_g} \text{-----} 4.71$$

$$A2 = \frac{h_{1r}}{\rho_g C_g \delta_g} \text{-----} 4.72$$

$$A3 = \frac{h_{1c}}{\rho_g C_g \delta_g} \text{-----} 4.73$$

$$A4 = 1 - (A1 + A2 + A3) \text{-----} 4.74$$

$$A5 = \frac{\alpha}{\rho_g C_g \delta_g} \text{-----} 4.75$$

↻ **For air gap**

$$\frac{dT_{ag}}{dt} = \frac{T_{ag,m}^{t+\Delta t} - T_{ag,m}^t}{\Delta t} \text{-----} 4.76$$

$$T_{ag,m}^{t+\Delta t} = (1 - 2 * A6 * \Delta t) T_{ag,m}^t + A6 * \Delta t * T_{g,m}^t + A6 * \Delta t * F * T_{p,m}^t \text{-----} 4.77$$

$$A6 = \frac{h_{c1}}{\rho_{ag} C_{ag} \delta_{ag}} \text{-----} 4.78$$

↻ **For absorber plate**

$$\frac{dT_p}{dt} = \frac{T_{p,m}^{t+\Delta t} - T_{p,m}^t}{\Delta t} \text{-----} 4.79$$

$$T_{p,m}^{t+\Delta t} = A7 * \Delta t * T_{g,m}^t + A8 * \Delta t * T_{ag,m}^t + A9 * \Delta t * T_{ins,m}^t + A10 * \Delta t * T_{f,m}^t + A11 * \Delta t * I_{Tt} + (1 - A12 * F * \Delta t) T_{p,m}^t \text{-----} 4.80$$

$$A7 = \frac{h_{1r}}{\rho_p C_p \delta_p} \text{-----} 4.81$$

$$A8 = \frac{h_{1c}}{\rho_p C_p \delta_p} \text{-----} 4.82$$

$$A9 = \frac{k_{ins}}{\rho_p C_p \delta_p \delta_{ins}} \text{-----} 4.83$$

$$A10 = \frac{\pi D_i h_{fi}}{\rho_p C_p \delta_p L} \text{-----} 4.84$$

$$A11 = \frac{\alpha \tau}{\rho_p C_p \delta_p} \text{-----} 4.85$$

$$A12 = A7 + A8 + A9 + A10 \text{-----} 4.86$$

↻ **For working fluid**

$$\frac{dT_f}{dt} = \frac{T_{f,m}^{t+\Delta t} - T_{f,m}^t}{\Delta t} \text{-----} 4.87$$

$$\frac{dT_f}{dy} = \frac{T_{f,m}^{t+\Delta t} - T_{f,m-1}^t}{\Delta z} \text{-----} 4.88$$

$$T_{f,m}^{t+\Delta t} = (1 - A13 * \Delta t - \Delta y) T_{f,m}^t + \Delta y T_{f,m-1}^t + A13 * \Delta t * F * T_{p,m}^t$$

$$A13 = \frac{\pi D_i h_{fi}}{\rho_f C_f A} \text{-----} 4.89$$

↻ **For insulation**

$$\frac{dT_{ins,m}}{dt} = \frac{T_{ins,m}^{t+\Delta t} - T_{ins,m}^t}{\Delta t} \text{-----} 4.90$$

$$T_{ins,m}^{t+\Delta t} = (1 - A16 * \Delta t) T_{ins,m}^t + A15 * \Delta t * T_{a,m}^t + A14 * \Delta t * F * T_{p,m}^t \text{-----} 4.91$$

$$A14 = \frac{h_{1c}}{\rho_{ins} C_{ins} \delta_{ins}^2} \text{-----} 4.92$$

$$A15 = \frac{h_{2c}}{\rho_{ins} C_{ins} \delta_{ins}} \text{-----} 4.93$$

$$A16 = (A14 + A15) \text{-----} 4.94$$

Where; an abbreviations of g, ag, p, f, and ins are glass, air gap, absorber plate, working fluid and insulation, respectively. T is a temperature, Di is for the internal diameter of the tube, F is for the fin efficiency of the absorber plate, C is for the specific heat capacity, ρ is for the density, k is for thermal conductivity, α is the thermal absorptivity of plate, τ is the thermal transmissivity of the glass, δ is for the thickness, \dot{m} is for the mass flow rate, N is the number of nodes in the flow direction, and V is the volume.

Initial Conditions @ t = 0 sec or at 12:00 PM morning

The glass cover and insulation materials are maintain at ambient temperature, 23°C.

The absorber plate temperature is equals to ambient temperature and 10°C ($T_p @ i=0 = 33$ °C).

The air gap temperature between plate and glazing equals its average of both temperature.

$$T_p @ i=0 = (23+33)/2 = 27.5 \text{ } ^\circ\text{C}$$

Heat transfer fluid (water) at a temperature of; $T_w @ i=0 = 23$ °C.

Boundary conditions

Temperature of fluid at the inlet of riser tube is equal to the ambient temperature ($T_f @ i=0 = 23$ °C).

Finally, the value of FDM analysis of all flat plate collectors are presented in result and discussion.

4.2.9 Estimating total heating load and solar energy

The energy demands to be met by a solar water heating system are hot water load and heat losses from a system components (storage tank and piping). The heat losses from the tank and piping are estimated as a fraction of the total hot water load which the fractions ranging from 10 to 25 percent are used by Mclaughlin et al., (1991).

The energy storage capacity of a hot water storage unit is given by; -

$$Q_s = Vst * \rho * c_p * \Delta T \text{-----} 4.95$$

Where, Q_s - total heat capacity of the storage tank [kWh]; Vst - Volume of storage tank and Density of the water ($\rho_w = 1000$ kg/m³)

c_p - Heat capacity of water and the value is 4.2kJ/kg.k (0.001167 kWh/kg.k);

ΔT - Temperature difference of hot and cold water in K.

4.2.10 Determining sizing of collector system

The common practice to determine the total area of collectors is simply founded dividing the total energy demand of the system to the average energy per month produced by the collector (solar

radiation, W/m^2). Besides, the size of the storage tank helps to determine the optimal sizing of the collector (A_c). Therefore, solar collectors are usually calculated to meet of DHW need in the period where solar intensity radiation is the least. The total area of the solar collector is given by:

$$A_{collector} = \frac{Q_{HWD} (W)}{\eta * I_{T,avg} (\frac{W}{m^2})} \text{-----} 4.96$$

Where, Q_{HWD} -is total hot water demand; η - thermal efficiency and $I_{T,avg}$ - is averagely solar radiation intensity.

4.2.11 Flat Plate Solar Collector Arrays Configuration

A solar water heater is a combination of a solar collector array, an energy transfer system, and a storage tank. The one part of a SWH is the solar collector array, which absorbs solar radiation and converts it to heat. The performance of solar collectors is dependent on how they are arranged, the flow rate through risers and the inlet temperatures to individual modules. Arrays of Solar Collector modules may be connected in series, parallel or combinations.

- (a) **Parallel connection:** -the riser and headers of each FPC are connected to increase the volume of water to be heated. The mass flow rate per FPC is the total mass flow rate divided by number of FPCs. The outlet-water temperature is the same at the outlet of each FPC. Such FPC modules can operate in natural as well as forced mode.
- (b) **Series connection:** -the outlet of one row of FPCs (the first module) is connected with the inlet to a second row of FPCs (second module) and so on. The mass-flow rates in such cases are the same for all rows. The outlet temperature depends on the number of rows of FPCs connected in series. Such series-connected FPC modules can only operate in forced mode.

For this study the solar collector array arranged in parallel is selected for an investigation of solar thermal water heating system component (Tiwari, 2016). The parallel configuration is the most common setting link and each row may or not have the same number of collectors in a parallel setting and aligned among each other. Therefore, to become fulfill or cover the daily hot water demand of the Adama Hospital Medical College is about 265 number of collectors required.

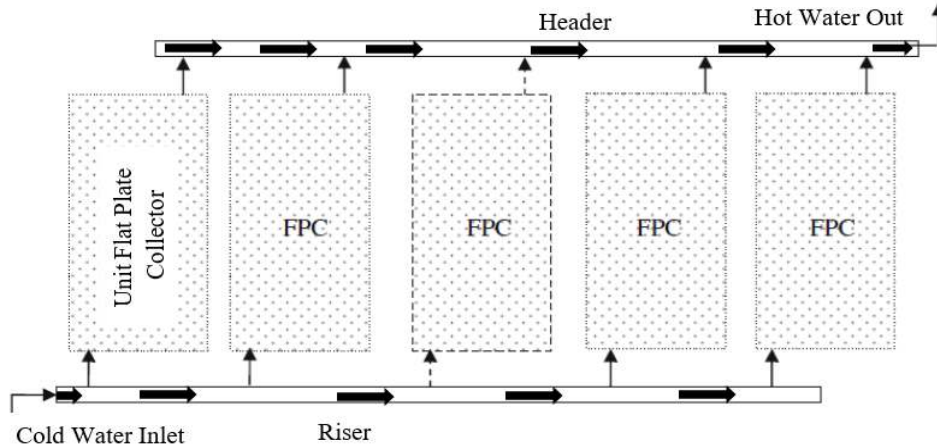


Figure 4.23 Diagram of FPC Parallel array configuration

4.2.12 Clearance between collector arrays

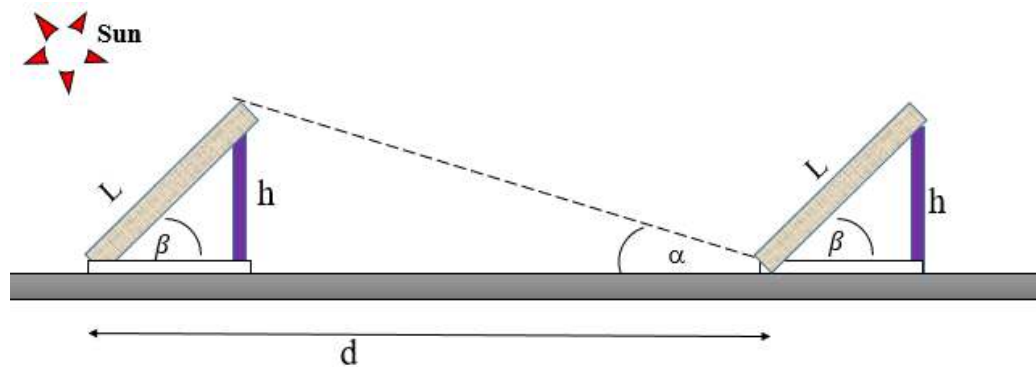
Before installing number of solar collector rows the suitable clearance between the collectors connection should be considered that to prevent the shading effects (Tiwari, 2016). As much as possible, the clearance between collector rows must be sufficient to prevent shading. As explained in previous section, for Adama weather condition with collector slope (20°), latitude, 8.54° and 2m length of FPC, the clearance distance between two neighboring collectors (d) calculated by the given equation (4.103).

$$d = \frac{h}{\tan(61^\circ - \varphi)} \text{----- 4.103}$$

Where, $h = L * \sin\beta = 2 * \sin 20^\circ = 0.684 \text{ m}$

β and φ –Inclination of the collector and latitude; L - Length of the collector

$$d = \frac{2 * \sin 20^\circ}{\tan(61^\circ - 8.54^\circ)} = 0.53 \text{ m}$$



L- Length of the collector d- Clearance between two collector

H – Collector height β - Collector angle of inclination α - angle of solar radiation

Figure 4.24 Clearance of collector arrays angle of inclinations

Next, for determining the number of collector per row, the space where the collector is installed is considered. Thus, the installation space used may be on the roof unless install collector on high elevation from the ground and calculated by equation (4.104)

$$\text{Number of collector per row} = \frac{\text{space width} - \text{free space}}{\text{collector width}} \text{-----} 4.104$$

Where, space width is 22 m, the chosen collector width is 1m and it is necessary to leave a 0.53m free space in the each row to facilitate the installation and maintenance.

$$\text{Number of collector per row} = 22 - 0.5 = 21.5$$

This indicates that, it's possible to install 21 solar collectors in each rows. For Adama hospital medial college, the estimated number of collector per row is the first 7th array and/or row have 21 soar collector and six collectors installed at the last row. The height of a collector is;

$$h_{coll} = h * \sin\alpha = 2 \text{ m} * \sin 20^\circ = 0.684 \text{ m}$$

4.2.13 Length of Pipe between solar collector and storage

The energy lost from ducts and pipes leading to and returning from the collector in a solar energy system can be significantly related to the pipe length, material property and insulation thickness.

I. Total Length of inlet Manifolds

↻ Total Length of collector in each array, $L_c = \text{No of collector} * \text{width of the collector}$

$$L_c = 21 * 1 \text{ m} = 21 \text{ m}$$

↻ Total Length of connection pipes, $L_{conn} = \text{No of collector} * \text{length of the connector between two collectors}$

$$L_{con} = 21 * 0.2 \text{ m} = 4.2 \text{ m}$$

In similar way, assuming the space between two collector and also between pipe bend and pipe joint. Definitely, there are 2 spaces between the joint (intake manifold and supply pipe) and connector pipe in both collector array of a system, and the height of the storage tank is considered. Approximately, the total length of space is 1.45 m needs. Finally, the total length of the intake manifold requires about 30 m.

$$L_1 = L_c + L_{con} + L_{space} \text{-----} 4.105$$

II. Total Length of Return Manifolds

It is suggested that the last array or 18th row have six number of collectors and total length of space between each collector's edge and pipe bend to intake manifold and also space two between the joint pipe and connector pipe is 1.5m. Width of the solar collector is 1m.

⇒ Total Length of collector in each array, $L_c = \text{No of collector} * \text{width of the collector}$

$$L_c = 21 * 1 \text{ m} = 21 \text{ m}$$

⇒ Total Length of connection pipes, $L_{con} = \text{No of collector} * \text{length of the coconnector between two collectors}$

$$L_{con} = 21 * 0.2 \text{ m} = 4.2 \text{ m}$$

⇒ The total length of the return manifold needed approximately 27 m.

$$L_2 = L_c + L_{con} + L_{space} \text{-----} 4.106$$

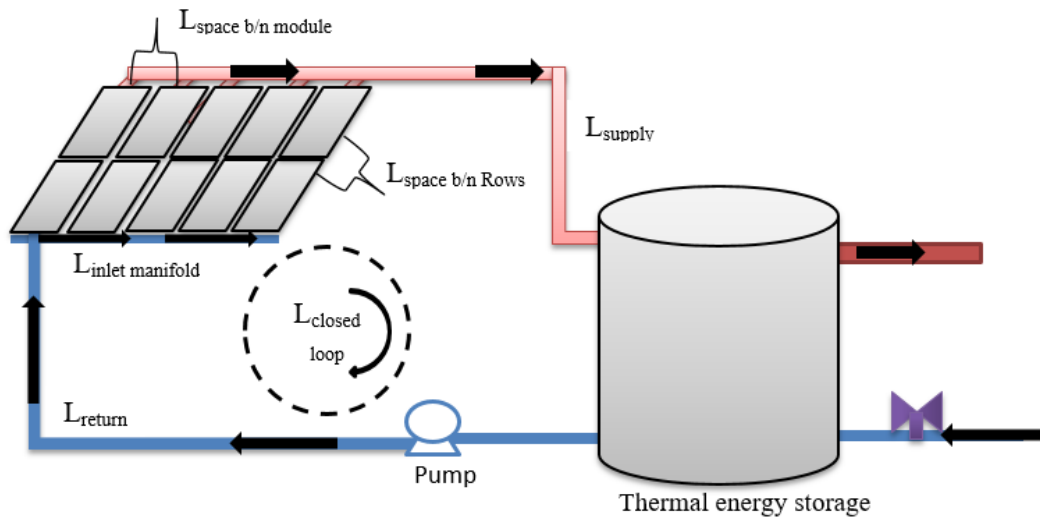


Figure 4.25 Schematic diagram of total length of pipe and network between solar collector and thermal storage system

4.2.14 Pressure drop in solar collector system

The common equation used to calculate the Pressure drop inside the collector can be:

$$\Delta P = f \left(\frac{L}{D} \right) \left(\frac{\rho u_{avg}^2}{2} \right) \text{-----} 4.97$$

For laminar flow; $Re \leq 2300$, $f = \frac{64}{Re}$

At average temperature, ($T_{avg} = 50^\circ C$) the property of the water is:

$$\rho = 988 \frac{kg}{m^3}; \mu = 5.47 * 10^{-4} \text{ N} \cdot \frac{s}{m^2}; k = 0.644 \frac{W}{m}; C_p = 4181 \frac{J}{kgk}; P_{sat} = 12.35 \text{ kPa}$$

$$Pr = 3.55; \dot{m} = 0.0145 \frac{kg}{s} = 0.0145 \frac{kg}{s} * 2 = 0.0276 \text{ kg/s. Volume flow rate of the fluid:}$$

$$\dot{V} = \frac{\dot{m}}{\rho} \text{-----} 4.58$$

Average velocity of the fluid in the tube

$$u_{avg} = \frac{\dot{V}}{A} \text{-----} 4.99$$

$$Re = \frac{\rho u_{avg} D}{\mu} \text{-----} 3.100$$

If $Re < 2300$ laminar flow, unless its turbulent flow. Pressure drop for fitting pipes calculated as:

$$\Delta P_f = K_f \frac{\rho u_1^2}{2} \text{-----} 3.101$$

If the bend is 90 degree and laminar flow, $K_f = 0.9$ and also Average velocity in the tube

upstream fitting is same as velocity in the header which is $u_1 = 0.0162 \text{ m/s}$. The total connection pipes length for a single collector is $L = 0.75 \text{ m}$.

The total pressure drop calculated as;

$$\Delta P_T = \Delta P_H + \Delta P_R + \Delta P_f + \Delta P_p \text{-----} 4.102$$

The total pressure loss due to viscous effect of the fluid in a single solar collector is the sum of pressure drop in all losses includes pressure drop through header, inside riser, fitting and connection pipes are tabulated in table 4.8.

Table 4.5 Total pressure drop in Solar Flat Plate Collector system

No	Parameters	Volume flow rate ($\frac{m^3}{s}$)	Area (m^2)	Average Velocity m/s	Reynolds Number	Total pressure drop Δp - (Pa)
1	Pressure drop Inside the Header (2) - ΔP_H	7.34 * 10^{-6}	4.524 * 10^{-4}	0.0162	703	0.732
2	Pressure drop Inside the Riser (10) - ΔP_R	7.34 * 10^{-7}	1.767 * 10^{-4}	4.154 * 10^{-3}	112.54	0.0613
3	Pressure Drop inside the Fitting - ΔP_f	-	-	0.0162	-	0.1181
4	Pressure Drop inside Connection pipes - ΔP_p					0.02
5	Total Pressure Drop in a single solar collector - ($\Delta P_T = \Delta P_H + \Delta P_R + \Delta P_f + \Delta P_p$)					0.9314
The total pressure drop through all of the solar collector (265 Flat Plate Collector) needed						246.821

4.2.15 Total Pressure Drop through the solar thermal system

With the intention of evaluation pressure drop over the solar collector, the pressure drop in each channel and manifold should be estimated properly.

a. Pressure drop in inlet manifold

The pump that circulates water through each collector is based on the total pressure drop that occurs following the longest path to the farthest collector. Approximating the length from the pump to the collector as 22.5 m, the total closed loop length will be 52 m. Total volume flow rate of the system;

$$\dot{V} = \text{Number of collector} * \text{volume flow rate} = 265 * 1.47 * 10^{-5} \frac{m^3}{s} = 4.65 * 10^{-3} \frac{m^3}{s}$$

The size of inlet and outlet diameter of the pipe assumed from the empirical correlation equation given below:

$$d_{pipe} \geq \sqrt{0.35 * \dot{V}} \text{-----} 4.107$$

Where, d_{pipe} and \dot{V} -pipe diameter and volume flow rate through the collector (L/hr). From the equation (4107), the minimum diameter of the pipe is 0.043 m or 43 mm is required. But, for this study the pipe having 60 mm diameter is selected $d_p = 60 \text{ mm}$.

$$A_{pipe} = \pi \frac{d_p^2}{4} = 0.00283 \text{ m}^2$$

Then average velocity is calculated as;

$$v_{avg} = \frac{\dot{V}}{A_{pipe}} = 1.643 \frac{m}{s}$$

$$Re = \frac{\rho v_{avg} d_{pipe}}{\mu} = \frac{v_{avg} d_{pipe}}{\vartheta} \text{-----} 4.108$$

Where, $\vartheta = \frac{\rho}{\mu}$ dynamics viscosity

$$Re = \frac{1000 \frac{kg}{m^3} * 1.643 \frac{m}{s} * 0.06m}{5.47 * 10^{-4}} = 1.8 * 10^5 \text{ (Since, } Re > 2300 \text{ the flow is turbulent).}$$

Relative roughness factor (ϵ): -often used for pressure drop calculations for pipes. It is an important parameter for determining friction factor (f) based on Reynold's number for flow in a pipe. Absolute Pipe Roughness of the pipe (ϵ) is a measure of pipe wall irregularities of commercial pipes. Relative roughness of a pipe is the ratio of absolute roughness to the pipe diameter.

$$\text{Relative roughness} = \frac{\epsilon}{D} \text{-----} 4.109$$

Table 4.6 Absolute Roughness Coefficient (enggyclopedia.com, 2011)

Surface Material	Absolute Roughness Coefficient - ϵ in mm
Aluminum, Lead	0.001 - 0.002
PVC, Plastic Pipes	0.0015
Fiberglass	0.005
Stainless steel	0.015
Drawn Brass, Drawn Copper	0.0015
Galvanized steel	0.15

Relative roughness $= \frac{\epsilon}{D} = \frac{0.15}{60} = 0.0025$ From the moody chart with corresponding Reynaldo's number $f = 0.0268$.

Total pressure drop for inlet and return manifolds;

$$\Delta P_{int} = f * \frac{L}{D} * \frac{\rho v_{avg}^2}{2} \dots\dots\dots 4.110$$

Pressure drop in Return manifold

$$\Delta P_{ret} = f * \frac{L}{D} * \frac{\rho v_{avg}^2}{2} \dots\dots\dots 4.111$$

b. Pressure drop in closed loop (return and supply) line

There are 2 circulation pipes; supplying hot water from solar collector to storage tank and the returning the water from the storage tank to the collector. Total length of closed loop is approximately 48 m $L = L_{supply} - L_{return}$ and diameter of the pipe is 55 mm. The total volume flow rate of the system is calculated is;

$$\dot{V} = 265 * \frac{1.47}{2} * 10^{-5} \frac{m^3}{s} = 2.323 * 10^{-3} \frac{m^3}{s}$$

$$A_{pipe} = \pi \frac{d_p^2}{4} = \pi \frac{(0.055m)^2}{4} = 0.00238 m^2$$

Then average velocity is calculated as;

$$v_{avg} = \frac{\dot{V}}{A_{pipe}} = \frac{2.323 * 10^{-3}}{2.38 * 10^{-3}} = 0.976 \frac{m}{s}$$

$$Re = \frac{\rho v_{avg} d_{pipe}}{\mu} = \frac{v_{avg} d_{pipe}}{\nu} \dots\dots\dots 4.112$$

$Re = 96,945.98$ (Since, $Re > 2300$ the flow is turbulent).

$$\Delta P_{loop} = f * \frac{L}{D} * \frac{\rho v_{avg}^2}{2} \dots\dots\dots 4.113$$

c. Pressure drop through the collector

Pressure drop through the whole collector is equal to drop pressure in a single collector time's number of collector needed.

ΔP_{loop} = drop pressure in a single collector * No of collector needs

d. Pressure Drop in bends

$$\Delta P_{bend} = K_f \frac{\rho u_1^2}{2} \text{-----} 4.114$$

Where, K_f -pressure loss factor and u_1 - Average velocity in the tube up stream of the fitting $u_1 =$

$0.25 \frac{m}{s}$. If the bend is 90° and laminar flow, $K_f = 0.9$. $\Delta P_f = K_f \frac{\rho u_1^2}{2} = 277.88 Pa$

e. Pressure drop due to inclination of the solar collector

$$\Delta P_{incl} = \rho g h_{coll} \text{-----} 4.115$$

Where, h-is height of the single collector, $h_{coll} = 0.684 m$

f. Total pressure drop in thermal system

$$\Delta P_{total} = \Delta P_{inl} + \Delta P_{ret} + \Delta P_{loop} + \Delta P_{coll} + \Delta P_{bend} + \Delta P_{incl} \text{-----} 4.116$$

Table 4.7 Total pressure drop through the solar thermal system for SWH system

No	Parameters	Total pressure drop (kPa)
1	Pressure drop in Inlet Manifold (ΔP_{inl})	17.87
2	Pressure drop in Return manifold (ΔP_{ret})	16.08
3	Pressure drop in closed loop (return and supply) line (ΔP_{loop})	11.923
4	Pressure drop through the collector (ΔP_{coll})	0.3
5	Pressure Drop in bends (ΔP_{bend})	0.278
6	Pressure drop due to inclination of the solar collector (ΔP_{incl})	6.63
7	Total pressure drop in solar thermal system (ΔP_{total})	53.081

Total specific work

$$Sp. work = Y = \frac{\Delta P_{total}}{\rho} \text{-----} 4.117$$

The maximum specific work is $54 m^2/s^2$.

Total Head

$$H = \frac{Y}{g} \text{-----} 4.118$$

The total head also calculated by using equation (4.118) and the result is approximately 7 m. The

total volume flow rate for each pump is $5.068 * 10^{-3} \frac{m^3}{s}$ or $18.245 m^3/hr$.

4.2.16 Selection of Pump

An active water circulation system of solar thermal water heating system is used to move the HTF from the storage tank to the solar collector in systems of pressurized. A solar system needs to move the cold water from the source to its demands. Since, the source is at a lower elevation than the thermal system and the user and the water must be raised to a higher level by external force to increase thermal system performance. The pump selection for SWH system is depending on amount water required to flows through the collector. Factors affects the selection of a specific component for SWH system are the amount of water that needs to be heated, Relative cost and efficiency, Simplicity of operation and Climate conditions in which the system will be used. The pumps are sized to get the best static and dynamic head pressure requirements in order to meet specific system design and performance flow rates. Among types of a pump, active solar systems use centrifugal pumps and selected pump is based on the following consideration: -

- ✓ System type (direct or indirect) and Heat collection fluid.
- ✓ Operating temperatures and Required fluid flow rates.
- ✓ Head or vertical lift requirements and Pressure drop due to friction losses.

Right selection of the centrifugal pump

Technical specification

Type	Electric drive centrifugal pump (PST-A70M/50Hz)
Application	Pumping of water for domestic
Maxi. Capacity	up to 409.14 gpm.
Max. Head	up to 60.7 m
Max. Operating pressure	800 kPa/8 bar
Temperature of pumped liquid:-10°C to +90°C.	

MOTOR

Type	3 phase
Rated power	0.75 kW
Voltage:	380-415 V
Frequency	50 Hz
Poles	2 poles

CHAPTER 5

5. Design and Performance Analysis of Solar Thermal Storage system for SHW

Due to time dependent nature of solar energy, thermal storage system is compulsory. Thermal reservoir tank is one of the most components in solar water heating system which stores the hot water coming from the solar collectors and the tanks are equipped with insulation to reduce heat loss. The providing and improving of a solar TES can reduce an auxiliary energy consumption to a great extent and increase solar load fraction substantially which conserving the valuable fossil fuel reserves and electric power. There are two techniques of store hot water for AHMC:

- A. Conventional solar hot water storage and
- B. Solar hot water storage with integrating phase change materials.

Under this chapter both conventional (sensible) and storage with packed thermal storage materials will discussed and comparisons occur to prefer the preeminent hot water storage for long period of time because the hospitals functions for 24 hours.

5.1 Numerical Investigation of Conventional Solar Thermal Storage System

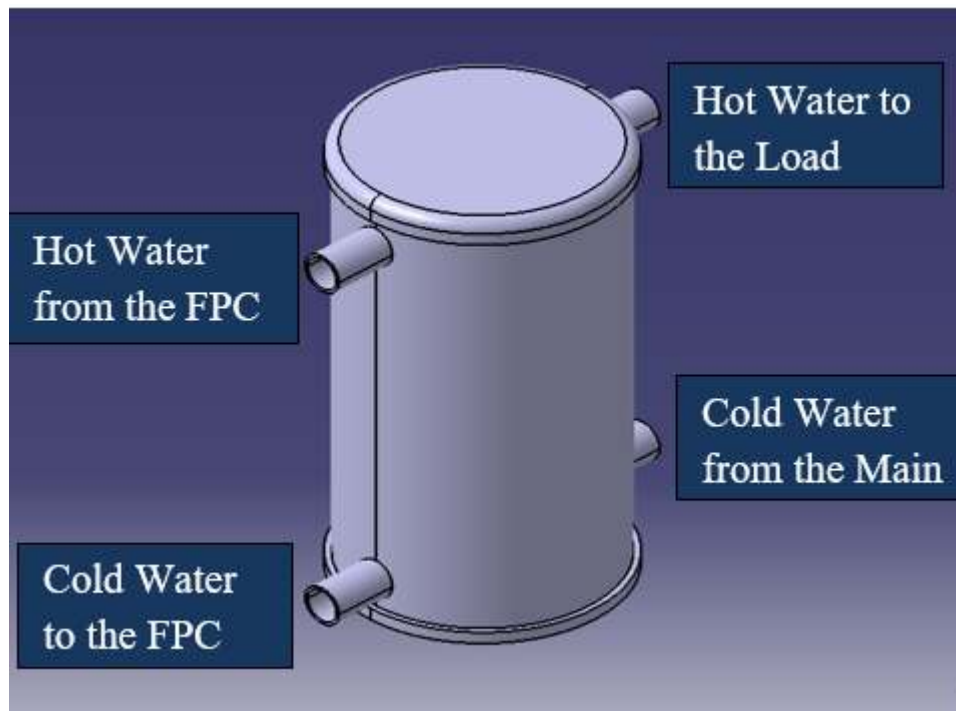


Figure 5.1 Schematic diagram of Sensible thermal storage tank for solar water heating system

5.1.1 Material Selection of Thermal Storage Tank

Materials for solar energy systems must be chosen very prudently with considering the most important factors such as safety, performance, durability and cost. Hot Water may be stored in copper, steel, galvanized metal, or concrete tanks. Whatever storage vessel is selected, it would be well insulated and large tanks and also recommended value of overall heat transfer coefficient is (0.57-1.13) W/m² K. However, storage tank with selective galvanization outer cover (fiber glass) have high efficiency in maintaining constant operating temperature of the storage tank by minimizing heat loss from the tank to the surrounding. In this study, mild steel plate storage tank is selected due to its low thermal conductivity, higher durability, lower cost of heat loss per cost of thickness and lower maintenance cost.

5.1.2 Modeling of the Sensible Thermal Storage for Solar System

Volume of thermal storage tank

The storage tank can be sized according to the daily heating load requirements. The recommend tank capacities ranging from 50 to 200 L per m² of collector for an annual system performance to be insensitive to tank capacity. A standard storage tank capacity of 75 L per m² of collector is used in solar water heating system design procedure (Hughes, 2006). The maximum volume capacity of hot water storage tank used to accomplish the total load HWD for hospital is 54 m³ and to achieve, two storage tank with each capacity of 27 m³ is looked-for. Occasionally, because of the required storage volume, more than one tank is used instead of one large one, if such a large-capacity tank is not available. Additional tanks offer, in addition to the extra storage volume, increased heat transfer surface and reduced pressure drop in the collection loop. The solar storage tanks usually used in domestic systems are within the range of aspect ratios H/D = 1.5 to 3.5. Assume, the geometry of the reservoir tanks are a right cylinder with height to diameter ratio of 2. So, the height of storage tank is given as:

$$h = 2 * D_i \text{ ----- 5.1}$$

Thermal storage tank diameter and height calculated from the volume of storage tank as:

$$V_{st} = \pi \frac{D_i^2}{4} h = \pi \frac{D_i^2}{4} (2 * D_i) = \pi \frac{D_i^3}{2} \text{ (m}^3\text{) ----- 5.2}$$

Internal diameter of a storage tank is founded as the following:

$$D_i = \frac{\sqrt[3]{2V_{st}}}{\pi} \text{ ----- 5.3}$$

Hence the two sensible storage tank with each have the capacity of 27 m³ should needs. The thermal storage tank required for the hospital has a parameters of $D_i = 2.58$ m & $h = 6.16$ m. Considering the surface area of thermal storage tank is used to recognize the space it occupies the place it for hospital that helps for proper space consumption tank.

$$A_s = \pi D_i h + 2 * \left(\pi \frac{D_i^2}{4} \right) = \frac{5\pi}{2} D_i^2 \text{-----5.4}$$

5.1.3 Optimization of Storage Tank and Insulation Thickness

Thermal insulation systems have been used in reduce heat loss from surfaces, control the process and surface temperatures, and provide a comfortable indoor thermal environment. To minimize the energy and insulation costs in addition to reducing the heat loss to the surroundings, the thickness of the insulation material needs to be optimized. The motivation for including pipe insulation is often to minimize the total cost, which includes the cost of the insulation, its installation and maintenance as well as the cost of the energy loss by convective or radiative heat transfer.

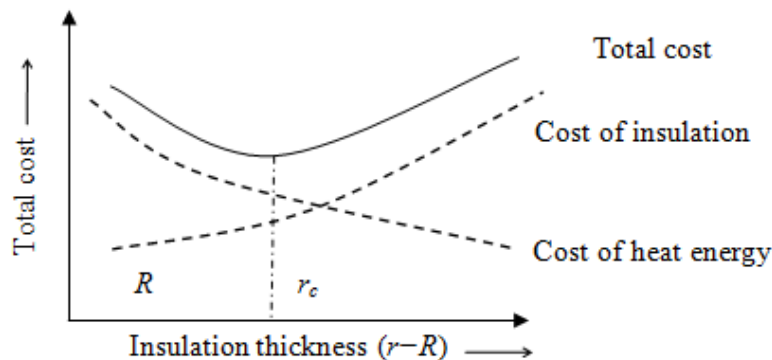


Figure 5.2 Optimization of insulation thickness from Sahu et al., (2015)

As shown in figure (5.2), the optimum insulation thickness can be determined at which the sum of the insulation cost and the cost of the heat loss is minimum (minimum total cost).

5.1.3.1 Insulation Thickness

The concept of an economic thermal insulation thickness considers an initial cost of the insulation system plus ongoing value of the energy savings over the expected service lifetime.

Cost of Insulation Thickness: -Glass fiber material is selected for the insulation of thermal storage tank and the cost of glass fiber gathered from market that is given as 0.3\$ or 9 birr/thickness (mm) per unit area (m²). The cost of glass fiber (CGF) estimated as:

$$CGF = \left(\frac{\text{Cost}}{\text{mm}} \right) * t_i(\text{mm}) = 9 \text{ Birr/mm} * t_i(\text{mm}) \text{-----5.5}$$

Price of Heat Loss: -The cost of energy per KWh in Ethiopia is equal (1.716 Birr/KWh). Then, the cost of heat loss (CHL) given by:

$$\text{CHL} = (\text{Cost}/_{\text{kWh}}) * Q_L(\text{kWh}) \text{-----} 5.6$$

Neglecting, the effect of the storage tank material on heat transfer, the temperature difference across the insulation is taken as ($\Delta T = T_s - T_a$). The rate of heat loss from the storage tank is given by:

$$Q_L = U_L A_S \Delta T = (U_L A)_S (T_s - T_a) \text{-----} 5.7$$

The overall heat loss coefficient (U_L) by the insulation of storage tank is:

$$U_L = U_{\text{ins}} + h_{\text{ina}} \text{-----} 5.8$$

Heat loss coefficient through insulation given as:

$$U_{\text{ins}} = k_{\text{ins}}/t_{\text{ins}} \text{-----} 5.9$$

The convective heat loss coefficient from insulation to ambient is given as:

$$h_{\text{ins-amb}} = 2.8 + 3V_w \text{-----} 5.10$$

Where, V_w & k_{in} are average wind speed ($2.95 \frac{\text{m}}{\text{s}}$) and thermal conductivity of the glass fiber ($0.036 \frac{\text{W}}{\text{m} \cdot ^\circ\text{C}}$) respectively.

Then, the overall heat loss coefficient (U_L) is calculated as:

$$U_L = \frac{0.036 \text{ W/mK}}{t_{\text{in}}} + 11.65 \text{ W/m}^2\text{K} \text{-----} 5.11$$

Therefore rate of heat loss from the tank is then equal to:

$$Q_L = \left[\left(\frac{0.036}{t_{\text{in}}} + 11.65 \right) A_S \Delta T \right] \text{-----} 5.12$$

By substituting the value of area A_S and change of temperature ΔT into equation (5.12); the rate of heat loss from the tank in a 24 hour is then given as:

$$Q_L = \left(\frac{1670}{t_{\text{in}}} + 540.864 \right) \text{ kWh} \text{-----} 5.13$$

Finally, the cost of heat loss from the tank calculated as:

$$\text{CHL} = \left(\frac{835}{t_{\text{ins}}} + 270.4 \right) \text{ Birr} \text{-----} 5.14$$

Total Cost: -Total cost is the sum of insulation material cost and heat energy loss cost. The relation between total cost and thickness insulation of the storage tank is given as:

$$\text{TC} = \text{CGF} + \text{CHL} \text{-----} 5.15$$

$$TC = \left[(9 * t_{in}) + \frac{835}{t_{in}} + 270.4 \right] \text{Birr} \text{-----} 5.16$$

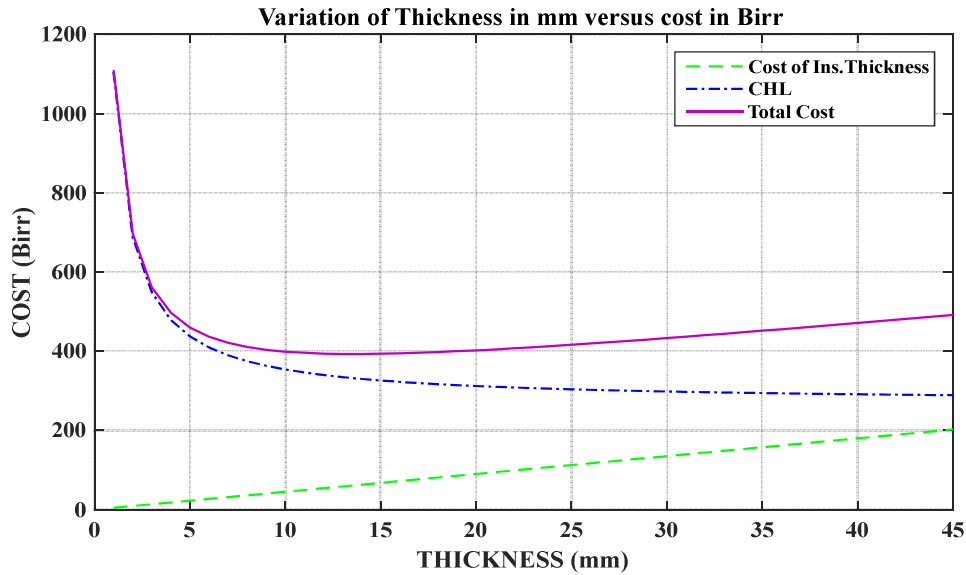


Figure 5.3 Optimum insulation thickness and cost

To obtain the specific value of insulation thickness for modeling, differentiating the total cost equation (6.11a) with respect to the thickness and setting it equal to zero.

$$\frac{dTC}{dt_{ins}} = 0 \text{-----} 5.17$$

At the end, the optimum value of insulation thickness is $t_{ins} = 13.6219 \text{ mm} \approx 14 \text{ mm}$ and for safety and long year operation storage tank insulation thickness $t_{ins} = 20 \text{ mm}$ is carefully chosen.

5.1.3.2 Sensible Thermal Storage Tank Thickness

It ought to be recognized that thickness of the reservoir tank does not eliminate heat transfer; it only reduces it. The thicker the storage tank, the lower is the rate of heat transfer but the cost of storage tank material is highest. For this reason, it should be needs to an optimize thickness and outer diameter of storage tank which corresponds to a least combined cost of storage tank material and heat lost. Now, consider the material cost that corresponding with the thickness. Cost of storage tank material (CSTM) is informed from the market as 135 Birr/thickness (mm) per unit area. Thus;

$$CSTM = (\text{Cost}/\text{mm}) * t_{st}(\text{mm}) = 135 * t_{st} \text{ Birr} \text{-----} 5.18$$

Cost of heat loss from the reservoir (CHL) is determined depends on power energy cost in Ethiopia. The latest energy cost per kWh is 1.716 Birr/kWh.

$$CHL = (\text{Cost}/\text{kWh}) * Q_L(\text{kWh}) \text{-----} 5.19$$

$$Q_L = U_L A_{St} \Delta T \text{-----} 5.20$$

$$U_L = U_{in} + h_{ina} + U_s + h_{ws} \text{-----} 5.21$$

The heat loss through storage tank material given as:

$$U_s = k_s / t_s \text{-----} 5.22$$

Convective heat loss coefficient from water to tank is given as:

$$h_{ws} = Nu_w k_w / d_i \text{-----} 5.23$$

Therefore, the overall heat loss coefficient (U_L) is calculated as:

$$U_L = (64 / t_{st} + 16.95) \text{ W/m}^2\text{K} \text{-----} 5.24$$

Therefore rate of heat loss from the tank is then equal to:

$$Q_L = [(64 / t_{st} + 16.95) \text{ W/m}^2\text{k}] A_S \Delta T \text{ kWh} \text{-----} 5.25$$

By substituting the value of area A_S and change of temperature ΔT into equation (6.16a); the rate of heat loss from the tank in a 24 hour is then given as:

$$Q_L = [(2971.2 / t_{st} + 787.2)] \text{ kWh} \text{-----} 5.26$$

The cost of heat loss from the tank is given as:

$$CHL = (1485.6 / t_{in} + 393.6) \text{ Birr} \text{-----} 5.27$$

Total cost is the sum of storage tank material cost and heat energy loss cost.

$$TC = CSTM + CHL \text{-----} 5.28$$

$$TC = [135 * t_{st} + 1485.6 / t_{in} + 787.2] \text{ Birr} \text{-----} 5.29$$

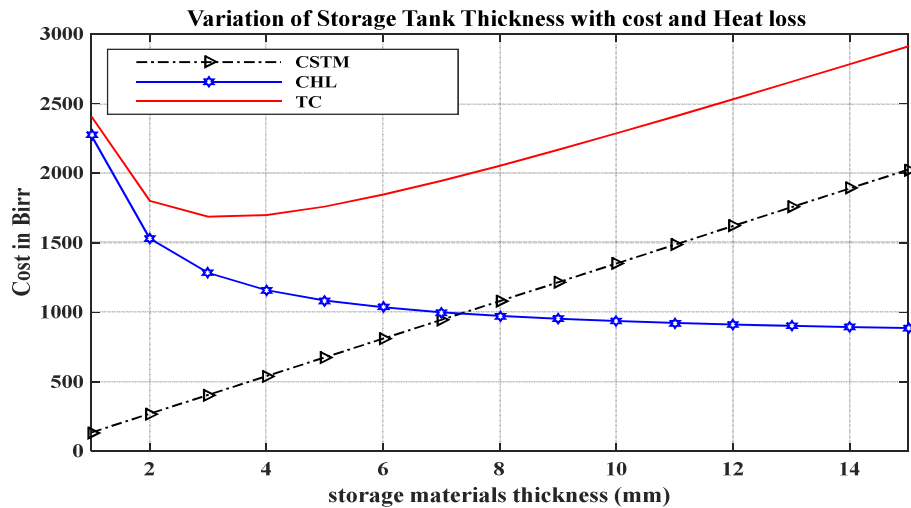


Figure 5.4 Sensible thermal storage tank thickness

Specifically, the value of insulation thickness for modeling is obtained by the differentiating the total cost equation (5.29) with respect to the thickness and setting it equal to zero.

$$\frac{dTC}{dt_{ins}} = 0 \text{-----} 5.30$$

The optimum value of insulation thickness is $t_{st} = 3.5\text{mm} \approx 4 \text{ mm}$ (for strengthen the tank wall).

An outer diameter of thermal storage tank is calculated as the following.

$$D_o = D_i + 2t \text{-----} 5.31$$

Where, $t = t_{ins} + t_{st} + t_{gv} = (20 + 4 + 1)\text{mm} = 25 \text{ mm}$

An external diameter of the storage tank is calculated and the result is 2.65 m.

5.1.4 Transient Analysis of Thermal Storage for Solar Hot Water System

An initial thermal analysis was performed to determine the performance of the solar water heater and aid in decisions regarding design modifications.

Assumptions and Conditions

Assumptions used in deriving the governing equation include:

- Inlet temperature of the system is an ambient temperature T_{amb} .
- The (cold) supply water temperature at T_{amb} or 23°C for Adama weather climate.
- The inlet water temperature to the collector would be the same as the mean storage tank water temperature.
- The temperature of the water entering the tank would be the same as the outlet water temperature of the collector.

Governing Equation

The thermal analysis assumes a lumped capacitance model for fluid in the tank. An energy balance on the system yields. Thus, the net energy stored in the water is equal to the net solar irradiation (insolation) minus thermal losses through the SWH and the flow of water out of the SWH to load and that is refilled at the same rate by cooler water supplied to the SWH. Applying the first law of thermodynamics over the control volume gives as the thermal energy balance of the storage tank.

$$E_{st} = E_{in} - E_{out} \text{-----} 5.32$$

$$Q_{st} = Q_u - Q_{loss} - Q_{load} \text{-----} 5.33$$

To determine the transient analysis of performance of the storage tank, finite difference schemes formed as the following. And also, to solve for the temperature distribution in the storage tank, a

set of N first-order, ordinary differential equations resulting from each node's energy balance (Newton, 1995) is assembled, and energy balance written about the i^{th} tank node is calculated as:

$$\frac{dT_s}{dt} = \frac{T_s^{t+\Delta t} - T_s^t}{\Delta t} \text{-----} 5.34$$

$$T_s^{t+\Delta t} = \frac{\Delta \tau}{(\rho c_p)_w V_s} [\dot{m} c_p (T_{f,i}^t - T_s^t) - (UA)_s (T_s^t - T_{\text{amb}}^t) + T_s^t] \text{-----} 5.35$$

$$T_s^{t+\Delta t} = A17 * \Delta \tau * T_{f,i}^t + A18 * \Delta \tau * T_{\text{amb}}^t + A19 * \Delta \tau * T_s^t \text{-----} 5.36$$

Where, $A17 = \frac{\dot{m} c_p}{(\rho c_p)_w V_s}$ and $A18 = \frac{(UA)_s}{(\rho c_p)_w V_s}$

$$A19 = 1 - (A17 + A18)$$

$T_s^{t+\Delta t}$ –New storage tank temperature after time interval (Δt). The furthestmost time period for this estimation is an hour because the solar radiation data are available on an hourly basis.

Initial condition and Boundary condition for storage tank

- The inlet water temperature to the collector would be the same as the mean storage tank water temperature. The temperature of the water entering the tank equal to the outlet hot water temperature of the collector. At initial time, the mean temperature of storage tank is equal to ambient temperature (23°C).

5.2 Performance Analysis of Solar Thermal Storage Tank Integrated with Phase Change Materials (PCM)

Modern technologies are being developed to extract energy from every available source and store the excess energy produced for later usage. One of the encouraging forms to store thermal energy is latent heat TES that can significantly enhance the performance of the SWH system, afford a smaller volume, lower cost and more efficient energy storage system compared to the other forms. TES systems based on latent heat are the most efficient alternative than other methods. Besides, these systems have a high energy density compared to sensible heat storage systems. The use of a latent heat thermal storage system using PCMs is an effective way of storing thermal energy with high-energy storage density and the isothermal nature of the storage process. It offers storage densities that are typically 5 to 10 times higher and half the volume of sensible heat thermal energy storage (Demirbas, 2006).

5.2.1 Thermal Storage Tank Integrated with incorporating PCM

The storage tank carries the water that has been heated via the solar collector. A cylindrical shape is preferable since it reduces the loss of heat. Besides, the heat exchange of water occurs inside the tank and a control system facilitates the charging and discharging of the thermal energy. With the purpose of intensification the heat capacity of thermal storage, PCM can be added into the hot water storage tank which typically the PCM in the form of cylindrical are inserted into the tank. The heat transfer fluid (HTF) used is hot water which comes from the flat plate collector. During the daytime, paraffin wax absorbs the heat from the water and stores it to use at night. Therefore, using water tanks for thermal energy storage has advantages of heat losses and volume in the tank should be minimized, and the tank should be properly designed for stratification. Furthermore, the tank should be large enough to store a sufficient amount of water to meet the peak daily demand. The geometry of the system is based on a configuration of shell and tube heat exchanger whose shell is filled with PCM while the HTF flows in the tube side.

5.2.2 Benefits of integrating PCM with Solar DHW Storage System

A PCM is a substance with a high heat of fusion which is melting and solidifying at a certain temperature, and is capable of storing and releasing large amounts of energy. Incorporating PCM to the storage tank is aimed to compensate the heat losses from the storage and to reheat the water after a period of discharge. So, these effects would improve the availability of hot water to the end-

user. Analysis of the performance of the PCM within the DHW system was usually addressed the following main aspects: -

- Heat transfer between the PCM and the surrounding water during charging process.
- The static behavior of a storage tank with PCM.
- Derive how long the storage can maintain a suitable temperature in readiness for end-user withdrawal and the recovery of heat from the PCM after a complete discharge.

5.2.3 Modes of Thermal Energy Storage System

There are three modes of a storage system which operates on:

Charging mode: - is start with circulation of the hot HTF heated in the collector system at a temperature higher than the PCM melting temperature. During this period, hot HTF enters the tube side at the top, transfers heat to the solid PCM and then HTF exits at the bottom of tubes. This mode occurs during day time and terminates with complete melting of the PCM, charging of the store does not terminate with complete melting of the PCM. If the inlet fluid temperature is above the melt temperature, charging of sensible heat continues.

Discharging mode: - is started by circulation of the cold HTF having inlet temperature lower than the PCM melting temperature. The cold HTF enters the system at bottom is heated by the storage PCM, and then exits at the top. This mode terminates with complete solidification of the PCM.

Standby mode: -This mode occurs when there is no further storage of energy occurring because of the thermal storage tank is completely charged or the energy is directly fed to the utility without using storage. There is no flow of HTF in the tube side and heat transfer within the system is dominated by axial conduction which acts to redistribute the axial temperature gradient formed in the system during charging. This is the transition period between the charge and discharge modes.

In this study, a one-dimensional heat transfer model for the charging process is developed for either a sensible or latent heat-absorbing process by using the basic conservation of energy principle. The time-dependent variables are discretized by using an explicit finite difference Scheme. And also for spatial variation, a finite difference scheme is used to discretize for solving a charging mode.

5.2.4 Design Consideration

The thermal storage material can be chosen based on availability, cost and compatibility. The major factors to be considered in the design of a LHTES unit containing a PCM include:

- The storage capacity of the tank.

- The configurations of the transfer fluid.
- The type of heat transfer fluid.
- Temperature limits with in which the units is to operate.
- The thermo-physical properties of PCM.

5.2.5 Design Assumption

- The hot water thermal storage tank is insulated to reduce heat loss to surrounding.
- The temperature of the HTF at the entry of storage tank is equal to the exit of solar FPC.
- The thermophysical properties for both HTF and PCM were constant with respect to T° .
- The initial temperature of the storage was uniform and it was in melting temperature.
- The HTF entering inside was laminar flow, and incompressible fluid.
- The thermal conduction in the axial direction is neglected for both PCM and HTF.

5.2.7 Sizing of Latent Heat TES System for Solar Heating application

A PCM storage tank is sized according to the required storage capacity under a rated operating condition. The cylindrical LHTES unit proposed for this study consists of concentric tubes whereby the HTF and PCM are segregated. The HTF flows through the inner tubes and exchanges heat with the PCM in the surrounding region (Tehrani al.et. 2016).

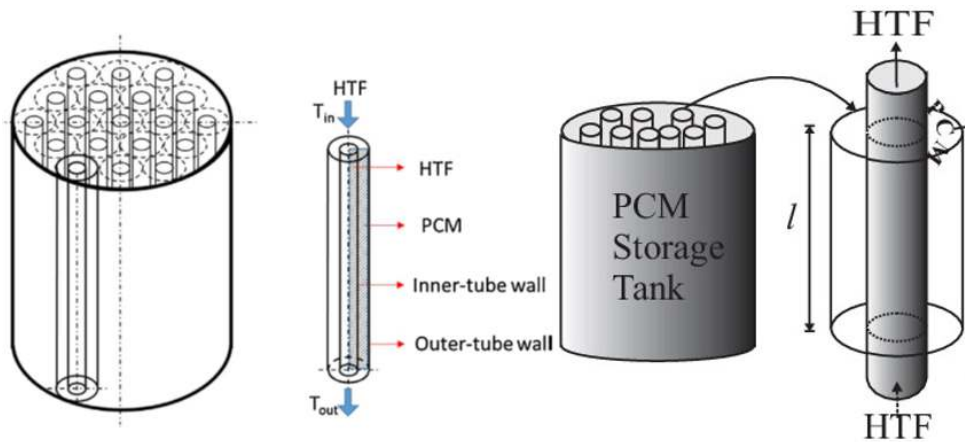


Figure 5.5 Schematic configuration of shell and tube latent heat thermal energy storage system (LHTES) unit with complete system, and concentric cylinders.

The thermal storage system under investigation consists of a shell and tube heat exchanger in Figure 5.6. The Heat Transfer Fluid (HTF) flows inside the tubes, are arranged in a regular pattern. For simplicity, in the PCM fictitious coaxial circular cylinders (tangent one to another) around every tube can be considered limiting the analysis to one single tube.

5.2.8 General Procedure for sizing LHTES unit for Solar Water Heating System

a. Selection of phase change material

PCMs are crucial components in the design of latent heat energy storage systems. The PCM used in the design of thermal-storage systems requires a desirable thermo-physical, kinetics chemical and economical properties (mentioned in Table 2.2). The selection of a PCM for a solar domestic hot water system should be made prudently in order to produce hot water at desirable range of temperatures and minimize safety concerns. So, the phase change material used is a Paraffin wax (n-Heptacosane) which has a melting point of 59°C with its thermo-physical properties are presented on the table 5.3 by Sharma et al., (2009).

Table 5.1 Thermophysical properties of selected Paraffin wax (n-Heptacosane) in design of SWH system.

Melting temperature (°C)	Latent heat of fusion (h_{pcm}) kJ/kg	Density kg/m ³		Specific heat J/kg°C		Thermal conductivity W/m°C	
		Solid	Liquid	Solid	Liquid	Solid	Liquid
59	236	861	780	1850	2384	0.21	0.15

b. Selection of working fluid (HTF)

The working fluid which is used as heat transfer fluid is water.

c. Determination of latent heat exchanger effectiveness

Effectiveness of LHTES is estimated at the beginning of the process (charging), when storage materials is in solid form and the inlet temperature of the fluid at the LHTS is fixed. Considering the conventional heat exchanger having capacity ratio (CR) defined by (Lienhard, 2006):

$$CR = \frac{c_{min}}{c_{max}} \text{-----} 5.37$$

So, effectiveness of heat exchanger given as:

$$\varepsilon = \frac{1 - \exp(-NTU(1+CR))}{1+CR} \text{-----} 5.38$$

For all condition $CR = 0$, since one side of the HX is isothermal (PCM is at melting temperature).

$$\varepsilon_{max} = 1 - \exp(-NTU) \text{-----} 5.39$$

$$NTU = \frac{AU}{mC_p} \text{-----} 5.40$$

d. Determination of parameters

The rate heat stored in HTF water:

$$Q_{HTF,total} = \int_0^t \dot{Q}_{HTF} dt \text{-----} 5.41$$

Then, the size of the LHTES unit calculated as:

$$V_{LHTS} = \frac{Q_{HTF,total} (W)}{\rho_{pcm,s} C_{P,s} (T_m - T_{ci}) + \rho_{pcm,l} h_{pcm} + \rho_{pcm,l} C_{P,l} (T_{co} - T_m)} (W/m^3) \text{-----} 5.42$$

Where, V_{PCM} -total volume of PCM of LHTES unit (m^3) and ε is a porosity; $Q_{HTF,total}$ -total heat energy capacity stored by water; $C_{P,s}$ and $C_{P,l}$ -specific heat of solid and liquid PCM (1.85 kJ/kg.k and 2.384 kJ/kg.k) respectively; $\rho_{pcm,s}$ and $\rho_{pcm,l}$ -density of solid and liquid PCM (861 kg/ m^3 and 780 kg/ m^3); h_{pcm} -latent heat of PCM, paraffin wax (236 kJ/kg); T_{co} , T_{ci} and T_m -outlet fluid or HTF temp, inlet fluid temp and melting temperature of paraffin wax, ($T_m = 59^\circ C$).

From the equation 5.42, the total volume of storage tank of LHTS with integrating paraffin wax is 39.52 m^3 . For determining the geometric parameters with aspect ratios H/D is 1.75, the diameter and length of the LHTS system are 3.076 m and 5.383 m and the porosity is 0.45. Equation 5.43 is used to compute mass of PCM is needed to store a certain amount of energy provided by solar collectors. So, total amount of paraffin wax needed given as:

$$m_{PCM} = (1 - \varepsilon) \rho_{pcm,s} V_{pcm} \text{-----} 5.43$$

Total number of shell and tube can be calculated by:

$$N_t = \frac{V_{pcm,total}}{V_{pcm,single}} \text{-----} 5.44$$

Selection of Geometric parameters

Determining the container LHTS unit of PCMs, geometric parametric design of shell and tube and several tubes in a shell should be computed. A comprehensive set of geometric parameters was used for that purpose is offered the non-dimensional radius ($R/r_{i,t}$) from 1.3 to 3 with tube length (L) range from 1- 5 m by Tehrani et al., (2016). The range of geometric parameters selected with values of $L = 1.5$ m; $0.03 < R_{sh,o} < 0.13$ and $0.01 < r_{t,i} < 0.1$. For this study, it takes the internal radius of the tube, $r_{t,i} = 0.06$ m and outer radius of the cylindrical shell is $R_{sh,o} = 0.12$ m. Where R_o and $r_{t,i}$ are an outer radius of the shell and inner radius of the tube respectively. To reduce the heat losses to the environment, the outer wall and the piping system was insulated with 20 mm thickness. In the LHTS unit, the total volume required to incorporate paraffin wax is 5.6 m^3 . This is the total volume needs to fill the paraffin wax (n-Heptacosane). Hence the storage unit is shell and tube configuration the single shell side filled by PCM has a volume of 0.055 m^3 and each shell has its own tube with 0.017 m^3 which HTF is flow through it. The total number of tube

used to fulfill the required demand is approximately 102. An amount of Paraffin wax required to store amount of energy provided by solar FPC is 2,651.88 kg.

5.2.9 Modeling and Simulation of Shell and Tube LHTES with integrating paraffin wax

This study leads to an analysis of the formulation of a mathematical model that defines moving solid-liquid interfaces. The transient heat transfer between the operating fluid (HTF) and the PCM is numerically investigated using a finite difference scheme. The numerical investigation of the shell and tube LHTES system employing numerical model and simulation with a MATLAB software package. The energy conservation is expressed in terms of total volumetric enthalpy and temperature for constant thermo-physical properties by equation 5.45.

$$\frac{\partial \rho H}{\partial t} + \nabla \cdot (\rho v H) = \nabla \cdot (k \nabla T) \text{-----} 5.45$$

Where, H -total volumetric enthalpy that is the sum of sensible and latent heats

$$H = h + \gamma h_{pcm} \text{-----} 5.46$$

$$h = h_{ref} + \int_{T_{in}}^T C_p dt \text{-----} 5.47$$

γ -refers to liquid fraction and indicates the fraction of a cell volume in liquid.

In order to determine the PCM state (solid, liquid or undergoing phase change), the liquid fraction:

$$\gamma = \begin{cases} 0 & T < T_{solidus} \\ (T - T_s)/(T_l - T_s) (0 < f < 1) & T_s \leq T \leq T_{liquidus} \\ 1 & T > T_{liquidus} \end{cases} \text{-----} 5.48$$

The energy equation becomes:

$$\frac{\partial \rho H}{\partial t} + \nabla \cdot (\rho v h) = \nabla \cdot (k \nabla T) - \frac{\partial \rho f h_{pcm}}{\partial t} - \nabla \cdot (\rho v f h_{pcm}) \text{-----} 5.49$$

The governing equations of the problem are the energy conservation equations written for the HTF (Heat Transfer Fluid), the wall and the PCM in a cylindrical orientation system. The main heat exchange mechanism within the HTF is convection. So, it is possible to model the heat transfer within the HTF through the definition of a convective heat transfer coefficient h . The computational domain is discretized using 12 nodes in the axial direction (Fortunato, 2012).

Convective heat transfer coefficient

Heat transfer starts as soon as HTF enters the tube, and the velocity and temperature profile start developing simultaneously. Cross sectional Area of the tube is given by:

$$A_t = \frac{\pi}{4} * D_t^2 = \frac{\pi}{4} * 0.06^2 = 0.00283 \text{ m}^2$$

$$\text{Average velocity of the HTF also; } u_m = \frac{\dot{m}}{\rho A_t} = \frac{0.0145}{988 * 0.00283} = 0.0052 \frac{\text{m}}{\text{s}}$$

$$\text{Reynold's number; } Re = \frac{\rho u_m D_t}{\mu} = \frac{988 * 0.0052 * 0.06}{5.47 * 10^{-4}} = 562.52$$

Since, the $Re < 2300$; then the flow is Laminar flow through the tubes.

$$\text{The prandtl number; } Pr = \frac{C_p * \mu}{K(T_{avg})} = \frac{4.2 * 10^3 * 5.47 * 10^{-4}}{0.64} = 3.589$$

$$\text{Nusselt number is obtained as; } NU = 1.86 * \left(Re Pr \frac{D_i}{L} \right)^{\frac{1}{3}} = 8.04$$

Finally, the value of the convective heat transfer coefficient calculated as:

$$h_f = \frac{NU * K(T_{avg})}{D_i} = \frac{8.04 * 0.64}{0.06} = 85.76 \frac{W}{m^2 K}$$

Energy conservation equation

The phase change can be taken into account in the heat equation using either the effective heat capacity method or the enthalpy method. The two methods have the advantages of allowing to use one formulation of the heat equation for the entire domain and of avoiding to solve the melting front position. In this study, the effective heat capacity is used to model the heat transfer due to the phase change because it gives reliable results. The basic equations for the PCM material:

$$\frac{\partial h_{pcm}}{\partial t} = \frac{\partial h_{pcm}}{\partial T} \frac{\partial T}{\partial t} = C_{PCM}(T) \frac{\partial T}{\partial t} \text{-----} 5.50$$

Where, $C_{PCM}(T)$ - analytical expression of the effective heat capacity

To avoiding the difficulty of discretization of the product the enthalpy becomes:

$$\frac{\partial H}{\partial t} = \frac{H(T^{i+1}) - H(T^i)}{\Delta t} = \frac{C_p [(T^{i+1}) - (T^i)]}{\Delta t} \text{-----} 5.51$$

a. Heat Transfer Fluid (HTF)

$$\rho_{HTF} C_{HTF} \frac{\partial T_{HTF}}{\partial t} = - \frac{\dot{m}_{HTF} C_{HTF}}{A_{t,HTF}} \frac{\partial T_{HTF}}{\partial y} + \frac{h \pi D_i}{A_{t,HTF}} (T_w - T_{HTF}) \text{-----} 5.52$$

Where, ρ_{HTF} , C_{HTF} and \dot{m}_{HTF} -density, specific heat and mass flow rate of HTF respectively.

h , D_i and $A_{t,HTF}$ - Convective heat transfer coefficient, internal tube diameter and tube cross section area of HTF respectively.

For discretization partial differential equation the finite difference scheme is: -

$$\frac{\partial T_{HTF}}{\partial t} = \frac{T_i^{\Delta t + \tau} - T_i^t}{\Delta \tau} \text{-----} 5.53$$

$$\frac{\partial T_{HTF}}{\partial y} = \frac{T_{HTF,i}^{\Delta t + \tau} - T_{HTF,i-1}^{\Delta t + \tau}}{\Delta y} \text{-----} 5.54$$

$$\frac{T_{HTF,i}^{\Delta t + \tau} - T_{HTF,i}^t}{\Delta \tau} = \frac{1}{\rho_{HTF} C_{HTF}} \left(\frac{\dot{m}_{HTF} C_{HTF}}{A_{t,HTF}} \left(\frac{T_{HTF,i}^{\Delta t + \tau} - T_{HTF,i-1}^{\Delta t + \tau}}{\Delta y} \right) + \frac{h \pi D_i}{A_{t,HTF}} (T_{w,i}^t - T_{HTF,i}^t) \right) \text{-----} 5.55$$

New temperature of HTF for each nodes are solved by the following equation.

$$T_{HTF,i}^{\Delta t+t} = \left(\frac{1}{1-AA*\frac{\Delta t}{\Delta y}} \right) * \left[(1 - \Delta t * BB) * T_{HTF,i}^t + AA * \frac{\Delta t}{\Delta y} * T_{HTF,i-1}^{\Delta t+t} + \Delta t * BB * T_{w,i}^t \right] \text{-----} 5.56$$

$$AA = \frac{\dot{m}_{HTF}}{\rho_{HTF} A_{t,HTF}} \text{-----} 5.57$$

$$BB = \frac{h\pi D_i}{\rho_{HTF} C_{HTF} A_{t,HTF}} \text{-----} 5.58$$

Where, $T_{HTF,i}^{\Delta t+t}$ - New temperatures of the heat transfer fluid at nodes i.

$T_{w,i}^t$ and $T_{HTF,i}^t$ - The previous time nodal temperature of wall and HTF at time t.

b. Wall

$$\rho_w C_w \frac{\partial T_w}{\partial t} = \frac{1}{\delta_w} \left(\frac{k_w A_{l,w}}{A_{t,w}} + R_w + \frac{k_{PCM} A_{l,PCM}}{A_{t,w}} \right) * (T_{PCM} - T_w) + \frac{h\pi D_o}{A_{t,w}} (T_{HTF} - T_w) \text{-----} 5.59$$

Where, A_w and δ_w -are the cross section area of the wall and thickness of the wall respectively; k_w and k_{pcm} are the thermal conductivity of the wall and the PCM, respectively; R_w -tube wall resistance is negligible; and $A_{l,w}$ and $A_{l,pcm}$ are the liquid side surfaces of the wall and the PCM, respectively.

Finite difference form:

$$\frac{T_{w,i}^{\Delta t+t} - T_{w,i}^t}{\Delta t} = \left(\frac{k_w A_{l,w}}{A_{t,w}} + \frac{k_{PCM} A_{l,PCM}}{A_{t,w}} \right) \frac{(T_{PCM,i}^t - T_{w,i}^t)}{\delta_w \rho_w C_w} + \frac{h\pi D_i}{A_{t,w} \rho_w C_w} (T_{HTF,i}^t - T_{w,i}^t) \text{-----} 5.60$$

$$T_{w,i}^{\Delta t+t} = (1 - \Delta t * CC - \Delta t * DD) T_{w,i}^t + \Delta t * CC * T_{HTF,i}^t + \Delta t * DD * T_{PCM,i}^t \text{-----} 5.61$$

$$CC = \frac{h\pi D_i}{A_{t,w} \rho_w C_w} \text{-----} 5.62$$

$$D = \frac{1}{\delta_w \rho_w C_w} \left(\frac{k_w A_{l,w}}{A_{t,w}} + \frac{k_{PCM} A_{l,PCM}}{A_{t,w}} \right) \text{-----} 5.63$$

Where, $T_{w,i}^{\Delta t+t}$ - New temperatures of the tube wall at node i.

$T_{w,i}^t$, $T_{PCM,i}^t$ and $T_{HTF,i}^t$ - The previous time nodal temperature of wall, PCM and HTF at time t.

c. Phase Change Materials (PCM)

The generic cell of the PCM;

$$\rho_{PCM} \frac{\partial H_{PCM}}{\partial t} = \frac{k_{PCM}}{C_{PCM}} \left(\frac{1}{r} \frac{\partial}{\partial r} \left(r \frac{\partial H_{PCM}}{\partial r} \right) \right) \text{-----} 5.64$$

In the time discretization the semi-implicit of first order accurate is adopted:

$$\frac{H_{PCM,i}^{\Delta t+t} - H_{PCM,i}^t}{\Delta t} = \frac{1}{2} \left(\frac{k_{PCM}}{C_{PCM} \rho_{PCM}} \left[\frac{1}{r} \frac{\partial}{\partial r} \left(r \frac{\partial H_{PCM}}{\partial r} \right) \right] \right)^{\Delta t+t} + \frac{k_{PCM}}{C_{PCM} \rho_{PCM}} \left[\frac{1}{r} \frac{\partial}{\partial r} \left(r \frac{\partial H_{PCM}}{\partial r} \right) \right]^t \text{-----} 5.65$$

The first cell of PCM adjacent to the wall

$$\rho_{PCM} \frac{\partial H_{PCM}}{\partial t} = \frac{1}{\delta_w} \left(\frac{k_w A_{L,w}}{A_{t,w}} + \frac{k_{PCM} A_{L,PCM}}{A_{t,w}} \right) * (T_{PCM} - T_w) + \frac{1}{\delta_w} \frac{k_{PCM}}{A_{PCM}} \left(\frac{H_{PCM}^{i+1} - H_{PCM}^i}{A_{t,w}} \right) \text{-----} 5.66$$

$$\rho_{PCM} C_P(T) \frac{\partial T}{\partial t} = \frac{1}{\delta_w} \left(\frac{k_w A_{L,w}}{A_{t,w}} + \frac{k_{PCM} A_{L,PCM}}{A_{t,w}} \right) * (T_{PCM} - T_w) + \frac{1}{\delta_w} \frac{k_{PCM}}{A_{PCM}} C_P(T) \left(\frac{T_{PCM}^{i+1} - T_{PCM}^i}{A_{t,w}} \right) \text{---} 5.67$$

$$\rho_{PCM} C_P \frac{T_{pcm,i}^{\Delta t+t} - T_{pcm,i}^t}{\Delta \tau} = \frac{1}{\delta_w} \left(\frac{k_w A_{L,w}}{A_{t,w}} + \frac{k_{PCM} A_{L,PCM}}{A_{t,w}} \right) * (T_{pcm,i}^t - T_{w,i}^t) + \frac{1}{\delta_w} \frac{k_{PCM}}{A_{PCM} A_{t,w}} C_P (T_{PCM}^{\Delta t+t} - T_{PCM}^t)$$

$$T_{pcm,i}^{\Delta t+t} = \left[\frac{1}{1 - \Delta \tau * FF} \right] * [(1 + \Delta \tau * EE - \Delta \tau * FF) T_{pcm,i}^t - \Delta \tau * EE T_{w,i}^t] \text{-----} 5.68$$

$$EE = \frac{1}{\rho_{PCM} C_P \delta_w} \left(\frac{k_w A_{L,w}}{A_{t,w}} + \frac{k_{PCM} A_{L,PCM}}{A_{t,w}} \right) \text{-----} 5.68a$$

$$FF = \frac{k_{PCM}}{\rho_{PCM} \delta_w A_{PCM} A_{t,w}} \text{-----} 5.68b$$

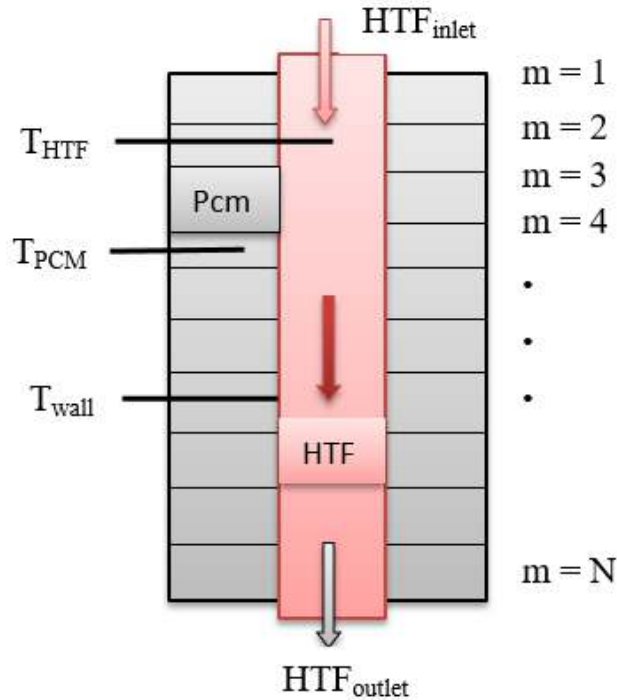


Figure 5.6 Schematic diagram of transient heat transfer flow through the shell and tube latent heat thermal storage system

5.2.10 Heat stored and available during charging and discharging process

The TES system involves a shell and tube configuration where paraffin wax is filled in the shell and water as HTF is passed inside the tube for both charging and discharging cycles.

Heat Energy during Charging (Melting) process

$$\dot{Q}_{stored} = C_{p,HTF} m_{HTF} (T_{HTF,in} - T_{HTF,out}) \text{-----} 5.69$$

$$\dot{Q}_{available} = C_{p,HTF} m_{HTF} (T_{HTF,in} - T_{pcm,in}) \text{-----} 5.70$$

Where, $T_{HTF,in}$ & $T_{HTF,out}$ - hot water (HTF) inlet and outlet temperature; $T_{pcm,in} = T_{cwi}$ - initially PCM temperature is equal to ambient temperature.

Initial and boundary conditions

In order to solve the discretized governing equation of the HTF and PCM an initial and boundary conditions are presented. Inlet temperature of HTF to storage tank is approximately outlet temperature of flat plate collector.

Initial condition: $T_{HTF}(y, t = 0) = T_{HTF,ini} = T_{fo}$

Wall temperature of the tube is an average of heat transfer and phase change temperature:

$$T_w = \frac{T_{pcm} + T_{HTF}}{2} \text{ at initial } t = 0$$

Initial temperature of paraffin wax is equal to ambient temperature:

$$T_{pcm}(y, t = 0) = T_{pcm,ini} = T_{amb}$$

Boundary condition: $-T_{HTF}(y = t, 0) = T_{HTF,ini}$ & $\frac{\partial T_{HTF}(y=l,t)}{\partial y} = 0$ $\frac{\partial T_w}{\partial y} = 0$ and $\frac{\partial T_{Hp}}{\partial y} = 0$

CHAPTER 6

6. Pipe Network and Water Distribution system

A water distribution system is a crucial infrastructure in the supply of water for domestic as well as industrial uses. PN is an investigating of the fluid flow through a hydraulic network containing several interconnected branches that determine the flow rates and pressure drops in the individual sections of the network. Pipe networks connect consumers to sources of water using hydraulic components such as pipes, valves, pumps, and tanks. As the discharges withdrawn from the network vary with time, it results in a continuous change in the nodal pressure heads and the link discharges. In the hospital, WDS is used to distribute hot water for each room. The main purpose of the water distribution network is to deliver hot water to the users/patients according to their demands on pressure and quality. WDS is composed of three components: pumping stations, storage tanks, and distribution piping. These systems are designed and investigated according to the loading conditions (pressure and demand) by Utkarsh et al., (2015). As shown on Figure (6.1), the total discharging of hot water (Q_{total}) is equal to the sum of all discharging rate distributed into each floor and room.

$$Q_{total} = Q1^{st} + Q2^{nd} + Q3^{rd} + Q4^{th} \text{-----} 6.1$$

Universally, Pipe flow is used to carrying hot fluids from storage tank to rooms and discharges and analyzed by using the continuity equation and the equation of motion. The continuity equation for steady flow in a circular pipe of diameter D is given by:

$$Q = \frac{\pi}{4} D^2 u \text{-----} 6.2$$

Where, u-average velocity of flow and Q -volumetric rate of flow (discharge).

The equation of motion for steady flow is given as:

$$P_i + Z_i + h_i + \frac{V_i^2}{2g} = P_o + Z_o + h_o + \frac{V_o^2}{2g} + h_L = \text{constant}$$

Where, Z_i and Z_o - Elevation of the centerline of the pipe at inlet and outlet, respectively.

h_i and h_o -pressure heads and V_i and V_o - Average velocity at inlet and outlet pipes

h_L - Head losses between inlet and outlet and composed of friction loss and minor losses.

$$h_L = h_f + h_m \text{-----} 6.3$$

Where, h_f - is friction loss (head loss on account of surface resistance); and h_m - Minor loss (head loss due to form resistance and on account of change in shape of the pipeline).

The head loss on account of surface resistance is given by the Darcy–Weisbach equation

$$h_f = f \frac{L V^2}{D 2g} \text{-----6.4}$$

Where, f -friction factor coefficient, L and D -length and diameter of the pipes, $g = 9.81 \text{ m/s}^2$

$$h_f = \frac{8fLQ^2}{\pi^2 g D^5} \text{-----6.5}$$

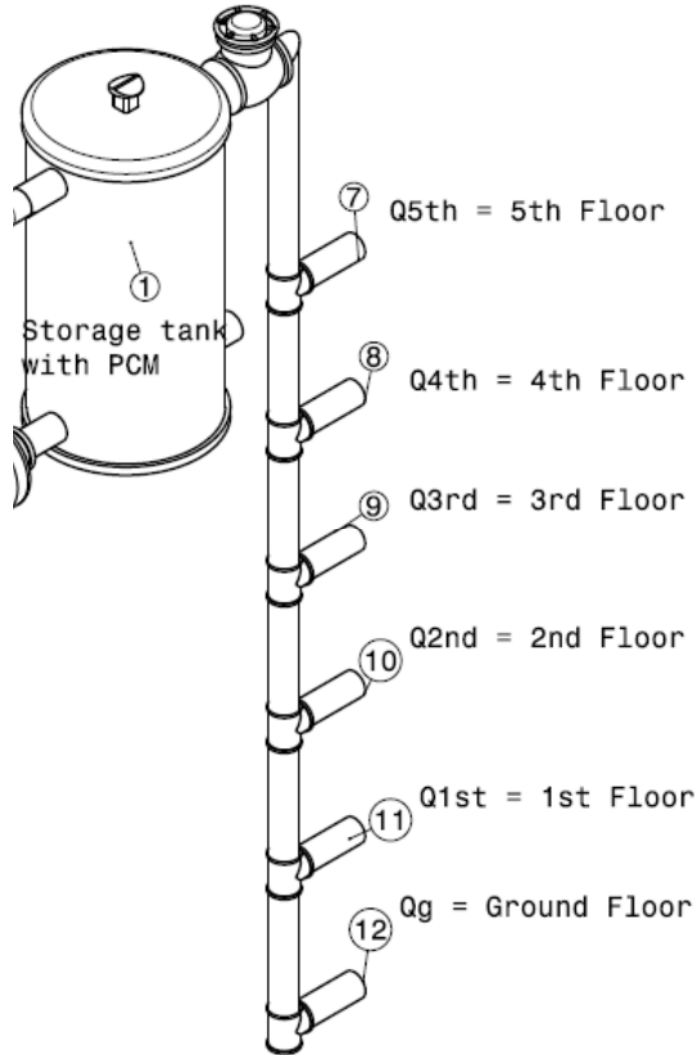


Figure 6.1 Layout of hot water discharging from storage tank to all floor building

In a water supply network, form losses play a significant role. The form-resistance losses (h_m) are due to bends, elbows, valves, enlargers, reducers, and so forth. Unevenness of inside pipe surface on account of imperfect workmanship also causes form loss. All these losses, when added together, may form a sizable part of overall head loss.

$$h_m = k_f \frac{V^2}{2g} = \frac{8k_f Q^2}{\pi^2 g D^4} \text{-----6.6}$$

Where, k_f -form-loss coefficient. For a service connection it taken as $k_f = 1.8$. In the case of pipe bend, elbows and valves; k_f depends on bend angle α and bend radius R.

The coefficient of surface resistance also depends on the Reynolds number of the flow, defined as

$$Re = VD/\vartheta \text{-----} 6.7$$

Where, ϑ -kinematic viscosity of fluid ($\vartheta = \mu/\rho$) or it can be obtained using the equation given by Swamee (2004)

$$\vartheta = 1.792 * 10^{-6} \left[1 + \left(\frac{T}{25} \right)^{1.165} \right]^{-1} \text{-----} 6.8$$

Where, T is the water temperature in °c.

μ and ρ -dynamic viscosity and density of the fluid.

6.1 Water Demand Pattern and Distribution System Design

All the rooms of the hospital are connected through service connections to water distribution network pipelines for supplying water. The maximum discharging rates occur in morning and evening hours. The maximum withdrawal rate in a pipe is a function of the number of rooms (patients) served by the service connections. In this study, to analysis and design the PN, the maximum discharge rate is considered. So, the maximum withdrawal rate for the hospital is functions for 24-hour. Since the total storage capacity of hot water for hospital calculated is 54,000 liter per day. The maximum drainage diameter of pipe is 38 mm and correspondingly pipe diameter selected to be 1 inch or 25.4 mm for pipe networks. For design of water distribution system, a typical ranges of design parameters like a velocities, diameter, hydraulic gradients and pressure drop are as the following.

Table 6.1 Design parameters ranges

Design parameters	Ranges
Velocity (m/s)	0.5 – 2.0
Hydraulic gradient (m/km)	1 – 5
Pressure drop (meter of water column (mwc))	20 – 30
Diameter of pipe (mm)	D < 50

In general, Pressures higher than 60 mwc should be avoided, due to increased leakage and risks of bursts in networks.

Design Data

Number of patients 1200 Length of the pipe 920 m

Specific demand	45 liter/person per day	Hourly peak factor K2	2.0
Daily peak factor K1	1.2		

Average discharges carried by distribution system can be calculated by:

$$Q_{avg} = N * spec. demand \text{-----} 6.9$$

Peak flow carried also can be calculated by:

$$Q_{max} = K_1 * K_2 * Q_{avg} \text{-----} 6.10$$

Average and maximum discharging rate for the end-users are calculated using equation (6.9 and 6.10) and their values are 0.625 liter per second and 1.5 liter per second respectively.

The hot water use rate (q) by persons per length of the distribution pipes is estimated by:

$$q = \frac{Q_{max}}{L_p} \text{-----} 6.11$$

Hot water use rate per total length of the pipe network in a building of 920 m is approximately 0.00163 liter per second per meter. For each floors, Hot water withdrawal rates are calculated according to the length of distribution pipe. The length of the pipe from storage tank to rooms of each floors is difference and the values are presented in tabulated form for each floor. Multiplying the total length pipe of each floor by the unit flow rate of hot water use (q) gives the demand (Q_d) along the floor pipe.

6.2 Water Distribution system and Hospital Building Geometry

Since the Adama hospital building pattern is rectangular looped shape, the single looped network is recommended. A new building of Adama hospital has a Base, Ground and five floors. Pipe lengths are obtained from the known geometrical layout of the hospital. The discharge rate and head loss of the pipe network and water distribution for each floor and room are analysed.

6.3 Estimation of discharging rate and head loss for each Room

To estimate the total discharge rate is calculated as:

$$Q_{max} = q * L_p \text{-----} 6.12$$

Where, q and L_p -are use rate of hot water and length of the pipe, respectively.

The total head losses are given by:

$$h_L = h_f + h_m = \frac{8fLQ^2}{\pi^2 gD^5} + \frac{8k_f Q^2}{\pi^2 gD^4} \text{-----} 6.13$$

The total discharge rate and total head loss are calculated for all rooms on each floor and the results are tabulated as the following.

A. First floor

1st FLOOR	Rooms	A1	B1	C1	D1	E1	F1	G1	H1
	Q(L/s)	0.0196	0.0061	0.0069	0.0069	0.0069	0.0069	0.0069	0.0069
	h_L(mm)	1.4623	0.0754	0.1020	0.1020	0.1020	0.1020	0.1020	0.1020
	Rooms	I1	J1	K1	L1	M1	N1	O1	P1
	Q (L/s)	0.0069	0.0069	0.0069	0.0134	0.0134	0.0069	0.0069	0.0077
	h_L (mm)	0.1020	0.1020	0.1020	0.5428	0.5428	0.1020	0.1020	0.1340
	Rooms	Q1	R1	S1	T1	U1	V1	W1	X1
	Q (L/s)	0.0069	0.0069	0.0069	0.0069	0.0069	0.0069	0.0053	0.0061
	h_L (mm)	0.1020	0.1020	0.1020	0.1020	0.1020	0.1020	0.0535	0.0754
	Rooms	Y1	Z1	AA1	BB1	CC1	DD1	EE1	FF1
	Q (L/s)	0.0175	0.0187	0.0163	0.0069	0.0077	0.0077	0.0069	0.0069
	h_L (mm)	1.0896	1.2894	0.8992	0.1020	0.1340	0.1340	0.1020	0.1020
	Rooms	GG1	HH1	II1					
	Q (L/s)	0.0069	0.0069	0.0257					
h_L(mm)	0.1020	0.1020	3.0599						

B. Second Floor

2nd Floor	SECTION	A2	B2	C2	D2	E2	F2
	DEMAND (L/s)	0.0245	0.0061	0.0069	0.0069	0.0069	0.0061
	H_{loss} (mm)	2.1777	0.0441	0.0619	0.0619	0.0619	0.0441

C. Third Floor

3RD FLOOR	Rooms	A3	B3	C3	D3	E3	F3	G3	H3
	Q (L/s)	0.0245	0.0061	0.0069	0.0069	0.0069	0.0069	0.0069	0.0069
	h_L(mm)	2.6773	0.0754	0.1020	0.1020	0.1020	0.1020	0.1020	0.1020
	Rooms	I3	J3	K3	L3	M3	N3	O3	P3
	Q (L/s)	0.0069	0.0069	0.0069	0.0134	0.0134	0.0069	0.0069	0.0077
	h_L(mm)	0.1020	0.1020	0.1020	0.5428	0.5428	0.1020	0.1020	0.1340
	Rooms	Q3	R3	S3	T3	U3	V3	W3	X3
	Q (L/s)	0.0069	0.0069	0.0069	0.0069	0.0069	0.0069	0.0053	0.0061
	h_L(mm)	0.1020	0.1020	0.1020	0.1020	0.1020	0.1020	0.0535	0.0754
	Rooms	Y3	Z3	AA3	BB3	CC3	DD3	EE3	FF3
	Q (L/s)	0.0175	0.0187	0.0163	0.0069	0.0077	0.0077	0.0069	0.0069
	h_L(mm)	1.0896	1.2894	0.8992	0.1020	0.1340	0.1340	0.1020	0.1020
	Rooms	GG3	HH3	II3					
	Q (L/s)	0.0069	0.0069	0.0297					
h_L(mm)	0.1020	0.1020	4.5925						

D. Fourth Floor

4th FLOOR	Rooms	A4	B4	C4	D4	E4	F4	G4	H4	
	Q (L/s)	0.0293	0.0061	0.0069	0.0069	0.0069	0.0069	0.0069	0.0069	
	h_L(mm)	4.4205	0.0754	0.1020	0.1020	0.1020	0.1020	0.1020	0.1020	
	Rooms	I4	J4	K4	L4	M4	N4	O4	P4	
	Q (L/s)	0.0069	0.0069	0.0069	0.0134	0.0134	0.0069	0.0069	0.0077	
	h_L(mm)	0.1020	0.1020	0.1020	0.5428	0.5428	0.1020	0.1020	0.1340	
	Rooms	Q4	R4	S4	T4	U4	V4	W4	X4	
	Q (L/s)	0.0069	0.0069	0.0069	0.0069	0.0069	0.0069	0.0053	0.0061	
	h_L(mm)	0.1020	0.1020	0.1020	0.1020	0.1020	0.1020	0.0535	0.0754	
	Rooms	Y4	Z4	AA4	BB4	CC4	DD4	EE4	FF4	
	Q (L/s)	0.0175	0.0187	0.0163	0.0069	0.0077	0.0077	0.0069	0.0069	
	h_L(mm)	1.0896	1.2894	0.8992	0.1020	0.1340	0.1340	0.1020	0.1020	
	Rooms	GG4	HH4	II4						
	Q (L/s)	0.0069	0.0069	0.0395						
h_L(mm)	0.1020	0.1020	10.1602							

E. Fifth Floor

5TH FLOOR	Node	A5	B5	C5	D5	E5	F5	G5	H5
	Demand (L/s)	0.0350	0.0060	0.0069	0.0069	0.0069	0.0069	0.0069	0.0619
	h_i (mm)	7.2474	0.0730	0.1020	0.1020	0.1020	0.1020	0.1020	36.4925
	Section	I5	J5	K5	L5	M5	N5	O5	P5
	DEMAND	0.0069	0.0056	0.0163	0.0069	0.0077	0.0077	0.0069	0.0399
	h_i	0.1020	0.0617	0.8992	0.1020	0.1340	0.1340	0.1020	10.4580

Now, after knowing the amount of discharging rate and head losses for each floor start from base up to 5th floor, it can simply be summarizes the total withdrawal rate and total head losses.

Table 6.2 Summary of discharging rate or demand for a hospitals

Floors	Length of pipe per floor (m)	Discharge rate (l/sec)	
Foundation	120	0.196	Q _B
1 st floor	195	0.318	Q1 st
2 nd floor	35	0.058	Q2 nd
3 rd floor	200	0.327	Q3 rd
4 th floor	210	0.343	Q4 th
5 th floor	145	0.237	Q5 th
Total	920	1.478	Q _{total}

As shown the above Table 6.2 the total sum of discharging rate for the hospital is less than the maximum withdrawal rate. This shows that the rate of hot water used is safe or fulfill the hot water for all rooms in each floors.

6.4 Pressure drop through water distribution system

Pressure drop over the length of pipe line calculated as:

$$\Delta P = \frac{32\mu LV}{D^2} \text{-----} 6.14$$

Where, ΔP -total pressure drop in the pipe network; L, V and D -are the length, mean velocity and diameter of the pipes respectively; μ -dynamic viscosity of the fluid.

Table 6.3 Total pressure drop throughout the pipe flow in a hospital.

Floor	Length of the pipe (m)	Q (L/s)	D (m)	Pressure drop (Pa)
Base	120	0.196	0.0500	4895.826
1st	195	0.318	0.0254	4726.66
2nd	35	0.058	0.0254	1370.958
3rd	200	0.327	0.0254	4788.84
4th	210	0.343	0.0254	3444.04
5th	145	0.237	0.0254	2468.73

As shown Table 6.3 total pressure drops are calculated for each rooms on each floors. Hence, the total pressure drop through water distribution to the end user or rooms is approximately 21,965.05 Pa. When a pump delivering hot water through a pipe to the rooms, the total loss pressure due to different factor is 22 kPa. The total pressure at outlet point of storage tank to end-user calculated by applying Bernoulli equation.

$$P_1 + \rho g z_1 + \frac{\rho u_1^2}{2} = P_2 + \frac{\rho u_2^2}{2} + \rho g z_2 + \Delta P_L \text{-----} 6.15$$

The total pressure at outlet point is approximately 22 kPa ($P_1 = 21,965 \text{ kPa}$).

6.5 Investigation of hot water flow from storage tank through pipeline

Simultaneously hot water flows from a storage tank and through a pipe to each appliance. While hot water is flowing, the fluid depth is decreasing as hot water distributed to each room. Continually, this action occurs with time, which implies that the deeper the hot water, the faster it flows from the tank. In this study, for unsteady flow hot water flow from a tank using FDM estimate the depth of the hot water in the tank with time throughout the day.

The mean velocity, V for hot water flow in a round pipe of diameter, D is given by;

$$V = \frac{D^2 \Delta P}{32 \mu L} \text{-----6.16}$$

Where, ΔP - the pressure drop over the length of L of pipe and at inlet pipe the pressure is;

$$\Delta P = \rho g h = \gamma h \text{----- 6.17}$$

The discharge pressure of hot water from the storage tank at the bottom calculated by Bernoulli equation as 21,965 *kPa*. Conservation of mass needs that the flow rate from the tank is related to the rate change of depth of hot water in the storage tank.

$$Q = -\frac{\pi}{4} D_t^2 \frac{dh}{dt} \text{----- 6.18}$$

Where, continuity equation ($Q = \frac{\pi}{4} D^2 V$); and the mean velocity becomes;

$$V = -\frac{\pi}{4} \left(\frac{D_t}{D}\right)^2 \frac{dh}{dt} \text{----- 6.19}$$

The mean velocity for laminar flow in round pipe is also given by:

$$V = \frac{D^2 \gamma h}{32 \mu L} \text{----- 6.20}$$

Where, the pressure drop over the length of pipe L is given by:

$$\Delta P = \gamma h \text{-----6.20a}$$

By combining equation 1 and 2, the partial differential equation becomes:

$$\frac{dh}{dt} = -Ch \text{----- 6.21}$$

Where, $C = \frac{\rho g h D^4}{32 \mu L D_t^2}$ is constant, D and h - Diameter of the pipe and height of the tank, respectively and D_t –diameter of the storage tank

Discretizing the equation 3 by using backward finite difference techniques gives:

$$\frac{dh}{dt} = \frac{h_i - h_{i-1}}{\Delta t} \text{----- 6.22}$$

Where, Δt is time step between the different nodes and its value is selected to be 15 minutes throughout the day and h_i and h_{i-1} are approximate values of h at nodes i and $i-1$. The total nodes are $N = 20$ and change in y -axis (Δy) is 0.25 m and analysis on one dimensional flow.

For $i = 2, 3, 4 \dots N$, the governing equation is given as the following:

$$\frac{h_i - h_{i-1}}{\Delta t} = -h_i$$

The depth of hot water in the storage tank is given by:

$$h_i = \frac{h_{i-1}}{(1 + \Delta t)} \text{----- 6.23}$$

Initial condition:

The total height is @ $i = 1$ equal to the total height of the storage tank ($h_1 = h_{tank}$). The final the equation used to simulation to solve the transient analysis depth of the hot water in a 24 hours for every day.

$$h_i = \frac{h_{tank}}{(1+\Delta t)^{i-1}} \text{-----} 6.24$$

6.6 Selection of pump for water distribution system

A wide range of pump types is available on the market. Prevailing local conditions and management capacities determine the type which is most suitable and sustainable. In selecting a pump type for a specific purpose the following methodological criteria need to be considered:

- Rate of delivery required (capacity)
- Vertical distance from pumping level to delivery level (pumping head)
- Variations expected in water levels at the source
- Durability of basic components
- Availability and cost of spares
- Ease of maintenance

6.6.1 The performance or characteristic curve of the pump

The pump characteristic curve show the relationship between discharge pressures vs. flow. The point of intersection between the pump performance curve and the system head curve represents the capacity at which the pump will operate. When select the pump, it is always advisable that it normally operate in a region of reasonable capacities i.e. not too far from their best efficiency point. From the characteristic curve of the pump the best efficiency point to discharge hot water is 70%. The power required for driving a pumping unit to achieve hot water to demand can be:

$$P_{req} = \frac{\rho g Q (H_{stat} + SL)}{\eta} \text{-----} 6.25$$

$$P_{req} = \frac{1000 * 9.81 * 1.5 * 10^{-3} (25 + 0.0085 * 920)}{0.70} = 690 \text{ W} = 0.70 \text{ kW}$$

Where, P_{req} = power required for pumping (Watts); Q = max. Pumping capacity (m^3/s); ρ = specific weight of water (kg/m^3); η = pumping efficiency (%); H_{stat} = static head (m); S = hydraulic gradient (m/km) and L = pipe length (m).

The pumping head is the total head, and comprises the static head plus the friction head loss for the design flow rate. Since, Centrifugal pump is high speed operation, smooth, even discharge,

efficiency range (50-85%) depends on operating speed and pump head and also it requires skilled maintenance and powered by electric power; is selected for pumping of hot water for domestic. A three-phase electric drive centrifugal pump selected has the following technical specification.

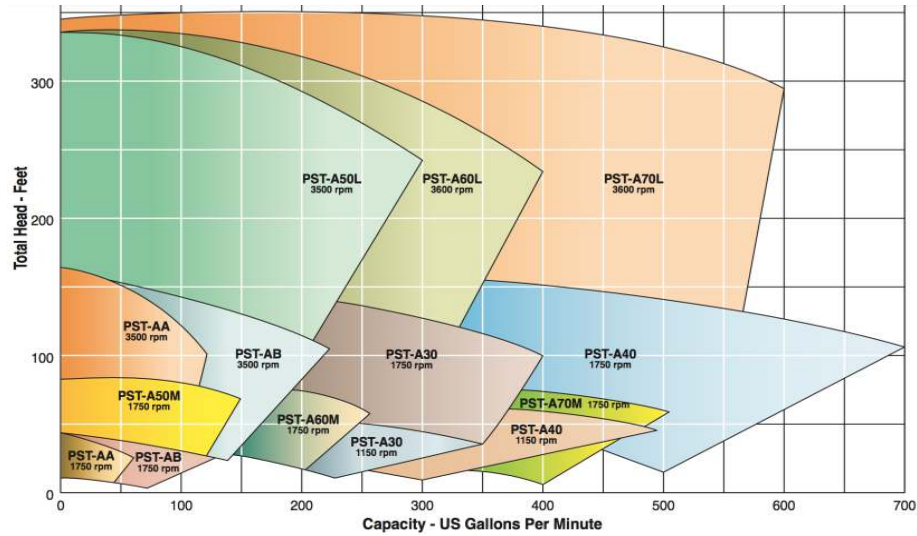


Figure 6.2 The selection chart to determine the appropriate Centrifugal pump model and size for water pumping application.

Technical specification

Type	Electric drive centrifugal pump (PST-A70M/50Hz)
Application	Pumping of water for domestic
Maxi. Capacity	up to 409.14 gpm.
Max. Head	up to 60.7 m
Max. Operating pressure	800 kPa/8 bar
Temperature of pumped liquid:	-10°C to +90°C.

MOTOR

Type	3 phase	Frequency	50 Hz
Rated power	0.75 kW	Poles	2 poles
Voltage:	380-415 V		

CHAPTER 7

7. Result and Discussion

7.1 Solar Intensity Radiation

The hourly average incident solar radiation in Adama for all months are estimated and its values are vary throughout the day. Here, the months such as February, January, June and July are mostly pointed and presented in Figure 7.1 to know the maximum and minimum results of solar radiation availability. Its shows that, months of January and February; the solar radiation intensity is higher than other. In case of the June and July months, the solar intensity is lower.

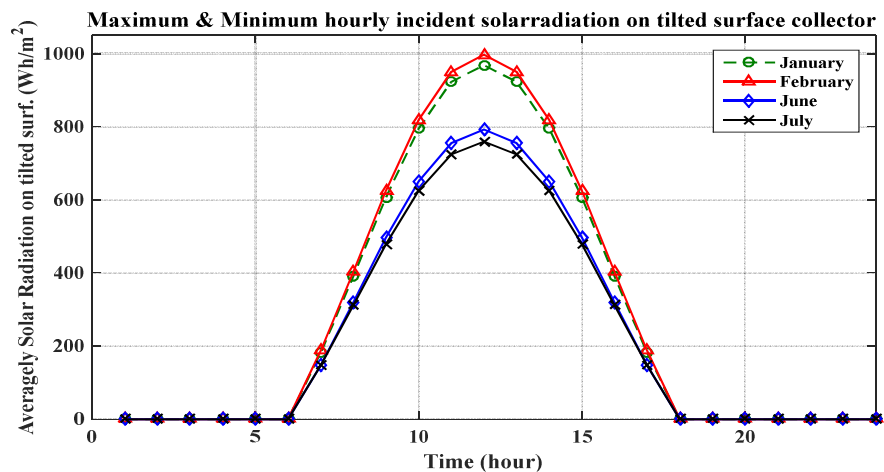


Figure 7.1 The hourly average SR for February, January, June and August in Adama.

7.2 Variation of Hot water Stream (HTF) Temperature

The hot water throughout the closed thermal system of the solar water heating which output from the flat plate collector and enter the storage tank and again recycle the loop is fluctuating throughout a day, months and a year. Depending on the variation of time outlet temperatures are calculated iteratively for all months throughout a year by MATLAB and Excel Microsoft package depends on hourly average solar radiation intensity incidence on the solar collector (FPC) and are intended on Figure 7.2 and 7.3. For all months, an outlet hot water temperature reaches a maximum at the mid-day (sun noon). The outlet temperature depends on the hourly solar radiation on a tilted surface and the mass flow rate of HTF for each collector. The simulation of the outlet temperature variation of all months is simulated and unsteadily calculated.

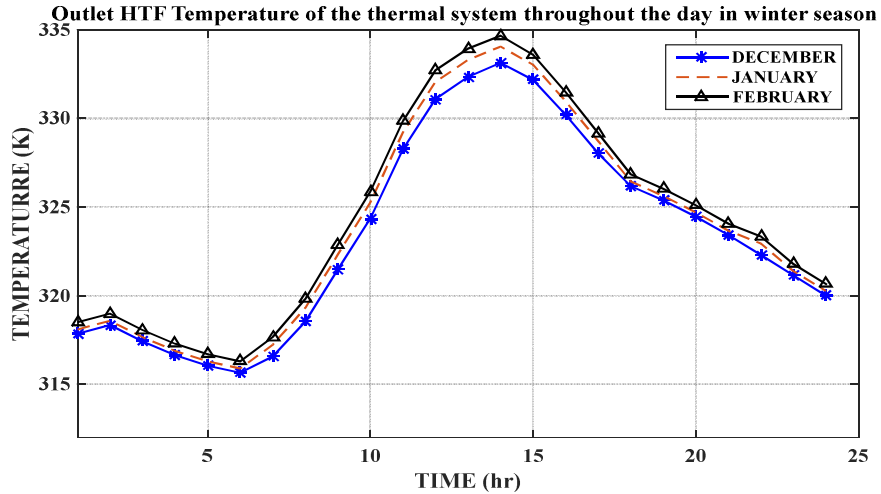


Figure 7.2. Fluctuation of Hot water stream temperature throughout the day in 24 hours for Winter Season (High solar radiation incidence).

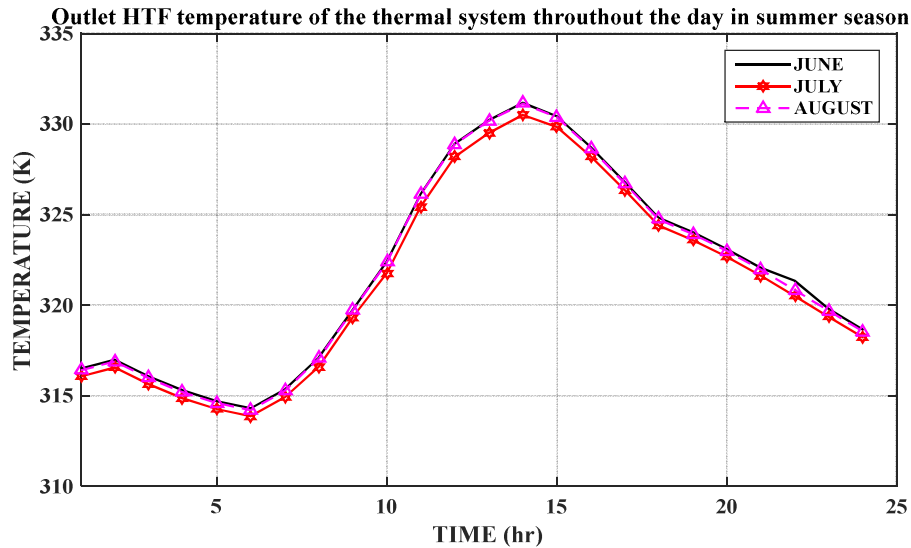


Figure 7.3. Fluctuation of Hot water stream temperature throughout the day in 24 hours for Summer Season (Low solar radiation Incidence).

As shown in Figure 7.3, during day time the flat plate collector starts to absorb solar radiation throughout the day start from sunrise to sunset hours. The fluid temperature continuously rises from sunrise to noontime and reaches a maximum, then decreases slightly up to sunset hour. For another season, hot water outlet temperature variations at the outlet of the solar collector (FPC) are presented at APPENDIX.

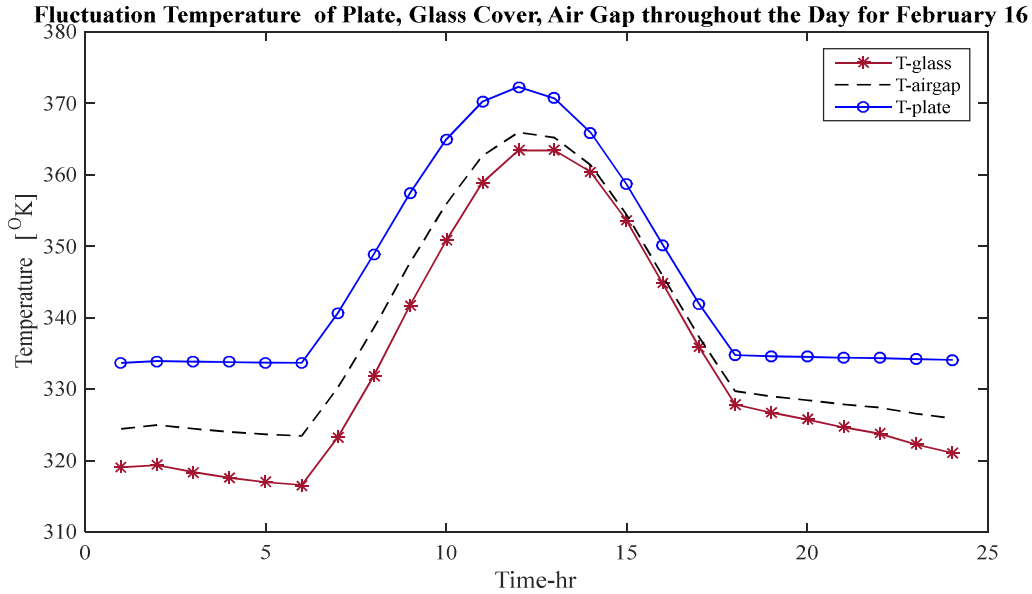


Figure 7.4 Temperature Fluctuation of absorber Plate, Glass Cover, Air Gap throughout the Day for February 16.

7.3 Solar Fraction

Averagely, hot water at collector outlet and delivered to thermal energy storage tank at temperature of 60 - 68°C for the maximum solar contribution to the heating load is achieved during the winter season in the month of February and the minimum is achieved during the summer season in the month of August lower solar fraction as shown in Figure 7.5. Thus, the result of solar fraction during August is 66.9% and during January is 98.6%.

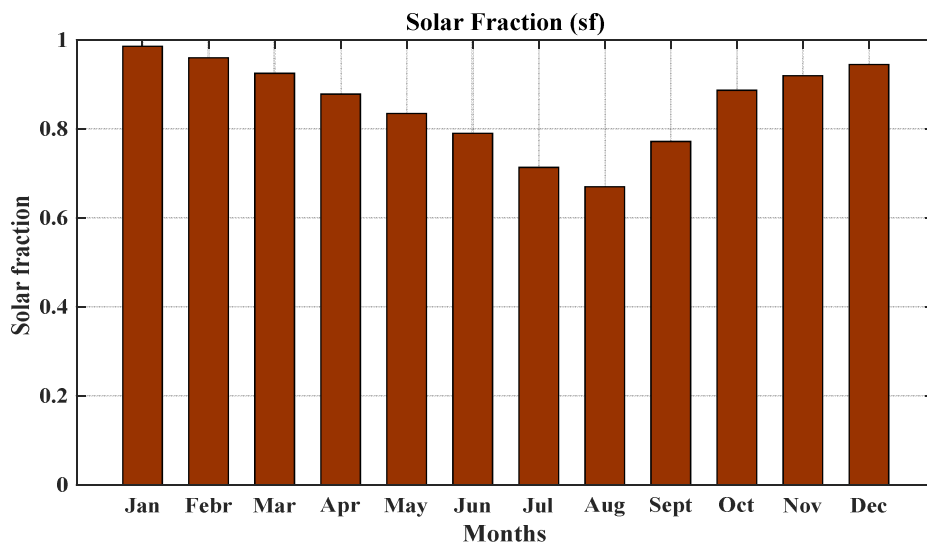


Figure 7.5 Monthly solar fraction (sf)

7.4 Instantaneous thermal efficiency

The instantaneous efficiency of the solar collector depends on mass flow rate, the water temperature at the collector outlet and available solar radiation. An efficiency was analyzed from the solar energy delivered from solar collector and instantaneous total solar radiation incidence on collector surface and variation is from sunrise to sunset. The Figure 7.6 reveals as a sample of a FPC instantaneous efficiency for February 16.

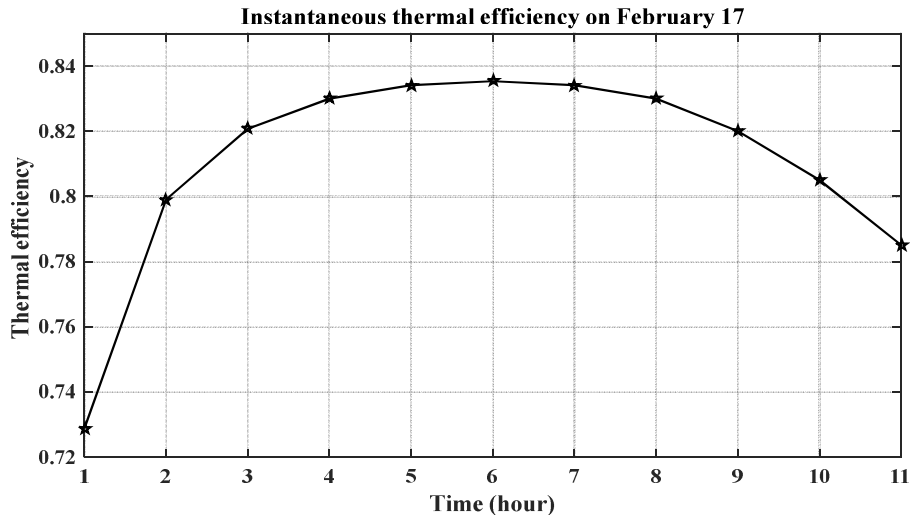


Figure 7.6 Variation of instantaneous efficiency of a flat plate collector for February 16.

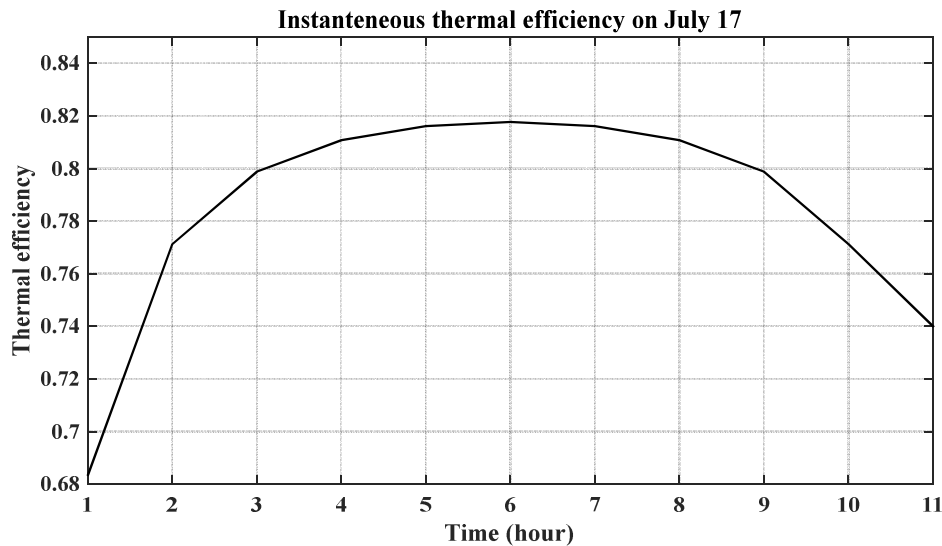


Figure 7.7 Variation of instantaneous efficiency of a flat plate collector for July 17.

As the time increases the system efficiency decreases during sensible heating of solid PCM and it remains nearly constant during phase change period and then it further decreases during sensible heating of liquid PCM. This is due to the fact that as charging proceeds the temperature difference

between the HTF and the PCM in the storage tank decreases. This decreases the amount of heat transferred to the storage tank and thus the energy stored decreases with increase in time.

The result reveals that the lowest instantaneous efficiency of a flat plate collector occurs at the sunrise hours. This is due to, some percent of solar radiation incidence on the surface of the collector was stored by a cover, air gap, plate, and tube materials; then the rate of heat absorbed by system components decreased. The highest value of efficiency occurs around noontime, because the sun comes to the overhead of the surface, due to this the major part of the radiation is beam radiation.

7.5 Estimated solar sizing system

In this study, to determine the size and number of collector based on the period from April to August or summer season because in this season least intensity of solar radiation is available. Since, from the specification of the flat plat collector for the system a single FPC is specified with dimensions of (2 m x1 m); then to fulfill the total energy demand for hospital number of FPC are needed and the number of solar collector needed obtained as the total area of FPC divided by the unit FPC which have area of 2 m². The results are tabulated in Table 7.1.

Table 7.1 Average effective area and total number of flat plat collector needed for each months

Months	Avg. effective Area (m ²)	Avg. Number of Collector required
January 17	523.099	261
February 16	470.068	235
March 16	482.730	241
April 15	468.058	234
May 15	556.320	278
June 11	600.912	300
July 17	630.967	265
August 16	546.744	273
September 15	544.732	272
October 15	517.528	259
November 14	474.982	237
December 10	514.742	257
Average Area	527.5735	265

As shown in Table 7.1, the total area of the solar collector to cover the total energy demand are designed for the all months of the year. The number of the collector is also considered from the specification of solar collector. According to the above results, the maximum effective area needed in July 17 that is 630.967 m^2 . Hence, during a summer season low solar radiation is acquired and the daily hot water demand of the Adama hospital is fulfilled by using 265 a number of solar flat plate collectors.

7.6 Variation of Storage tank Temperature throughout the day

The hot water temperature from the solar collector outlet equal to the inlet temperature of the storage tank, hence the temperature losses through the pipes are small. As shown below in figure the fluctuation of storage temperature varies with hourly an ambient temperature, and maximum storage tank temperature occurred at noontime and slightly decreased up to sunset time. From Figure 7.9 the high temperature of the storage tank is obtained on February 17 and similarly, the low temperature of a storage tank is obtained on July 17 in Figure 7.8. Hot water temperature in the storage tank for winter and summer season have schemed below and for autumn and spring-summer seasons schemed in APPENDIX.

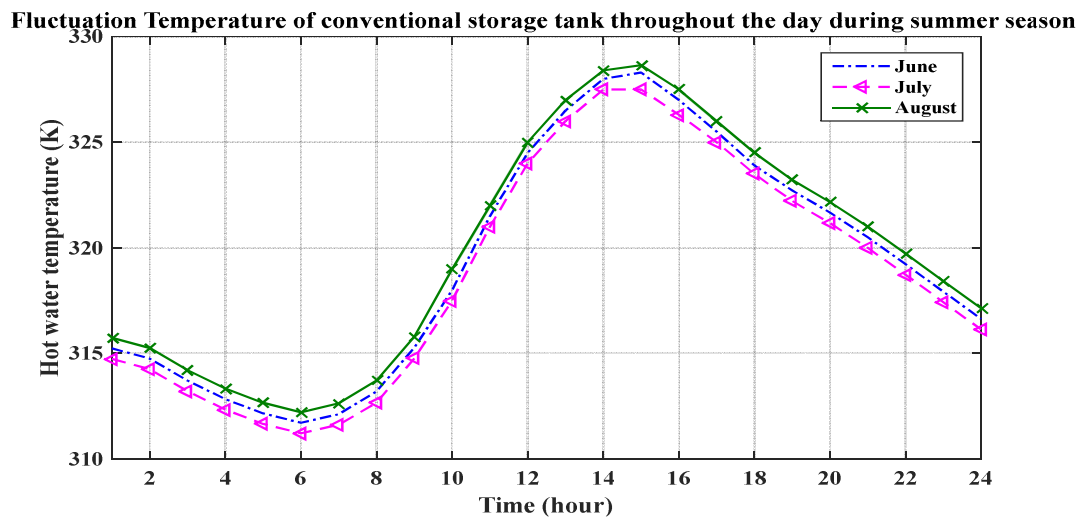


Figure 7.8 Simulated hourly variation temperature of hot water during summer season

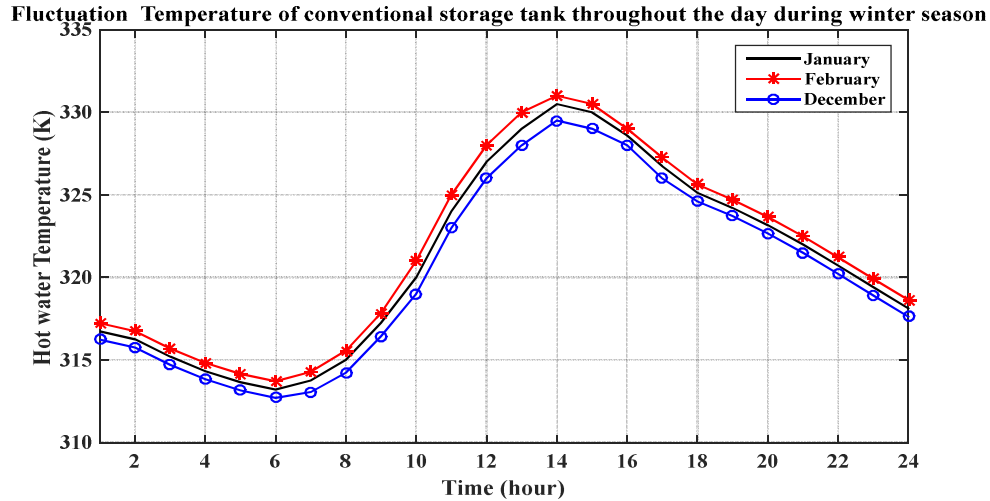


Figure 7.9. Hourly variation temperature in storage hot water tank during winter season

7.7 Useful Energy gained by Solar Collector

7.7.1 Hourly average useful solar energy throughout the day

Useful energy collected from solar collected are simultaneously calculated hourly from sun rise to sunset as shown in Figure 7.10, the energy collected usually high at noon time. Conventional, solar energy delivered is found as outlet fluid temperature variation of FPC throughout the day times the temperature rise of the HTF to its mass flow rate and specific heat capacity of the fluid.

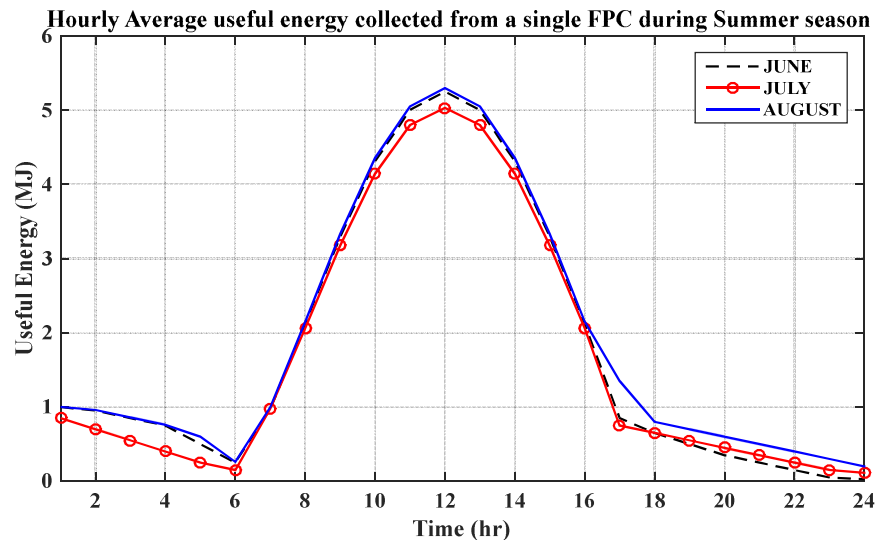


Figure 7.10 Hourly average useful energy collected throughout the day from a single FPC for Summer Season (Minimum value of Useful energy gain)

For all season weather such as winter, autumn and spring seasons; hourly average useful solar energy gain are listed in APPENDIX.

7.7.2 Monthly average of useful solar energy throughout a year

Thermal storage tank stores hot water for later use. The storage tank deliver hot water for a demand at temperature of 60°C succeeds a maximum temperature solar contribution to the load are in winter season in the month of February and achieves a minimum solar contribution during a summer season in months of July. Since in Ethiopia, high solar radiation attains during winter season and low solar intensity during summer season.

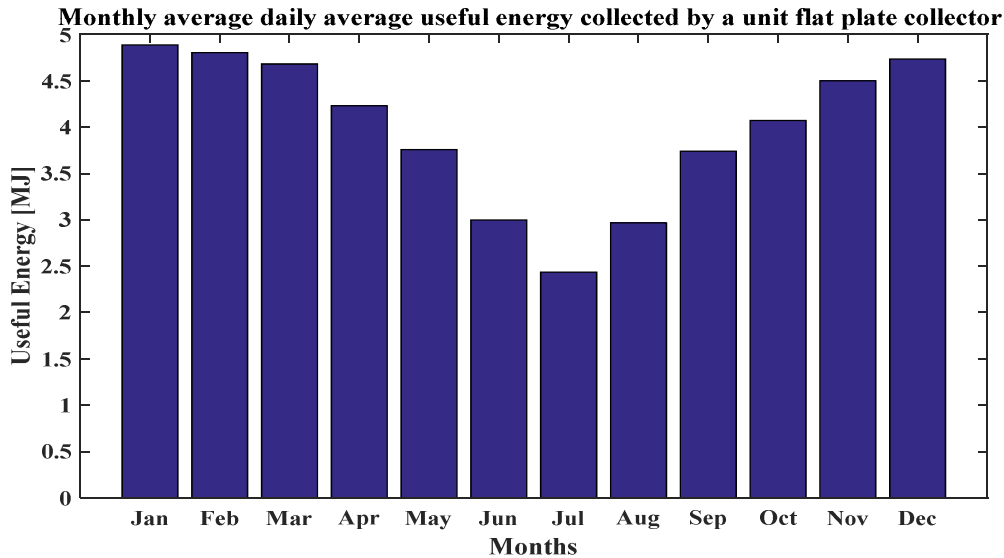


Figure 7.11 Monthly average daily average useful energy collected by a single FPC

Generally, to summarizing from the result of simulation and shown from Figure 7.11 the total amount of useful energy collected by a single flat plate collector per day are obtained from minimum value 2.435 MJ during summer season on July to maximum value collected 4.806 MJ during winter season on February. This implies that average daily solar radiation on February is higher rather than other months in a years and lowest value of solar intensity reaches in summer season especially on July. Besides, to get the total annual useful energy by multiplying daily useful energy and 365 of day per a year. In this study, analysis of flat plate collector is investigated only on a single solar collector; so, it is possible to analyse transients analysis on the total solar collector required. Thus, from a simulation the total number of collector used to cover the daily energy demand for AHMC is 265 solar FPC and all are configured in parallel arrangements. The total mass flow rate of hot water or heat transfer fluid is 4.582 kg/s or 275 kg/min.

7.7.3 Solar thermal energy losses throughout the day

The rate of useful energy decreases with increasing temperature difference. The thermal loss to the surroundings is an important factor in the determination of the performance of a FPC. The lower the rate of thermal losses, the higher rate of useful energy output. The rate of useful energy lost by absorber to the atmosphere is obtained by overall heat transfer coefficient times the temperature difference. According to the simulation heat losses to atmosphere are presented in Figure 7.12.

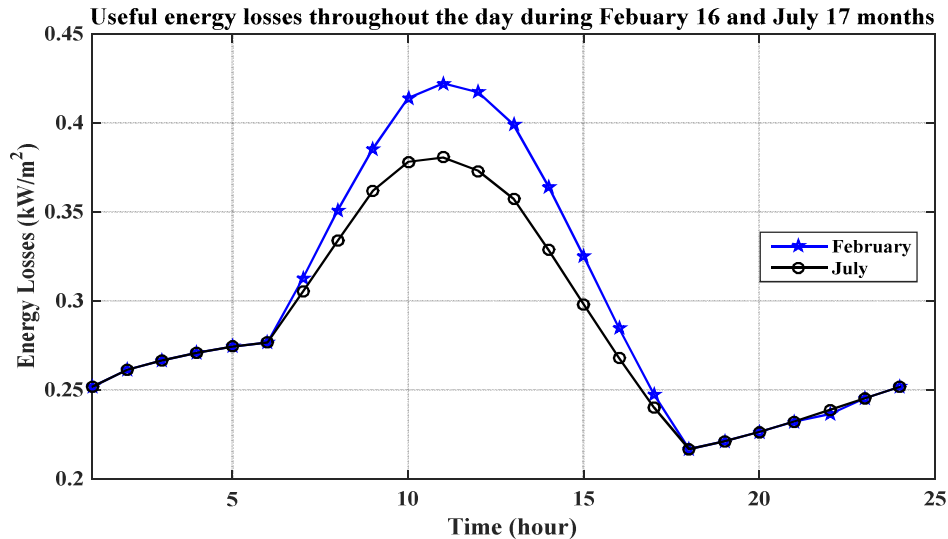


Figure 7.12 Simulation of Useful Energy losses throughout the day for February 16th and July 17. As shown in Figure 7.12, the thermal energy losses during maximum solar radiation intensity on February and minimum solar radiation on July 17. Thus, the rate of useful energy losses are maximum during the noon time for both months. Parallel, useful energy absorption and energy losses are proportional occurred throughout the day. In summer season thermal energy losses are very low rather than winter, correspondingly solar radiation incidence is also minimum.

7.8 Fluctuation Temperature of Thermal Storage Tank integrating Phase Change Materials (Paraffin wax)

7.8.1 Variation temperature of Paraffin storage tank during charging process

The variation of paraffin wax (n-Heptacosane) temperature during charging processes is investigated with variation of HTF throughout the day at inlet point. The inlet temperature of HTF is approximately same as outlet temperature of HTF from the solar collector. Initially, both PCM and HTF have the same temperature which is greater than/equal to ambient temperature. Then, the melting process is occurs with sensible heating initial point for one hour and half minutes. During

melting process, phase change process happens within a slightly temperature range 0.5-1.5 °c. The melting process occurs approximately for seven and half-hours' of time duration. After paraffin wax phase change process ends, simultaneously sensible heating continues.

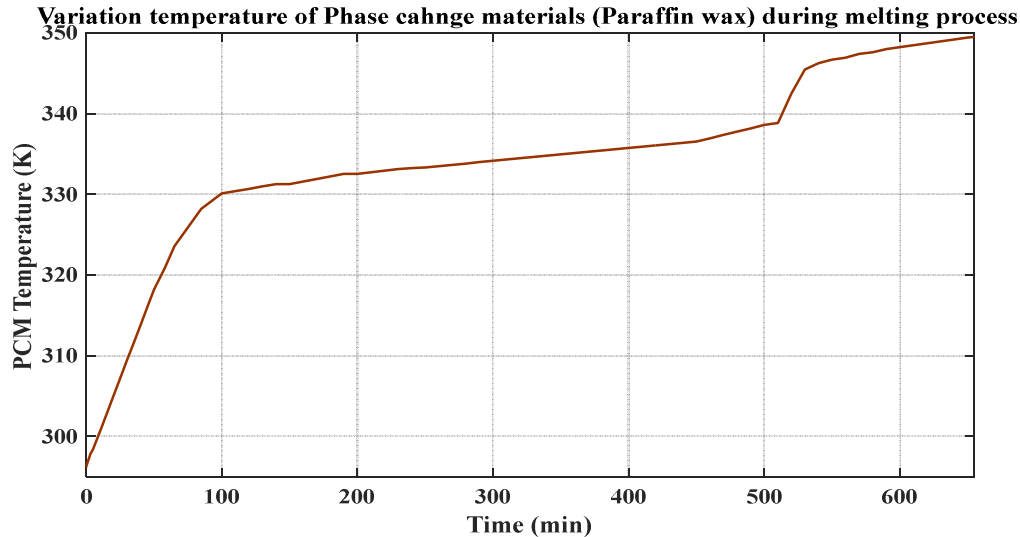


Figure 7.13: Temperature variation of Paraffin wax during melting process during February 16.

The PCM experiences three phase during charging processes; solid, liquid and mushy. The solid and liquid phases have sensible heat and the mushy one has latent heat as shown in Figure 7.13. From a simulation and modeling thermal storage tank with integrating PCM, the total volume required to integrate paraffin wax is 5.6 m³ i.e. the total volume needs to fill the paraffin wax. The paraffin wax (n-Heptacosane) filled in shell or concentric cylindrical shape on outer surface of the tube and a porosity ($\epsilon = 0.45$), through which hot water (HTF) flows. Hence the storage unit is shell and tube configuration the single shell side filled by PCM has a volume of 0.055 m³ and each shell has its own tube with 0.017 m³ which HTF is flow through it. The total number of tube used to fulfill the required demand is approximately 102.

7.8.2 Validation

To verify the reliability of the numerical model, the mathematical results are compared with the previously published thesis. The simulation of the thermal storage system with integrating PCM during the charging process is indorsed with the same work of experimental and numerical analysis of Reddigari et al., (2012). Graphically results of the numerical analysis of phase change materials have a similar shape, only the difference is melting time and amount of heat energy. Since the geometrical size of the latent heat storage system and the meting point's pf PCM used are different, their melting time and temperature limits vary, good agreement as shown in Figure 7.14.

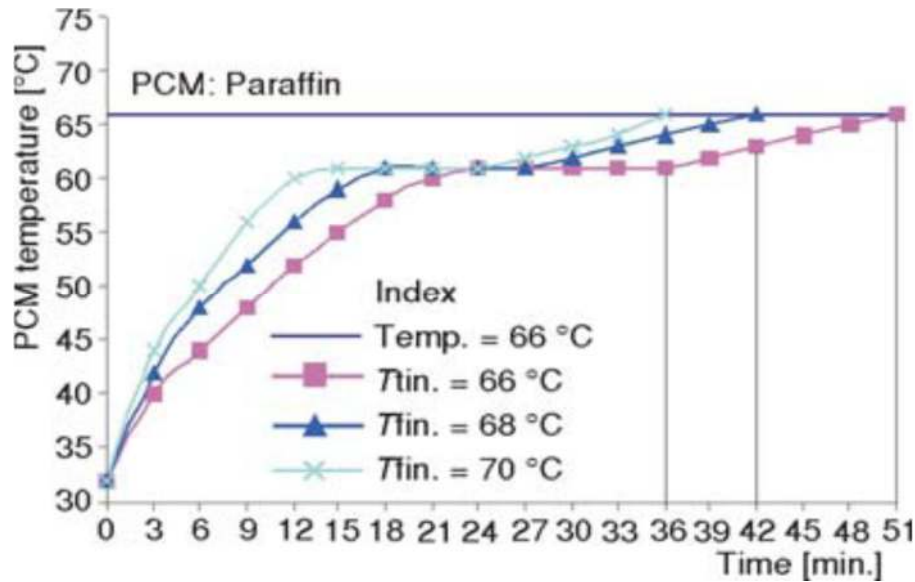


Figure 7.14: Variation Temperature of phase change materials for different heat transfer inlet Temperature during charging process Reddigari et al., (2012).

7.9 Summary and Comparison of LHTES and Conventional SHS solar water heating system

A thermal energy storage system has been developed for the use of hot water for domestic applications using conventional sensible and latent heat storage concept (Figure 7.15 and 7.16).

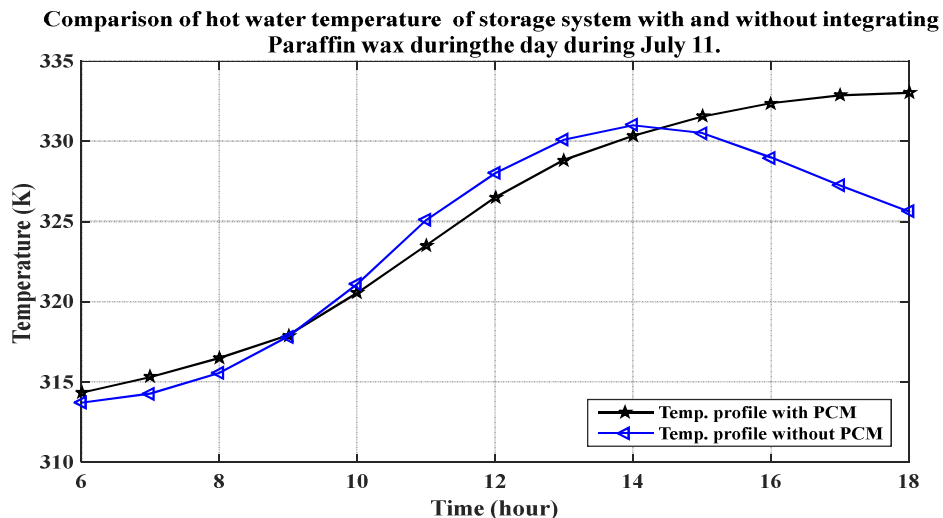


Figure 7.15 The time wise variation of the hot water temperature in the solar water heating system with and without PCM during charging processes on July 11th.

Figure 7.15 reveals that shows the time variation of the water average temperature in the storage tank for the SWH without PCM and with PCM during sunshine and the analysis solar water heater

with paraffin wax, hot water temperature increases and achieves its maximum value. But, SWH without PCM where the temperature decrease directly. Paraffin wax is remains constant at this maximum value which is nearly equal to the melting temperature of the PCM, the phase change occurs during this period, and the water temperature decreases next. This is due to the specific characteristic of the solid/liquid transition of the PCM which is its isothermal behavior. An integrating of paraffin in SWH is best alternatives option to affect the heat transfer from the storage tank that can improve the thermal performance of solar thermal system and numerical results show that their advantage for night thermal losses reduction.

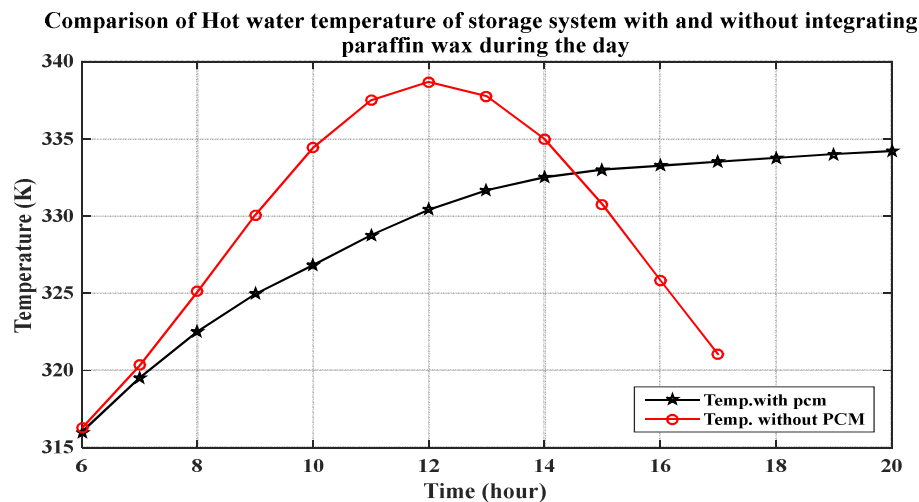


Figure 7.16: The time wise variation of the hot water or HTF average temperature of the storage tank for the SWH system with and without PCM on February 16th during charging processes

Both Figure 7.15 and 7.16 shows that including the PCM could result in temperature advantage in stored hot water temperature over extended periods of time and helps to minimize for reducing the time lag between the peak radiation and peak water temperature. In the case of extreme consumption during evening hours, the existence of PCM can partially recover the temperature of water. Thus, extending the effective operational time of the SDHW system. Furthermore, the integration of PCM in the hot water tank improves the storage capacity with the potential to save energy and to shift and/or smooth peak power demand.

Effect of flow rate of the HTF (\dot{m}): - has significant effect on the heat extraction rate from the solar collector that affects the rate of charging of the TES tank. Increase in mass flow rate has a large influence on the phase transition process of PCM. As the flow rate increases the time required for the complete charging becomes smaller. This is because an increase in fluid flow rates translates into an increase in surface heat transfer coefficient between the HTF and PCM capsules.

Solar water heating without PCM TES system: -is known as conventional sensible heat storage (CSHS). From the simulation result the following draw backs are arise:

- The size of storage system volume or space is large (total volume SHS tank is 54 m³).
- The peak solar radiation usual occurs near noon, but the peak heating demand is in the late evening or early morning. So, there is mismatch between supply and demand, and high heat losses are occurs at noontime as shown in Figure 7.16.
- The T_{hwo} decreases continuously with time as it goes to sunset.
- Employ the direct mixing of cold water with hot water in the conventional storage tank.
- Low heat storage capacity per unit volume and Non-isothermal behaviour.

SWH with paraffin wax TES system (LHTES): -by using the latent heat storage system, it is possible to rectify the back draws of variation in water outlet temperature experienced in the conventional SHS system and the outcomes:

- Provide a high-energy storage density and its characteristics to store heat at a constant temperature corresponding to the phase transition temperature of PCM.
- The peak solar radiation occurs at noontime are stored for late use.
- The size of the storage tank is reduced appreciably compared to conventional system and is best suited for applications where the requirement is intermittent.

7.9.1 Validation

The physical validity of the proposed numerical model has been checked by comparison between numerical results and data published. Since the geometrical size of latent heat storage system and melting points of PCM used are different; due to this their melting time, ambient and outlet temperature limits are vary. However, there is a good agreement of a present study result and published paper by Padmaraju et.al., (2008).

7.10 Water distribution system and pipe network

A hot water distribution system is an essential infrastructure in the supply of water for each rooms and end users. It connects consumers to sources of water, using hydraulic components, such as pipes, valves, pumps and tanks. The hospital buildings whose elevation is more than the main tank height come under this category. In general the buildings having elevation G+5 come under the pressure network.

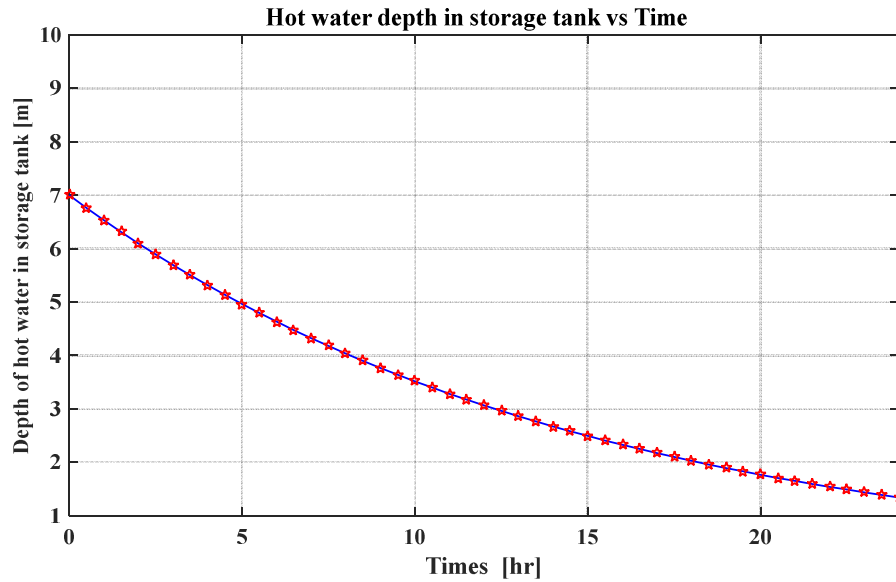


Figure 7.17. Depth of hot water in thermal storage tank

The maximum velocities attained in Pressure network are 0.78 m/s. The total head to be generated meets the needs of all the buildings floors. Figure 7.17 shows the depth of hot water in storage tank is slightly decreases as the customers are used. The maximum height of the fluid is approximately 7.5 m with the volume of reservoir 60 m³.

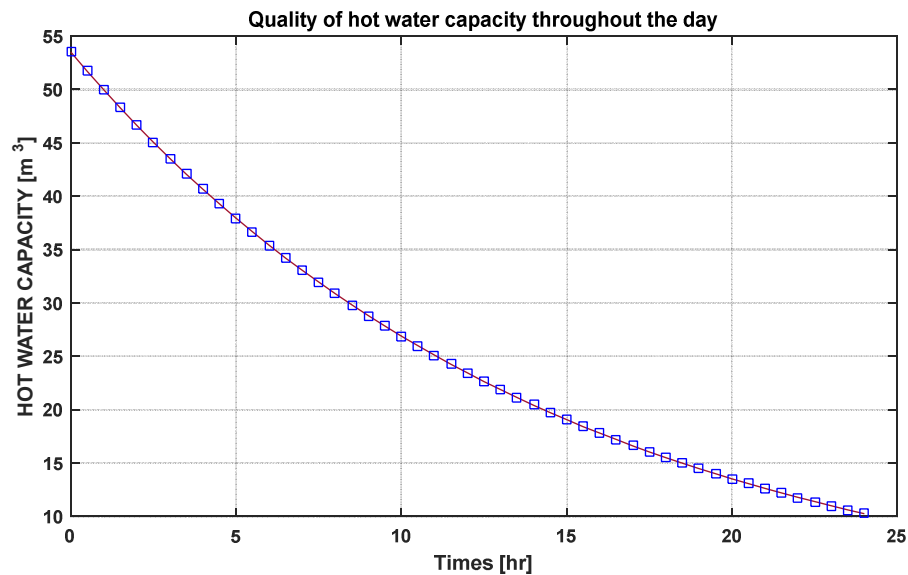


Figure 7.18. Quality of hot water withdrawal rate capacity versus operating time used.

CHAPTER 8

8. Estimation of Economic Analysis of DHW for AHMC

8.1 Economic Analysis of Solar Thermal System

Investment in solar energy technology is encouraged as the merits such as pollution free environment, free renewable and energy source, high reliability and low maintenance costs. Although solar radiant energy is free but the equipment required to convert it to a useful form is not free. So, a cost must be assigned to solar thermal that reflects the conversion equipment cost prorated on the number of kWh delivered by the solar energy which is less than the cost of other energy sources that can perform the same task (Kalogirou, 2014). Thus, there is an economic incentive to use solar energy. Generally, solar processes are characterized by high first cost and low operating cost. Investments in purchasing and installing solar energy equipment are major factors in solar processes economics.

The main goal cost evaluation is the determination of the least cost method of meeting the energy required considering both solar and non-solar alternatives and also solar energy equipment is bought today to reduce tomorrow's fuel bill. In our country, solar water heaters (SWH) are becoming increasingly attractive in sustainable development and efforts are continuously made to reduce their costs to make them more affordable. A SWH is designed for supplying a specified quantity of hot water per day at a specified temperature. Thus, annual heating load for water heating becomes:

$$Q_a = 365 * \rho_w C_p V_{st} (T_{hot} - T_{cold}) \text{-----} 8.1$$

While a solar fraction of this heating load is covered by solar energy and rest is met by auxiliary energy supply system. So, annual contribution of solar energy to the system;

$$Q_{a,solar} = sf * Q_a \text{-----} 8.2$$

Economic analysis parameters

Inflation rate	10%	Debt ratio	50%
Discount rate	10%	Debt interest rate	8%
Salvage rate	10%	Loan period	10 year
Energy escalation rate	15%	Cost of fuel	1.72 ETB
Cost of electricity	1.716 ETB		

8.2 Financial and Unit prices of components of SHW system with integrating PCM as Thermal energy storage

No:-	Item	Specification	Unit cost (ETB)
1	Solar flat plate collector, FPC	(1*2) m ²	972,218.75
2	Storage tank inside	2 mm steel sheet	5512.5
	Insulation	Glass fiber thick-1.95 mm (1.2*3) m	37012.5
	Insulation cover	Galvanized steel with 1 mm thick	3466.97
	Manufacture	30% of material cost	16097.20
	Total		62,089.17
3	Pipe External pipe for joining collector Tee, Elbow 90°, and fitting pipe	Length = 6 m (standard) 1 inch 1 ¼ inch 1 inch	24,666.75
4	Pump	Electric drive (2)	37,400
5	Controlling system and accessories	PRV, Check valves, block valves, vacuum and air vent, safety, RTD, thermostat and pump controls	35,500
6	Cylindrical and tube Latent Heat Storage Copper tube sheet		49,306.00
7	Paraffin wax (PCM)	Requirement by weight 2651.88 kg	62,266.142
8	Pipe Network for water distribution (L=6m std) Elbow and fitting	Total Length 920 (Galvanized Steel Piping) 1 inch 1 ¼ inch	118,906.7
9	Labor and installation cost	20% solar collector cost	194,443.75
Total component system cost			
10	Operating cost (Maintenance and pumping cost) [M&O]	15% of system cost	224,519.59

8.3 Maintenance, Operating and Replacement Cost

At the outset, investment and installation of project associated with solar energy process, system operation cost should be considered. Operating cost if continues operation that includes energy cost for pump operation, controllers and other accessories needs a system as a whole. Repair and replacement costs are a critical issues to the success of solar thermal systems. It has to be mentioned that the replacement and repair cost depends on the manufacturer and the type of the system used. The reason for this is the best approximation of the life cycle costing. In terms of lifetime and replacement this is the most difficult section solar water heating system component to evaluate. From the various companies manufacturing solar flat plate collectors were not able to give an exact average replacement age. Most of them qualified that the solar collectors would last for at least 20-25 years. Similarly for storing a thermal energy, various companies recommend the average lifetime of hot water storage reservoir replacement from 8 to 12 years. For an active solar water heating system, one basic components needs is a pump, but after lifetime is over, it should be replaced. The recommend pump for solar thermal system is an average age of pumps substituted from 5 up to 10 years.

8.4 Analysis of investment cost

An investments in buying and installing solar energy equipment are important factors in solar process economics. Installed costs of solar equipment can be shown as the sum of two terms, one proportional to collector area and the other independent of collector area:

$$C_I = C_A * A_C + C_E \text{-----} 8.3$$

Where, C_I -total cost of installed solar energy equipment (Birr); C_A - Total area dependent cost (Birr/m²); A_C -Area collector (m²); and C_E - Total cost of equipment independent of collector area.

There are many factors (interest rate, inflation rate, unit cost of electricity, operation & maintenance cost and solar water heater service life) are to be considered while evaluating life cycle cost of solar water heating system. All these factors are affected by fluctuations in the economy, government policies, electricity tariff and etc. (Kalogirou S. A., 2014)

Life cycle cost (LCC): -is the sum of all costs associated with an energy delivery system over its lifetime, taking into account the time value of money and can also be estimated for a selected period of time.

The life cycle cost of solar water heating system is determined from the investment cost and the present value of maintenance and pumping cost distributed over the life as follows;

$$LCC = CI + C_m \frac{1}{i} \left(1 - \frac{1}{(1+i)^n}\right) \text{-----} 8.4$$

Where, *CI* and Investment cost of solar water heating system

C_m-annual maintenance and pumping cost and *n*-period of time (years).

Life cycle savings Energy (LCS): -is defined as the difference between the LCC of a conventional fuel-only system and the LCC of the solar plus auxiliary system. This is equivalent to the total present worth of the gains from the solar energy system compared to the fuel-only system. The life cycle saving of solar water heater is the energy cost saved due to replacement of electricity or/and fuel by solar. Annual energy saving calculated as:

$$AES = sf * Q_{ann} \text{-----} 8.5$$

$$LCS = P_e * sf * Q_{ann} * \left(\frac{1+i_e}{i-i_e}\right) \left[1 - \left(\frac{1+i_e}{1+i}\right)^n\right] \text{-----} 8.6$$

Where, *LCS*-life cycle saving energy, [kWh]; *sf* and *Q_{ann}*-solar fraction of load supplied by solar energy and annual heating load [kWh] respectively.

i and *i_e*-annual market discount rate and annual market rate of energy escalation.

Unit price of Solar Energy

To determine the unit price of solar energy cost, the life cycle cost has to be equal to the life cycle savings of the solar water heater during its life time.

$$LCC = LCS \text{-----} 8.7$$

$$CI + C_m \frac{1}{i} \left(1 - \frac{1}{(1+i)^n}\right) = P_e * sf * Q_{ann} * \left(\frac{1+i_e}{i-i_e}\right) \left[1 - \left(\frac{1+i_e}{1+i}\right)^n\right] \text{-----} 8.8$$

Unit price of solar energy for solar water heating system

$$P_e = \frac{CI + C_m \frac{1}{i} \left(1 - \frac{1}{(1+i)^n}\right)}{sf * Q_{ann} * \left(\frac{1+i_e}{i-i_e}\right) \left[1 - \left(\frac{1+i_e}{1+i}\right)^n\right]} \text{-----} 8.9$$

Payback period (Np): -is the number of years needed to exactly recover the initial investment cost, *CI*, i.e. the time required for the annual solar savings to become positive and the time required for the cumulative solar savings to become zero (Mishra, 2012). Thus;

0 = -initial investment, *CI* + sum of annual cash flows, *CF* (means that *CI* = *CF*)

To determine the pay-back period, assume the maintenance cost is very low rather than other cost.

Hence the investment of the solar water heater has to be pay-backed by the life cycle saving of electric cost (*LCS*).

$$LCS = C_f * sf * Q_{ann} * \left(\frac{1+i_e}{i-i_e}\right) \left[1 - \left(\frac{1+i_e}{1+i}\right)^n\right] \text{-----} 8.10$$

Where, $LCS = CI$ at $n = Np$; C_f -unit cost of electricity for 1st year [Birr/kWh] and LCS -life cycle saving of electric cost [Birr]

$$CI = C_f * sf * Q_{ann} * \left(\frac{1+i_e}{1-i_e}\right) \left[1 - \left(\frac{1+i_e}{1+i}\right)^{Np}\right] \text{-----} 8.11$$

$$Np = \frac{\ln\left[1 + \frac{CI\left(\frac{i_e-i}{1+i_e}\right)}{C_f sf Q_{ann}}\right]}{\ln\left[\frac{1+i_e}{1+i}\right]} \text{-----} 8.12$$

8.5 Summary of Cost Estimation for the project installation

COST SUMMARY OF THE PROJECT FOR INSTALLATION						
Total initial cost of the projects (ETB)	Total Life Cycle cost (LCC)	Total Life Cycle saving (LCS)	Unit cost of Solar Energy	Unit cost of diesel fuel	Unit cost of Electricity and fuel	Payback period
ETB	Birr	Birr	Birr/kWh	Birr/kWh	Birr/kWh	years
1,496,797.262	3,408,259.1	3,442,935.87	0.17	1.72	0.572	3.85

CHAPTER 9

9. Conclusions and Recommendations for Future work

9.1 Conclusions

When going over the main points, AHMC needs total daily hot water consumption of 54 m^3 with the sizing of a solar collector over 630.96 m^2 that needed 265 number of collectors to fulfill the demands. An essential numerical derivation and model are developed for the flat-plate solar collector cross-sections (cover, air gap, absorber, working fluid, and insulation), sensible storage tank, and LHTES unit. Besides, after investigating both the thermal storage tank with and without integrating paraffin wax (n-Heptacosane) are examined. From the simulation result, an integrating of paraffin in SWH is a best alternative option to enhance the performance of the system overall and the heat transfer from the storage tank can improve the thermal performance of a solar thermal system, increases the operating periods and their advantage for fulfilling demand at night time. Generally, incorporating the PCMs in TES for SWH system can conserve the outlet water temperature, especially when the inlet water temperature is less at night time.

A hot water distribution system is also an essential infrastructure in the supply of hot water for each room and end-users and it connects consumers to sources of water using hydraulic components. The hospital buildings whose elevation is more than the main tank height and having G+5 come under the pressure network. Thus, the thesis has analyzed the pipe network and water distribution system. Then, the pump is selected to drive the water up to the end-users.

For the installation of the project, the cost estimation is calculated. To install the AHMC requires an initial capital cost of 1,496,797.26 ETB, which a total of 3,408,259.1 Birr per project through its lifetime and life cycle cost saving will be 3,442,935.87 Birr per project. Finally, the unit price of solar thermal energy is 0.17 ETB/kWh with the payback period of 3.85 years. This indicates that the unit price of the solar energy is less than the unit price of a diesel fuel (1.72 Birr/kWh) and the unit price of electricity (0.572 Birr/kWh).

9.2 Recommendations

- Waterborne organisms like *Legionella* grow within free-living amoebae and highly replicate between 20 - 45°C, with fastest growth as temperatures approach 40°C. Since, solar radiation is always an intermittent especially in a summer season, at that time the solar collector may not fulfill the desired temperature. So the auxiliary heating system as a backup will be actions helps to prevent Legionella contamination of hospital water distribution systems.
- The solar water heating is a green technology and an energy efficient technology which is economically viable in the long run and will reduce electricity generation and where it can have the further investigation areas for modern life.

9.3 Future work

In future many researchers willing to transform and familiarize the modern solar technology with our societies while solar energy are utmost application rather than other energy sources. Adama hospital medical college being a center of excellence in our country and has the long term plan to expand the construction and reduce the intermittent of heat energy sources. Therefore, it recommend that the solar thermal system should be optimized with different parameters to improvement of the solar system for hospital.

- ✚ Using different phase change materials as thermal energy storage with varying its thermophysical properties and numerical analysis for simulation of charging and discharging processes. Optimization of solar thermal system and phase change materials is suggest.
- ✚ The same work with this thesis and the thermal performance of LHTES units by considering the 2st law of thermodynamics approaches on TES system is recommended.
- ✚ Analysis of thermal losses after thermal storage for a period of time in case of thermal energy storage using phase change materials and compare it with energy storage using water.
- ✚ Investigation of PCMs that have a high thermal conductivity in order to be employed as phase change materials for thermal energy storage and analyzing its performance.

References

- Agbanigo, A. O. (2017). Performance Evaluation of Solar Water Heating System with PCM Thermal Storage;. *vol 5*.
- Al-Hinti, Al-Ghandoor, A., Maaly, A., Nageera, I. A., Al-Khateeb, Z., & Al-Sheikh, a. O. (2010). Experimental investigation on the use of water-phase change material storage in conventional solar water heating systems. 1735-1746.
- AnuarSharif, M., A.A.Al-Abidi, S.Mat, K.Sopian, M.H.Ruslan, M.Y.Sulaiman, & M.A.M.Rosli. (2015). Review of the application of phase change material for heating and domestic hot water systems. 557-568.
- Ayompe, D. a. (2013). Analysis of the thermal performance of a solar water heating system with flat plate collectors in a temperate climate.
- Bekele, A. (2007). Large scale application of Solar Water Heating system in Ethiopia; Masters thesis of Mechanical Engineering;.
- Brochure, M. (2015). "Energy Efficiency in Hospitals". 05.
- Christopher A. Homola, P. (2010). Solar Domestic Hot Water Heating Systems Design, Installation and Maintenance.
- Demirbas. (2006). An overview of Thermal energy storage and phase change materials. *Energy Source Part B Econ. Plan. Policy, 1(1)*, 85-95.
- Duffie, & Beckman. (2013). *Solar Engineering of Thermal Processes* (Fourth Edition ed.).
- ELPA. (2019). Retrieved from <https://www.costtotravel.com/cost/electricity-in-ethiopia>.
- Endale, A. (2019, 1167-1176). Analysis of status, potential and economic significance of solar water heating system in Ethiopia. (132).
- EngineeringToolBox. (n.d.). Thermal Conductivity of some common Materials and Gases. Retrieved from <http://www.engineeringtoolbox.com/thermal-conductivity>
- Fei, L., Yin, Z., Qinjian, L., Zhenghao, J., Xinhui, Z., & Enshen, L. (2017). 'Experimental study on TES performance of Water Tank with Phase Change Materials in Solar Heating System'. 3027–3034.
- Fortunato.B, C. T. (2012). Mathematical Model of Thermal storage with phase change materials (PCM). (2), 241-248.
- G.N. Tiwari, R. M. (2016). *Advanced renewable energy sources*.

- Garg, Chakraverty, & Agnihotri, S. a. (2003). Advanced tubular solar energy collector—a state of the art. *Energy Conversion and Management*. 157–169.
- Homola, & Christopher. (2010). *Solar Domestic Hot Water Heating Systems Design, Installation and Maintenance*.
- Hossain. (2011). Review on solar water heater collector and thermal energy performance of circulating pipe. *Renewable Sustain Energy*, 15(8), 380-392.
- IEA. (2015). Energy conservation through energy storage (ECES) programme. *International Energy Agency, Brochure*. Retrieved from http://www.iea-ec.es.org/files/090525_broschuere_eces.pdf
- Kalogirou. (2014). *Solar Energy Engineering; Processes and Systems* (Second Edition ed.).
- Kebede, D. (2016). ‘Design and Analysis of Solar Thermal System for Hot Water Supply to Minilik II Hospital New Building’ , June,.
- Kumar, Mahesh, Mubarak, Sreejith, & Vibin, a. (2016). “Experimental Investigation of Performance on A PCM Assisted Solar Water Heater”. *Vol 5(06)*.
- Liang, F., Zhanga, Y., Liua, Q., Jina, Z., Zhaoa, X., & Longa, a. E. (2017). ‘Experimental study on TES performance of Water Tank with Phase Change Materials in Solar Heating System’. 3027–3034.
- M.A. Kibria, M. A. (2014). Numerical and experimental investigation of heat transfer in a shell and tube thermal energy storage system. (13), 71-78.
- M.F.Demirbas. (2006). An overview of Thermal energy storage and phase change materials. *Energy Source Part B Econ. Plan. Policy*, 1(1), 85-95.
- M.R.Reddigari, Nallusamy, N., Bappala, A. P., & Konireddy, H. R. (2012). Thermal Energy storage system using Phase Change Materials (PCM). *THERMAL SCIENCE*, 16(04), 1097-1104.
- Mehling H, C. L. (2009). PCM-module to improve hot water heat stores with stratification. *Renew Energy*. 699–711.
- Mishra, G. N. (2012). *Advanced renewable energy sources*. RSC Publishing.
- Murali, G., Mayilsamy, K., & Arjunan, a. T. (2015). An Experimental Study of PCM-Incorporated Thermosyphon Solar Water Heating System, *International Journal of Green Energy*. 978–986.

- Padmaraju, Vignesha, & Nallusamy, a. (2008). "Comparative study of sensible and latent heat storage systems integrated with solar water heating unit". *1*.
doi:<https://doi.org/10.24084/repqj06.218>
- Panapakidis, D. (2016). Solar Water Heating Systems Study Reliability, Quantitative Survey and Life Cycle Cost Method, MSc. thesis, Department of Mechanical eng., University of Strathclyde in Glasgow.
- Rai, G. D. (2001). Solar Energy Utilization, fifth edition, Delhi.
- Renyuan, Z., & Xiufang, K. (2005). Applications of latent heat energy storage technology in peak load regulation of power system. *electric power*, 35, 21-24.
- Rosen, I. D. (2007). Thermal energy Storage (Systems and applications); (S. edition, Ed.)
- Salah., A. M. (2012). Modeling of flat-plate solar collector operation in transient states.
- Sarbu, I., & Sebarchievi, C. (2015). Solar Heating and cooling systems; Fundamentals, experiments and Application.
- Sharma, A., Chen, & Buddhi, a. (2009). Review on thermal energy storage with phase change materials and applications. *Renewable and Sustainable Energy Reviews*, 13, 318–345.
- Solomon, G. (2018). Potential use of solar thermal as an Alternative energy source for Adama General Hospitals and Medical College.
- Tay, M. B. (2011). Designing a PCM storage system using the effectiveness number of transfer units method in low energy cooling of buildings. *Energy and buildings*.
- Tehrani, Taylor, R. A., Saberi, P., & Diarce, G. (2016). Design and feasibility of high temperature shell and tube latent heat thermal energy storage system for solar thermal power plants. 130-136.
- Tiwari, G. T. (2016). *Handbook of Solar Energy; Theory, Analysis and Applications*. New Delhi & Saudi Arabia.
- Trp, A. (2005). An experimental and numerical investigation of heat transfer during technical grade paraffin melting and solidification in a shell-and-tube latent thermal energy storage unit. (79), 648-660.
- UNCC. (2002). Proceedings of Energy Conference 2002 UNCC, Addis Ababa.
- Utkarsh, Tiwari, Yadav, Mehta, a., & Darshan. (2015). Water Distribution Network Re-design for Svnit Surat Campus. *IJAREST*, 02(05), 2394-2444.

APPENDIX

ANNEX A: Incident solar radiation on inclined surface collector

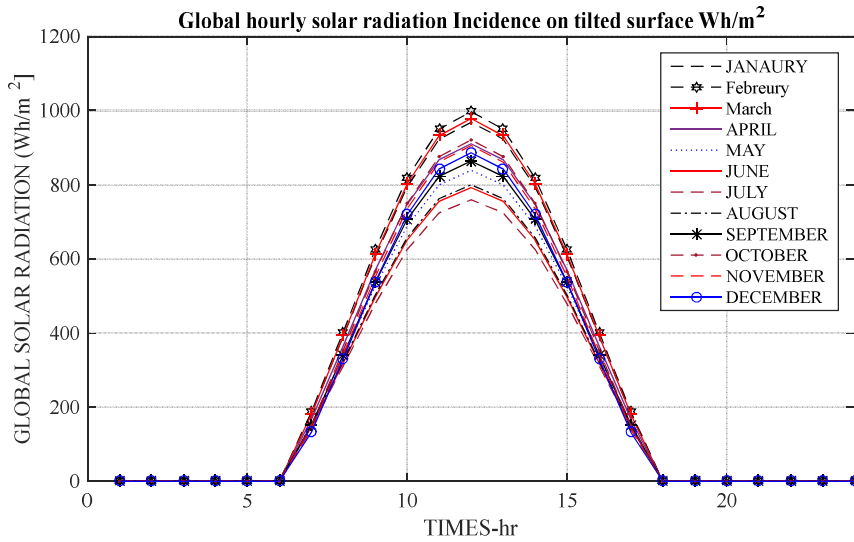
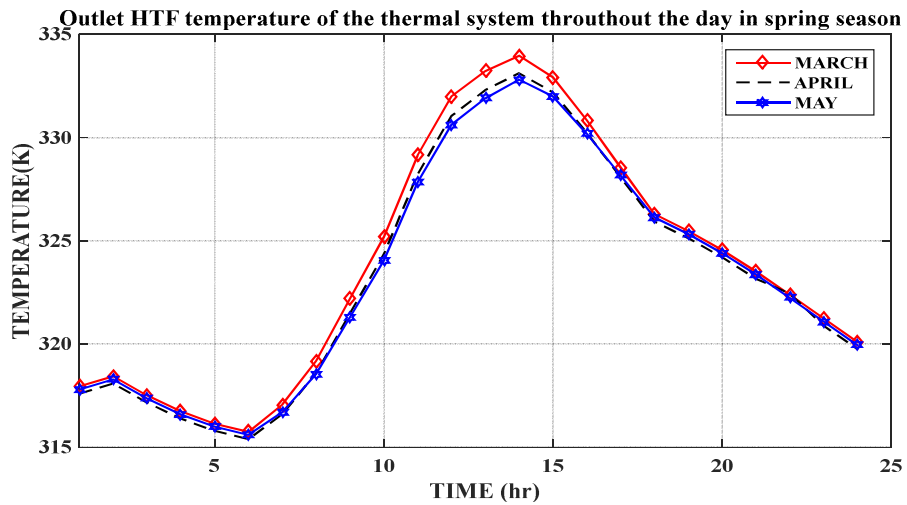


Figure A.0.1 Incident solar radiation on inclined surface collector

ANNEX B: Graph of Outlet heat transfer fluid temperature



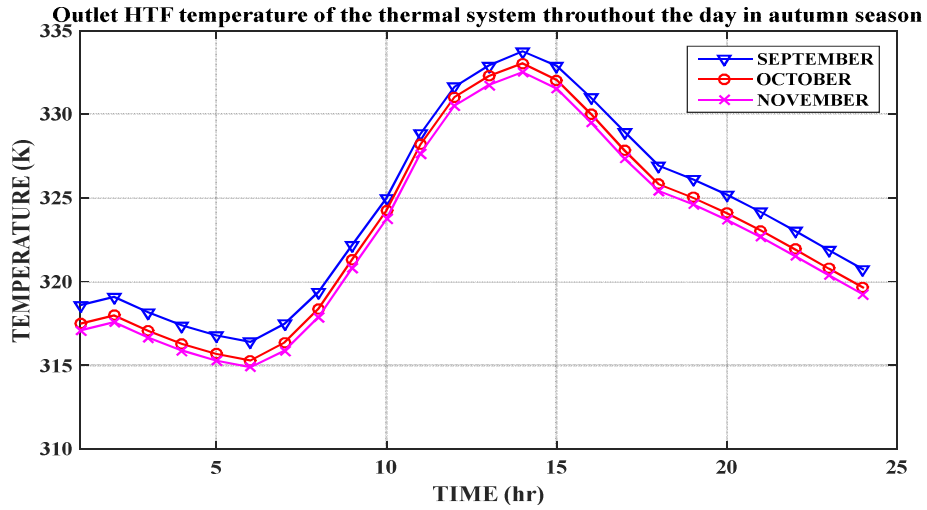


Figure B.0.2 Outlet temperature of HTF during all months in a year

ANNEX C: Temperature of plate absorber, air gap and glass cover

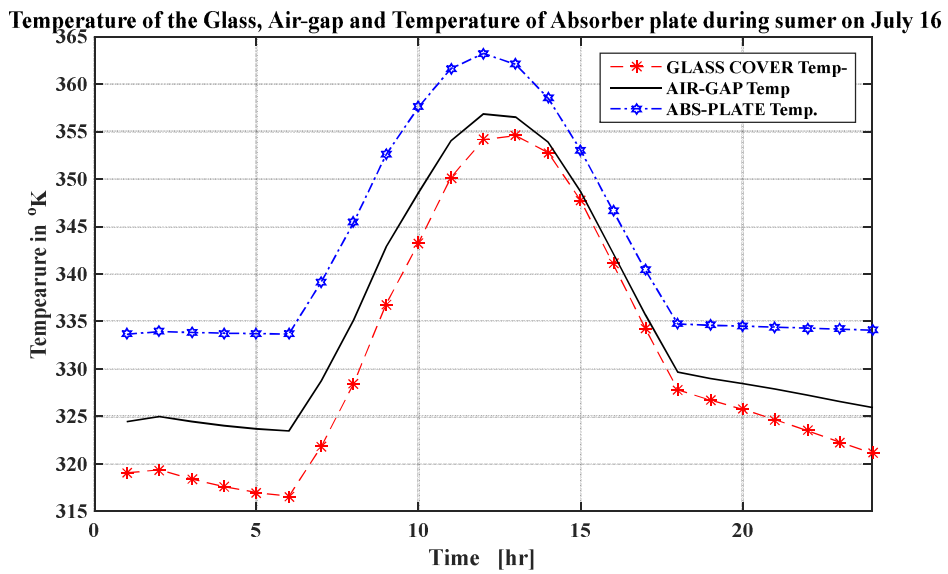


Figure C.0.3 Temperature of Glass cover, absorber plate, and air gap during summer season

ANNEX D: Useful solar energy gain for every months

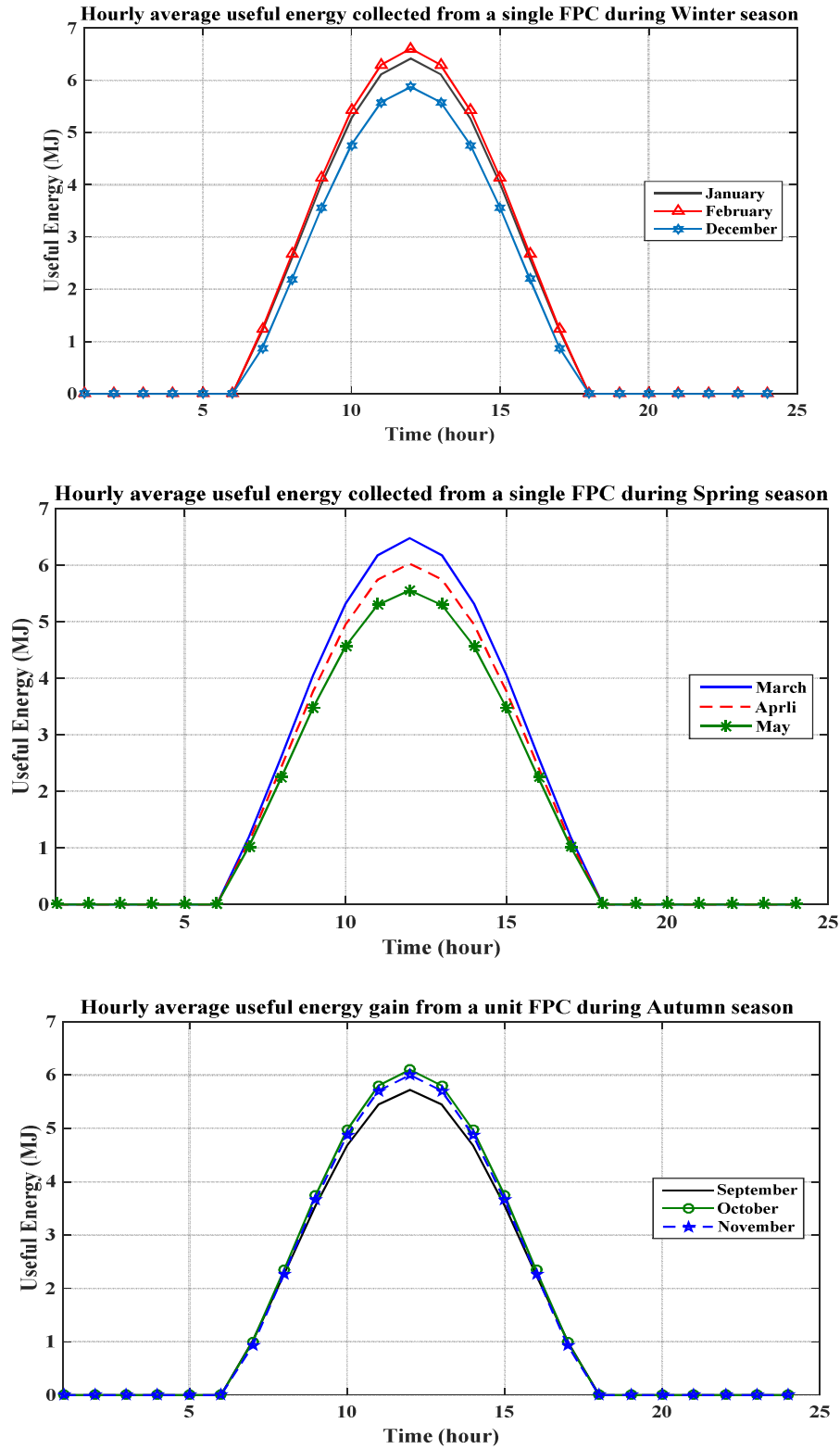


Figure D.0.4 Hourly average useful energy solar gain by a single flat plate collector

ANNEX E: Variation of daily temperature of hot water with and without phase change materials for June 17.

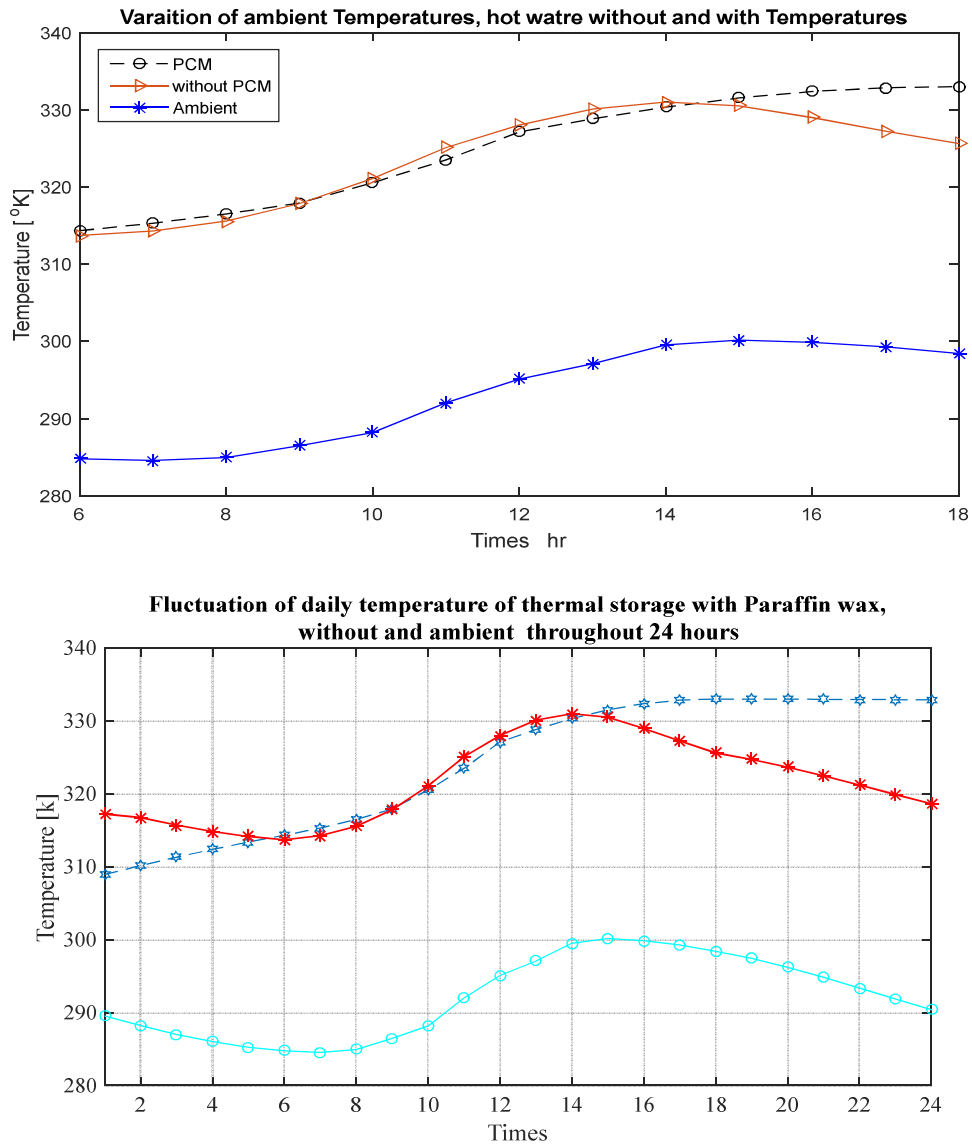


Figure E.0.5 Variation of daily temperature of hot water with and without phase change materials, and ambient temperature.

ANNEX F: Moody chart

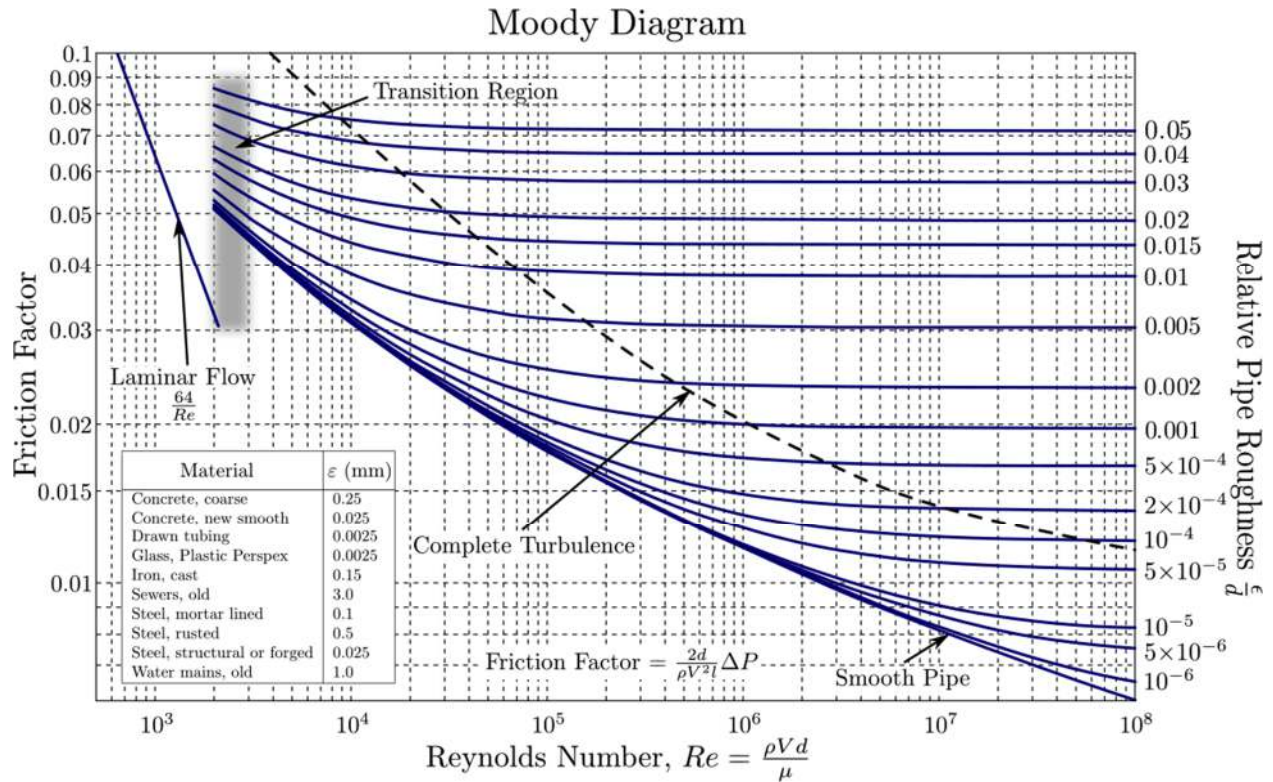


Figure F.0.6 Moody chart

ANNEX G: Thermal Conductivities of Absorber Materials

Table G.0.1 Thermal conductivity of absorber plate materials.

MATERIALS	THERMAL CONDUCTIVITY (W/m.K)
Copper	385
Aluminium	205
Mild Steel	54
Stainless steel	24
Polyethylene	0.3 – 0.4
Fiber glass	0.36
PVC(Polyvinyl Formal)	0.16
Paraffin wax	0.15 – 0.4
Water	0.64